Harnessing Spinel Ferrites: A Comprehensive Review of Their Role in Water Treatment

Alibasha Akbar,[a] Bhavani Lakshmi M,[a] Mihir Ghosh[a*]

[a] Department of Chemistry, SRM Institute of Science and Technology, Kattankulathur- 603203, Tamil Nadu, India.
Email: mihirg@srmist.edu.in

Abstract

Addressing water pollution effectively has led to the recognition of spinel ferrites as highly promising materials due to their inherent stability, magnetic characteristics, and photocatalytic capabilities. This review evaluates recent progress in employing spinel ferrites for the degradation of organic contaminants in water, highlighting their beneficial properties such as low bandgap energy, hydroxyl radical generation under light, and ease of separation through magnetic properties. Despite considerable research efforts, optimizing the synthesis techniques and photocatalytic performance of spinel ferrites remains a challenge. Key areas needing further exploration include improved doping methods, modifications to enhance photocatalysis, and evaluations of reusability, durability, and scalability. This review addresses these issues by providing a thorough analysis of recent innovations in spinel ferrite-based photocatalysts, including novel hybrid materials and advanced synthesis techniques like sol-gel, co-precipitation, and hydrothermal processes. This review offers an in-depth examination of the latest advancements in spinel ferrite photocatalysts, focusing on their applications in water purification. It investigates the influence of operational parameters; such as pH, temperature, light intensity, and catalyst dosage on efficiency and explores emerging composite materials and previously unexplored spinel ferrite systems. By incorporating recent research developments, the review underscores the significant potential of spinel ferrites and their composites for enhancing sustainable water treatment technologies.

1. Introduction:

One of the essential components of human civilization, water, has been well-researched. Roughly 71% of the Earth's surface is made up of water, 97% of which is salty. Freshwater makes up the remaining 3%, of which just 1% is fit for human use. Additionally, this 1% is dispersed unevenly around the world, which makes freshwater availability a critical problem for many countries.[1, 2] Water stress occurs when there is a lack of insufficient water for usage in homes, businesses, or agriculture. This covers various physical aspects of water resources, such as water availability, flow in the environment, and water quality.[3-5] Several important factors, including population growth, industrialization, urbanisation, aquifer depletion, climate change, and water pollution cause long-term water crises.[6-9] Meeting the worldwide demand for clean drinking water in the long-term prospects seems to be unachievable because the total amount of water in the hydrologic cycle stays essentially constant, existing in many forms such as ocean, surface and groundwater, and rains.[10, 11] Nevertheless, climate change is anticipated to impact both the quality and quantity of potentially accessible drinking water by intensifying floods, worsening droughts, and increasing the toxicity of chemical pollutants in the environment.[12, 13] Water contaminants may be classified into two primary categories: point source and nonpoint source. Point source pollution is derived from specific and easily identified sources, while nonpoint source pollution is derived from a variety of various sources. In addition, water pollutants may be categorized into several categories depending on their basic physicochemical characteristics. These types include radioactive in nature, thermal energy, microorganism-related, nutrient-based, suspended elements and sediments, as well as organic and inorganic pollutants.[14-16] The toxic nature of industrial effluent-containing dyes poses a considerable concern since they contain damaging and carcinogenic contaminants such as heavy metals, volatile organic substances, strong odours, and other hazardous elements. This poses a substantial threat to both human welfare and aquatic ecosystems.[17, 18] The main sources of these hazardous pollutants are from sectors such as textiles and clothing, leather products, printing, paper production, cosmetics, also medicines, processing of food, and animal feed making.[19, 20] Every year, approximately 1.6 million tons of dyes are manufactured. The dyeing industry commonly utilizes various organic components, predominantly employing reactive dyes, dispersed dyes, vat dyes, and direct dyes.[21, 22] Various industries, including metal plating, mining, tanneries, painting, automotive radiator production, and agriculture, significantly impact the pollution of heavy metals in

aqueous waste streams. These industries produce toxic waste that contains non-biodegradable heavy metals like Cu, Zn, Cr, Pb, Hg, and Cd, which contaminate water resources, including groundwater. The accumulation of these heavy metals in living organisms can result in various health issues. For example, Chromium poses a severe threat to both plants and animals, causing catastrophic illnesses. This review aims to address the issue of environmental pollution caused by dyes and heavy metals. To tackle this problem, spinel ferrites are proposed as a potential solution. This type of material has shown promising results in effectively removing these pollutants and mitigating their harmful effects on humans, animals, and the environment.

1.1. Spinel Ferrites

Spinel ferrites are a family of elements that possess remarkable stability, magnetic characteristics, and photocatalytic efficacy due to their unique cubic crystal structure. Figure 1 from the Scopus database provides proof that spinel ferrites have been employed for the past 13 years. The statistics of publications indicate that there have been 11,751 publications on spinel ferrites in the past 13 years. Over time, a growing body of research on spinel ferrites was carried out. They consist of trivalent (octahedral) and divalent (tetrahedral) metal cations, which are represented by the general formula AB_2O_4 in Figure 2. The photocatalytic behaviour of these cations is significantly influenced by the presence of transition metals. These metals cause the bandgap to become concentrated in electronic states, which effectively separates charges, which is an essential part of photocatalysis. The remarkable properties of spinel ferrites such as their remarkable chemical stability, low bandgap energy, and ability to generate hydroxyl radicals in response to light have drawn a lot of attention. These qualities provide great promise for water restoration procedures and make them perfect for the effective degradation of organic contaminants. Their ability to separate easily from the reaction liquid is due to their magnetic characteristics, which improve process efficiency and lower secondary pollutants. We present a comprehensive overview of the latest advancements in spinel ferrite-based photocatalysts in this work. We study synthesis methods that significantly affect ferrites' size, shape, and surface properties, all of which affect how well they photocatalyze. We also look at doping schemes and changes that improve their photocatalytic activity, such as heterojunction creation and bandgap engineering. Furthermore, we use spinel ferrites to study the processes behind the photocatalytic degradation of contaminants. We focus on the role played by reactive oxygen species (ROS) and charge carrier separation and transfer mechanisms. We also investigate the effects of various operating parameters on the photocatalytic process, including pH, temperature, light intensity, and catalyst dosage. Lastly, we draw attention to the difficulties and constraints that still exist in the real-world use of spinel ferrites for the remediation of water pollution, including issues with reusability, long-term stability, and scaling up the photocatalytic process for commercial uses. We wrap up by talking about potential avenues for future studies, such as investigating new composite materials, exploring unexplored spinel ferrite systems, and incorporating these materials into cutting-edge water treatment technologies. According to this review, spinel ferrites hold a great deal of promise as adaptable materials to fight water pollution. The present study aims to provide an overview of the potential, difficulties, and state-of-the-art related to the use of these materials in advanced material science and environmental sustainability.

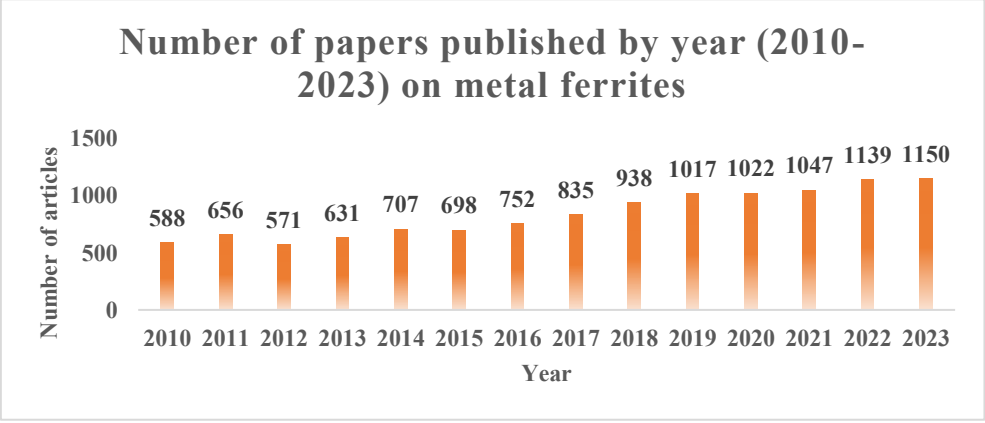

Figure 1. Scholarly publications released between 2010 and 2023, organized by year. The Scopus Database provided this information (This data was obtained from the Scopus Database).

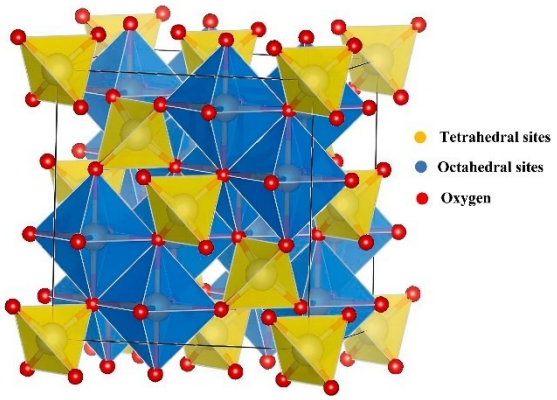

Figure 2 The diagram mentioned above illustrates the structure of spinel ferrites which is depicted with distinct colours representing oxygen atoms (depicted in red), tetrahedral sites (depicted in yellow), and octahedral sites (depicted in blue).

2. Spinel ferrites as a photocatalyst:

Zhang et al. synthesized $CoFe_2O_4$-graphene hybrid materials (CFGHs) with different GO/$CoFe_2O_4$ weight ratios by employing Dafeng et al.'s combustion technique. The as-synthesised CFGHs outperformed pure $CoFe_2O_4$ in their ability to photocatalytically degrade Methylene Blue (MB) when exposed to visible light.[23] The hydrothermal method was used to manufacture multi-walled carbon nanotube (MWCNT) hybrids and spinel nickel ferrite with different concentrations of MWCNT. The study aimed to explore the photocatalytic activity of $NiFe_2O_4$/MWCNT hybrids in decolourizing Congo Red (CR) in an aqueous solution using simulated solar light irradiation. This innovative fusion has the potential to effectively address a wide range of dyestuff effluent on a large scale.[24] Using GO and various metal ions as starting materials, Bai et al. developed a one-pot solvothermal synthesis process to create hybrids of reduced graphene oxide (rGO) supported ferrite (MFe_2O_4, M = Mn, Zn, Co, and Ni). These hybrids have proven to be highly effective adsorbents for removing dye pollution. Researchers have discovered that a concentration of 0.6 g/L of combinations can eliminate 100% of MB and over 92% of Rhodamine B (RhB) in 2 minutes, with a 5 mg/L concentration. The hybrids also show improved photocatalytic activity in MB and RhB degradation. This research could make a new, straightforward separation platform for decontaminating wastewater available.[25] Sun et al. devised a straightforward hydrothermal synthesis technique to create a magnetically separable photocatalyst composed of P25/$CoFe_2O_4$/graphene. The quantity of P25 in the catalyst was varied. The result shows that the P25/$CoFe_2O_4$/graphene photocatalyst surpasses other photocatalysts, such as $CoFe_2O_4$/graphene, P25/$CoFe_2O_4$, and P25/graphene, in terms of both the adsorption process and photocatalytic degradation.[26] Xiong et al. have developed a simple two-step hydrothermal cadmium sulfide-ferrite nanocomposite (NC) (CdS-MFe_2O_4, where M can be either Zn or Co) with different ferrite concentrations. The addition has improved photocatalytic stability and efficiency under visible light irradiation, and it may be employed as a magnetically recoverable photocatalyst. When exposed to visible light, the degradation of 4-chlorophenol (4-CP) and RhB in a water-based solution was assessed to determine the material's photocatalytic performance.[27]

Fu et al. devised a simple technique for creating a $CuFe_2O_4$-graphene hetero-architecture through hydrothermal fabrication. This structure has a variety of uses, including magnetic cycling, increased photocatalytic activity when exposed to light, and remarkable electrochemical behaviours that make it suitable for use as the anode in lithium-ion batteries. The photocatalytic activity data show that the formerly inert $CuFe_2O_4$ drastically changes and becomes a highly active catalyst for the breakdown of MB when coupled with graphene.[28] Ji, Haiyan, et al. used a straightforward chemisorption approach to create new magnetic graphitic carbon nitride g-C_3N_4/$NiFe_2O_4$ photocatalysts. After five runs with hydrogen peroxide (H_2O_2) and visible light illumination, the 7.5% g-C_3N_4/$NiFe_2O_4$ composite exhibits high and stable photocatalytic activity as prepared.[29] Zhang et al. used a one-step chemical coprecipitation method to successfully create magnetic composites of $ZnFe_2O_4$ and $BiVO_4$. By doping $ZnFe_2O_4$ with a narrow band gap, $BiVO_4$'s photocatalytic activity was enhanced. This resulted in a larger production of photo-produced electrons and a higher absorption of visible light when compared to pure $BiVO_4$.[30] Yao et al used a simple reflux approach to synthesize magnetic $ZnFe_2O_4$-C_3N_4 hybrids. They employed graphitic C_3N_4 sheets and $ZnFe_2O_4$ nanoparticles (NPs) (about 19.1 nm in size) in methanol at 90°C. The catalytic activity of heterogeneous $ZnFe_2O_4$-C_3N_4 catalysts was assessed utilising orange II's

photo-Fenton discolouration procedure. This approach involved the use of H_2O_2 as an oxidant as well as visible light irradiation (> 420 nm). The results of five distinct studies consistently demonstrated that the heterogeneous $ZnFe_2O_4$-C_3N_4 hybrid operated successfully and without loss of activity. This demonstrates a realistic use for the photo-oxidative degradation of organic contaminants.[31] Wu, et al. proposed a simple method for incorporating magnetic $ZnFe_2O_4$ NPs into a rGO network. This was accomplished by utilising highly reactive $ZnO_x(OH)_y$ and FeO_x colloids as precursors. The precursors were synthesised by laser ablation of metallic zinc (Zn) and iron (Fe) targets in distilled water. The resulting nanocrystals significantly improved the photodegradation efficacy of the MB dye. Furthermore, the remarkable magnetic characteristics of the $ZnFe_2O_4$ NPs enable facile catalyst recovery by magnetic separation from the solution. This study expands the potential use of $ZnFe_2O_4$ NPs as photocatalysts, which may be triggered by visible light to destroy organic contaminants. Furthermore, it devised a unique method for synthesising $ZnFe_2O_4$-rGO (NCs).[32]

Khadgi et al. used a straightforward one-pot hydrothermal method to commercialize $ZnFe_2O_4$, a photocatalyst that is responsive to visible light, by combining it with graphene oxide (GO) and silver NPs. Consequently, they synthesized NC referred to as $ZnFe_2O_4$-Ag/rGO. This NC was evaluated for its photocatalytic efficiency using visible light to degrade 17-ethinylestradiol (EE2), a non-dye chemical compound regarded as an emerging pollutant with endocrine-disrupting effects.[33] Chen et al. researched the degradation of 2,4-dichlorophenol (2,4-DCP) using a new photocatalyst composed of a magnetically separable NC of rGO, $ZnFe_2O_4$, and silver phosphate (Ag_3PO_4). The photocatalyst was created using the solvothermal and in situ precipitation methods. According to the study, rGO/$ZnFe_2O_4$/Ag_3PO_4 NC demonstrated superior photocatalytic activity and stability compared to pure Ag_3PO_4.[34] Kulkarni et al. reported that magnetically separable core-shell $ZnFe_2O_4$@ZnO NPs could break down aqueous Methyl orange (MO) under visible light by photodegradation. $ZnFe_2O_4$@ZnO NPs are efficient solar photocatalysts because they can be easily separated using a magnet, have a surface area of 41 m^2/g, and can absorb visible light. $ZnFe_2O_4$@ZnO NPs have superior UV photocatalytic efficiency compared to ZnO. This is a result of the massive generation of electron-hole pairs. It has been documented for the first time that $ZnFe_2O_4$@ZnO NPs can be utilized for visible light photodegradation of MO. The $ZnFe_2O_4$@ZnO NPs have high photocatalytic efficiency and can be reused multiple times, indicating their applicability for solar photocatalytic applications.[35] N-doped TiO_2/$ZnFe_2O_4$ catalysts were effectively synthesised using one-pot vapor-thermal coupling of nitrogen-modified TiO_2 and $ZnFe_2O_4$. Yao et al. examined the hybrids' UV-vis photocatalytic capabilities. Furthermore, the effects of catalyst stability, dye type, and amount on the photodegradation of organic dyes were examined. This study presents an easily recyclable photocatalyst for water filtration, as well as a simple method for creating N-doped TiO_2/$ZnFe_2O_4$ hybrids.[36]

Wu et al. produced Ag/ZnO/$ZnFe_2O_4$ ternary composites with hollow and porous nanostructures using a straightforward calcination procedure. $Zn_3Fe(CN)_6.xH_2O$, an Ag-loaded Prussian blue analogue, served as the precursor for this synthesis (Ag-ZnPBA). Compared to its binary cousin, ZnO/$ZnFe_2O_4$, the ternary Ag/ZnO/$ZnFe_2O_4$ demonstrated noticeably greater photocatalytic activity in the degradation of organic dye. This result emphasises how important Ag is to the photocatalytic process. The study offers a quick and efficient method for creating multi-component, homogenous NCs with interesting topologies and a range of uses.[37] Ren et al. used a hydrothermal approach and a microwave-assisted synthesis process to create unique $NiFe_2O_4$/Bi_2O_3 heterostructures. These structures have visible light photocatalytic activity and were used for the degradation of antibiotics. The photocatalytic activity of the $NiFe_2O_4$/Bi_2O_3 heterostructures was significantly higher than that of a single semiconductor in removing tetracycline from water.[38] Fu et al. plan to manufacture a magnetically separable $NiFe_2O_4$-graphene photocatalyst with varying graphene contents using a straightforward method. It is intriguing to note that when $NiFe_2O_4$ NPs and graphene sheets are combined, the inert $NiFe_2O_4$ undergoes a dramatic transformation into a highly active catalyst capable of breaking down MB when exposed to visible light.[39]

3. Spinel ferrites based on synthesis methods

3.1 Sol-gel Method:

Ivanets, Andrei, et al. used Fenton-like catalyst $MgFe_2O_4$ and metal-loaded MFe_2O_4 NPs [(M)-Mn^{2+}, Co^{2+}, Ni^{2+}, and Cu^{2+}] to degrade MB in water in a recent work. The primary emphasis of the investigation was on the catalytic breakdown of MB and the impact of metal ions absorbed into $MgFe_2O_4$. The outcomes show that $MgFe_2O_4$ may be a useful

adsorbent and catalyst for eliminating organic pollutants and dangerous metal ions from multi-component water solutions.[40] Magnetic $CuFe_2O_4$ spinel NPs were synthesised by Feng et al. These NPs were used as catalysts to activate H_2O_2 for sulfanilamide heterogeneous degradation via external energy-free Fenton-like processes.[41] Desai and his team have utilised the auto-combustion method to produce $MnFe_2O_4$ NPs. They used a combination of $MnFe_2O_4$ and mM solutions of H_2O_2 for the degradation of MB dye by photocatalysis under sunshine.[42] In this study, Trier et al. used the sol-gel method to synthesise $Cu_{1-x}Co_xFe_2O_4$ spinel ferrite NPs for 6 hours at 600 °C with cobalt content (x = 0, 0.3, and 0.5).[43] Sol-gel technology was employed to produce $MnFe_2O_4$ spinel ferrite NPs as catalysts for the oxidative disintegration of MO. These NPs feature delicate magnetic response properties and a large specific surface area. The tests showed that they have a strong catalytic activity for the breakdown of MO. Due to their unique properties, $MnFe_2O_4$ spinel ferrite NPs may be used in water treatment.[44] Jasrotia, Rohit, and colleagues employed sol-gel auto-combustion to synthesise Ni-Cu-Zn nanosized spinel ferrites doped with Ag^+, Mn^{2+} and Cr^{3+} ions. The chemical formula of the synthesised specimens is $Zn_{0.3}Ag_0Ni_{0.4}Cu_{0.3.4x}Cr_{0.3x}Mn_{0.3x}Fe_{2-x}O_4$ (ZANCuCrMFO) (where x = 0.0, 0.05, 0.10, 0.15). The study aimed to investigate synthesised specimens' microstructural, optical, magnetic, and electrical properties.[45] Muhammad et al. utilised the sol-gel method to prepare copper ferrites with indium (In) substitution, having the nominal composition $CuIn_xFe_{2-x}O_4$ (where x = 0.00 to 0.32). The synthesised ferrites exhibited low coercivity and dielectric parameters, indicating the potential benefits of using indium-substituted copper ferrites in high-frequency and switching applications.[46] Khirade, Pankaj P. et al. investigated how different synthesis methods affected the qualities of the structure, microstructure, magnetic, electrical, and dielectric of $Mg_{1-x}Zn_xFe_2O_4$ nanocrystals prepared using the ceramic and environmentally friendly sol-gel method (where x = 0.00 to 0.32).[47] Researchers Samoila and Petrisor and their team used sol-gel auto combustion with citric acid as the fuel agent to create nanosized spinel ferrites MFe_2O_4 (where M can be Ni, Co, or Zn). They discovered that using $NiFe_2O_4$ as an adsorbent, a single-objective optimisation produced an impressive 98.995% colour removal efficiency. Furthermore, the adsorption capacity and removal efficiency improved due to the multi-objective optimisation.[48]

3.2 Co-Precipitation method

Wu, et al. tested the efficacy of magnetic ferrite $CuFe_2O_4$ powder as an adsorbent and catalyst for adsorption-catalytic combustion in this work using Acid Red B (ARB), an organic pollutant. The study concentrated on three key areas: the material's reusability as an adsorbent and catalyst; the powder's catalytic activity for the discharge of ARB and the characterization of the resultant products;[49] and P. Annie et al. employed a rapid and cost-effective co-precipitation technique to create several metal ferrites (MFe_2O_4 = Co, Ni, Cu, Mn, and Sr). The spinel metal ferrite NPs have garnered much attention because of their extraordinary properties, particularly their optical and magnetic properties. The resultant metal ferrites are employed as a nanocatalyst in the photo-degradation process of MB dye, a prominent organic dye used in the textile industries.[50, 51] $MgFe_2O_4$ NPs were synthesised by Kaur N et al. using sol-gel, solution combustion, and co-precipitation techniques.[52] The $Mg_{1x}Zn_xFe_2O_4$ NPs (x ranging from 0 to 0.9) were produced using the sol-gel process by Reyes-Rodríguez et al. The study found that certain water suspensions of $Mg_{0.9}Zn_{0.1}Fe_2O_4$ and $Mg_{0.7}Zn_{0.3}Fe_2O_4$ could heat up to 42°C within 10 minutes, indicating the NPs' magnetic properties.[53] The research conducted by Ajeesha, T. et al. involved using the chemical co-precipitation method to create NPs of spinel $Mg_{1-x}Ni_xFe_2O_4$ (where x = 0.0, 0.6, and 1.0). The synthesised materials were tested for their suitability in photocatalytic applications by using them to degrade MB. These materials demonstrated absorption activity in the visible spectrum, according to optical studies.[54] Irshad, Amna, et al. successfully made cobalt-substituted magnesium-zinc ferrites (MZF) in this work by using the co-precipitation technique. Through the photodegradation of coloured and colourless pollutants in the presence of light, they assessed the photocatalytic activity. This study's main goal was to look into the photocatalytic degradation of hazardous materials including MB and benzimidazole. When cobalt was added, the MZF's ability to function as a photocatalyst was increased. The highest cobalt level, MZF3, resulted in the greatest amount of MB photodegradation. As a result, it can be said that $Mg_{0.5}Zn_{0.5}Co_xFe_2O_4$ is a promising catalyst for treating wastewater.[55]

3.3 Hydrothermal method

Su et al. used a hydrothermal process to produce nanocrystals of meso-$ZnFe_2O_4$ by reacting cetyltrimethylammonium bromide (CTAB) with $ZnFe_2O_4$. The quantity of ZnFe2O4, the concentration of H2O2, and the degradation of Acid Orange II (AOII) at various sintering temperatures

were used to assess the photocatalytic activity of $ZnFe_2O_4$ under visible light. Furthermore, $ZnFe_2O_4$ preserved its degradation effectiveness throughout multiple subsequent batch runs, illuminating the accurate photocatalytic mechanism.[56] Liu et al. created a $NiFe_2O_4$ NPs magnetic species that catalyzed the degradation of RhB in the presence of oxalic acid through a photo-Fenton catalytic property. The best breakdown rates were achieved at pH 3.0 with 1.0 mM oxalic acid. The magnetic catalyst was highly active, extremely stable, and simple to separate using an external magnet, according to seven cyclic tests for the deterioration of RhB. Thus, this magnetic catalyst shows promise for the removal of organic pollutants.[57] Owing to the synergistic interactions between Fe and Cu ions, $CuFe_2O_4$ containing Cu^+ ions can serve as highly effective heterogeneous Fenton catalysts. As a result, a technique by Moreno-Castilla, Carlos, et al. for creating $CuFe_2O_4$ nanospheres (CFNS) was chosen that also allows cuprite to develop, yielding a CFNS composite that was then calcined at a temperature of 400 °C. Nearly all of the phenols had been completely degraded after 95% elimination of the total organic carbon (TOC).[58] Three spinel ferrites $CuFe_2O_4$, $MgFe_2O_4$, and $ZnFe_2O_4$ were the subject of a study by Kurian, J. et al. examined their structural, optical, and magnetic characteristics. Under the same physical circumstances, these ferrites were made in an autoclave using various liquid media and surfactants. In the hydrothermal method, water was used as the medium and trisodium citrate as the surfactant. In the solvothermal approach, ethylene glycol was utilized as the solvent while polyethylene glycol served as the surfactant.[59] As heat sources for magnetic hyperthermia therapy, Fotukian, Seyedeh Maryam, et al. planned to prepare monodisperse $CuFe_2O_4$ and Fe_3O_4 NPs in this study utilizing a solvothermal approach. This is the first report on the solvothermal synthesis of monodisperse $CuFe_2O_4$ NPs with an average particle size < 50 nm, as far as in the literature.[60]

3.4 Microemulsion method

Cobalt, nickel, and zinc nanosized spinel-type ferrites (MFe_2O_4, M: Co^{2+}, Ni^{2+}, and Zn^{2+}) were made by Arturo Adrián, et al. utilizing an original oil-in-water microemulsion process. These compounds, especially those created by microemulsion, have not been thoroughly examined for H_2 production by the water-splitting mechanism.[61] Pemartin et al. demonstrated the potential of oil-in-water microemulsion reactions as an eco-friendly alternative for synthesizing mixed oxide spinels with magnetic properties.[62] By using the micro-emulsion process, Ca-Ni co-substituted samples of nanocrystalline spinel ferrites with the chemical formula $Mg_{1x}Ca_xNi_yFe_{2y}O_4$ (x=0.0-0.6, y=0.0-1.2) were created by Rajjab et al. and they were then annealed at 700°C for 7 hours. The improved magnetic properties of synthetic materials make them ideal for switching and high-frequency applications, while their reduced dielectric qualities make them ideal for high-frequency applications.[63] La-doping Typical micro-emulsion approach used by Ketan A et al. to manufacture Ni-rich nano Ferro spinel compounds.[64] Neodymium (Nd^{3+}), a rare earth element, and its impact on the characteristics of $LiNi_{0.5}Nd_xFe_{2x}O_4$ spinel ferrites were covered by Zaheer Abbas, et al. These ferrites were produced using a simple microemulsion method.[65] After employing a multi-microemulsion strategy, a reverse micelle method was used by Uskoković, V. et al. to create stoichiometric nanocrystalline nickel-zinc ferrites.[66] The study by Misra et al. demonstrates the microemulsion technology's ability to synthesize a narrow size distribution of various nanocrystalline ferrites, including nickel and zinc ferrites.[67]

3.5 Template method

Using appropriate salts of nickel, cobalt, or magnesium as templates, Gu et al. presented a two-solvent technique in this study to fabricate one-dimensional spinel $NiFe_2O_4$, $MgFe_2O_4$, and $CoFe_2O_4$ nanowires from iron nitrate.[68] Gao, et al. produced magnetic mesoporous spinel $NiFe_2O_4$ with a high surface area (up to 301.6 m^2 g^{-1}) and a well-defined pore size distribution ranging from 2.5-16.2 nm using a single-phase multi-component precursor. There was no pore-generating template used in the procedure. Acid Orange 7 (AO7) was successfully adsorbed by the mesoporous material, which may also be used as a magnetically separable adsorbent to remove AO7 from wastewater. AO7 adsorbed on the adsorbent can be quickly removed by heat breakdown, and the synthesized mesoporous $NiFe_2O_4$ can be easily recycled while maintaining its adsorption property.[69] By annealing $Mg(OH)_2$-deposited -FeOOH nanorods, Enlei, Zhang, et al. reported a highly active magnetic $MgFe_2O_4$ nanorod catalyst. The breakdown rate of CR solution reached 95% after 2 hours when the Fenton oxidation of CR was catalyzed by the $MgFe_2O_4$ nanorods in their as-prepared state. After five cycles, the catalytic activity was still quite high. This opens up new possibilities for the efficient treatment of aqueous hazardous dye and the manufacture of a one-dimensional magnetic catalyst based on a template technique.[70] Using mesoporous silica SBA-15 as a host matrix, spinel $CoFe_2O_4$ nanowires were effectively created by El-Sheikh SM et al. and the

precursors were slowly thermally decomposed inside the silica-based template.[71] Yu et al. produced spherical mesoporous nanocrystal clusters of nickel and cobalt ferrite, featuring a large surface area and uniform size distribution. They achieved this using a template-free solvothermal technique in ethylene glycol, followed by heat treatment.[72] Yourdkhani et al. fabricated highly ordered spinel ferrite $M_xFe_{3-x}O_4$ (M = Ni, Co, Zn) nanotube arrays using anodic aluminium oxide templates with a pore size of 200 nm. This was achieved by combining a liquid-phase deposition technique with a template-assisted approach.[73] Zhao, B. et al. synthesized spherical La^{3+} doped zinc ferrite clusters without the use of a template or surfactant using a simple and effective one-pot solvothermal synthetic method. The clusters as-prepared also performed well when it came to adsorbing contaminants like MO from water.[74]

3.6 Sono chemical method

Low-power sonochemical coprecipitation was used by Kaur et al.to create $CuFe_2O_4$ NPs.[75] Single-phase $CoEu_xFe_{2-x}O_4$ (CEFO) ($0.00 \leq x \leq 0.10$) nanosized spinel ferrites were synthesized by Abdullah et al. via a sonochemical approach.[76] $MnFe_2O_4$ single-phase spinel ferrite structure synthesized by Yadav et al. using a sonochemical approach.[77] For the first time, $Zn_{0.35}Fe_{2.65}O_4$ (ZFO) nanostructures were created by Yousefi, S. R. et al. using the sonochemical approach. By changing the synthesis procedure, a pure ZFO nanostructure was created. In the presence of light, these nanomaterials demonstrate significant photocatalytic activity.[78] Sonochemically produced $CoFe_{2x}Gd_xO_4$ (CFG) NPs with x = 0.00, 0.05, 0.10, 0.15, and 0.20 by Yadav et al. To create extremely crystalline single spinel crystal phase NPs, sonochemical synthesis is advantageous. Gd^{3+} substitution in $CoFe_2O_4$ NPs changes the magnetic characteristics, enhanced ac conductivity and dielectric constant.[79] In this study, Amulyaet al. utilized the sonochemical approach to create $NiFe_2O_4$ NPs cost-effectively and simply. The research demonstrated that $NiFe_2O_4$ NPs functioned as an effective photocatalyst and a reliable electrode material, exhibiting high electrode reversibility when detecting paracetamol. Therefore, it is expected that the sonochemically synthesized $NiFe_2O_4$ NPs will offer valuable insights into their versatile applications.[80] MNPs made of $NiFe_2O_4$ and $CoFe_2O_4$ were created by Ilosvaiet al.using a sonochemical process and combustion.[81] Goswami, Partha P., et al. studied the sonochemical method for producing $CoFe_2O_4$ NPs.[82] In this study, Almessiere, Munirah Abdullah, et al. discussed the benefits of using ultrasonic irradiation to produce nano spinel ferrites (NSFs) consisting of Dy-Y co-substituted Mn-Zn spinel-type. Two different methods were used to synthesize the $Mn_{0.5}Zn_{0.5}Fe_{2-2x}(Dy_xY_x)O_4$ (MZFDYO) (0.0 x 0.05) NSFs, namely citrate sol-gel combustion and ultrasonic irradiation.[83] Goswami, Partha Pratim, et al. used acetate precursors to describe the sonochemical production and characterization of Mn-ferrite NPs.[84]

3.7 Electrochemical method

$MnFe_2O_4$ NPs were produced by Mazarío et al. using a combination of electrochemical/chemical techniques.[85] $CoFe_2O_4$ NPs of uniform size have been produced electrochemically in one step.[86] Zahra et al. employed electrochemical synthesis to create ferromagnetic iron oxide (Fe_3O_4) NPs in a quick and low-cost process. The synthesized substance was employed as a heterogeneous electro-Fenton catalyst for decolorizing solutions containing Acid Scarlet and Acid Blue 92. Moreover, the Fe_3O_4 NPs can be easily recycled through magnetic separation, thus preventing them from becoming a secondary pollutant in the environment.[87] The magnetic characteristics and cytotoxic effects of MNPs made from magnetite and Mn, Co, and Ni ferrites and synthesized electrochemically are examined by Ovejero et al. in this study.[88] A novel electrochemical technique was used by Mazario, E., et al.to create $CoFe_2O_4$ NPs.[89] A team of researchers led by Lakshmi Ranganatha V. has introduced a simple, cost-effective, and eco-friendly approach for producing $ZnFe_2O_4$ NPs. They assessed the photocatalytic performance of MB in the presence of visible light, achieving a removal efficiency of 96%. Furthermore, the nano-catalyst showed effective reusability.[90]

3.8 Flame spray pyrolysis method

Kotsikau et al. reported that a single-phase $Zn_{0.5}Mn_{0.5}Fe_2O_4$ ferrite was fabricated via spray pyrolysis from a water solution containing iron and manganese nitrates.[91] Hong, Dachao, and his team utilized Pluronic F127 as a structure-directing agent to fabricate submicron-sized mesoporous spheres of $NiFe_2O_4$ using an aerosol spray pyrolysis technique. The researchers then tested these spheres for photocatalytic activity in an aqueous methanol solution by irradiating them with visible light (>420 nm) to produce hydrogen (H_2). The high surface area and crystallinity of the $Ni6Fe_2O_4$ led to a significant photocatalytic activity, resulting in the evolution of H_2 from water with methanol.[92] Chavan et al. successfully produced $Li_{0.5-x/2}Mg_xFe_{2.5-x/2}O_4$ ($0.0 \leq x \leq 1.0$) thin films using the spray pyrolysis process to

create nanocrystalline films.[93] Unique chainlike MFe_2O_4 nano aggregates have been made by quickly pyrolyzing nitrates/ethanol as a precursor in a flame

application.[94] Using the spray pyrolysis process, $Ni_{1-x}Cu_xFe_2O_4$ thin films with a wide range of compositions (0.0 x 1.0 in steps of 0.2) were created in the current work by Chavan, Apparao R., et al.[95] Mesoporous carbon spheres filled with $NiFe_2O_4$ NPs were created by Zheng, Jingwu, et al.in a single step using ultrasonic spray pyrolysis.[96] Aerosol spray pyrolysis (ASP) was utilized to create oxygen-deficient doped ferrite structures that would be utilized by Lorentzou, S et al. as redox materials in a two-step thermochemical water-splitting cycle to produce solar hydrogen from water.[97] Ozdemir et al. used flame spray pyrolysis (FSP) to create $MnFe_2O_4$ NPs.[98]

3.9 Electrospinning

By using the electrospinning (ES) technique, $MgFe_2O_4$ nanostructures were successfully created by Maensiri S et al.[99] Kaur, et al. described the electrospinning process shown in Figure 3. It is used to create a new nanofiber membrane comprising $CoNiFe_2O_4$-Polyvinylidene Fluoride (PVDF). The sol-gel combustion process was used to create the $CoNiFe_2O_4$ NPs.[100] El-Rafei et al. successfully created $CaFe_2O_4$ nanofibers using the ES technique which are three-dimensional random calcium ferrites. These NFs are suggested for photocatalysis applications in water purification since they generate active hydroxyl radicals under simulated solar light irradiation.[101] The preliminary findings of the polyvinyl alcohol (PVA) nanofiber study were used by Na, Kyeong-Han, et al. in this work to optimize the ES conditions for the synthesis of ferrite (α-Fe_2O_3) nanofiber.[102] The optical, electrical, and dielectric characteristics of electrospun $Ni_{0.5}Co_{(0.5-x)}Cd_xNd_{0.02}Fe_{178}O_4$ (x = 0.25) nanofibers were investigated in a work by Alahmari, F., et al.[103] In this study, an ES process was used by Dorneanu, et al. to successfully generate pure PVDF and PVDF/$CoFe_2O_4$ magnetic fibre composites for oil spill sorption applications.[104] Nilmoung, S., et al. described the production of carbon/cobalt ferrite (C/$CoFe_2O_4$) composite nanofibers and their spray process by Li, Yunfeng, et al. Flame spray pyrolysis is a reliable method for creating binary or complex oxides with the potential for industrial

characteristics after being carbonized in an environment of mixed air and argon.[105] Sertkol et al. created different $Co_{0.5}Ni_{0.5}Bi_xFe_{2-x}O_4$ spinel ferrite nanofibers (CoNiBi SFNFs) using the ES method in their study.[106] Jun et al. utilized sol-gel-assisted ES to produce composite fibres comprising Ni-Zn ferrite and polyvinylpyrrolidone (PVP). Upon calcination of the composite fibres at high temperatures, cubic spinel-structured $Ni_{0.5}Zn_{0.5}Fe_2O_4$ nanofibers were obtained.[107] The ES has been successfully used by Li et al.to create $NiFe_{2x}Ce_xO_4$ (x = 0-0.03) nanoribbons, which were then calcined in oxygen at 500°C.[108]

3.10 Laser ablation method

Almessiere et al. used both sol-gel and green pulsed laser ablation in liquid (PLAL) methods to produce samples of $ZnFe_2O_4$ (ZFO) spinel ferrite NPs (SFNPs), $Co_{0.5}Ni_{0.5}Ga_{0.01}Gd_{0.01}Fe_{1.98}O_4$ (CNGaGdFO) SNPs, and NCs of $(CNGaGdFO)_x/(ZnFe_2O_4)_y$.[109] The application of a pulsed laser beam was used by Almessiere, et al. to synthesize the NCs of $CoTm_{0.01}Tb_{0.01}Fe_{1.98}O_4$ (soft) and $SrGd_{0.03}Fe_{11.97}O_{19}$ (hard) in various ratios using the green PLAL method.[110] By using the alternating target laser ablation deposition technique, epitaxial $CuFe_2O_4$ thin films were formed by Yang, Aria, et al. on MgO substrates.[111] The magnetic $Co_{0.5}Ni_{0.5}Fe_2O_4$ (CNFO) with varying (x%) Se (x = 0.00-0.20) were made by Sadiq Mohamed, et al. using a sophisticated green laser ablation technique in conjunction with the sol-gel combustion pathway.[112] Özçelik et al. investigate structural, magnetic, photocatalytic properties & blood compatibility of $MnFe_2O_4$ NPs produced by sub-nanosecond laser ablation in water.[113] MgO substrates and a variety of $CoFe_2O_4$ thin film samples were created by Yang, Aria, et al. for alternating target laser ablation deposition and traditional pulsed laser deposition methods.[114] By applying the laser-ablation approach, Mn-Zn ferrite films with a coercive force of roughly 4 kA/m were produced by Nakano, et al. in a low-temperature process.[115]

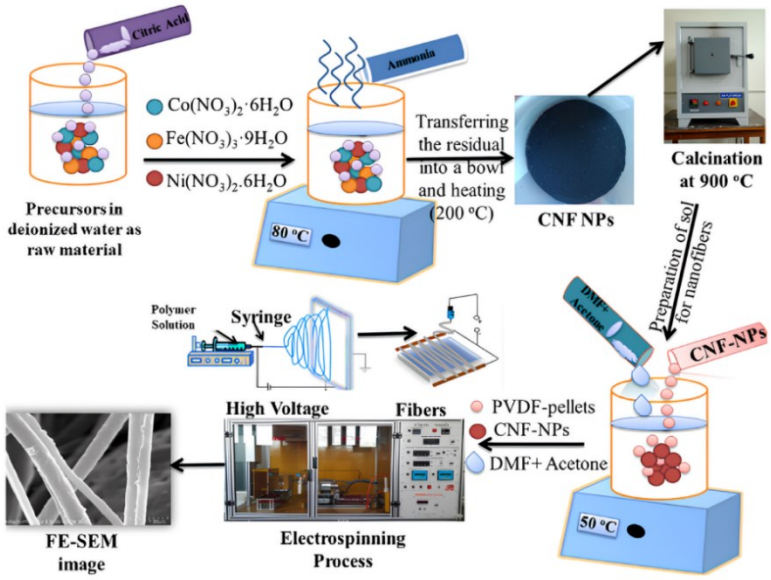

Figure 3. The schematic diagram of $Co_{0.5}Ni_{0.5}Fe_2O_4$-PVDF nanofiber membrane preparation. (Reprinted with permission from Mamta et al. (2020). Copyright 2020 Elsevier).

Table 1. Wastewater contaminants removal using different spinel ferrite materials by various synthesis techniques.

S. No	*Material*	*Synthesis method*	*Contaminant*	*Ref*
1	$NiFe_2O_4$/MWCNTs hybrid	Hydrothermal method	CR dye	[24]
2	MFe_2O_4	Solvothermal method	RhB and MB dye	[25]
3	CdS-MFe_2O_4	Hydrothermal synthesis	RhB dye	[27]
4	$ZnFe_2O_4$/$BiVO_4$ composite	Coprecipitation approach	RhB dye	[30]
5	$ZnFe_2O_4$-C_3N_4 hybrid	Reflux process	Orange II	[31]
6	$ZnFe_2O_4$-Ag/rGO	Hydrothermal approach	17-ethinylestradiol (EE2)	[32]
7	RGO/$ZnFe_2O_4$/Ag_3PO_4	Solvothermal synthesis	2,4-dichlorophenol (2,4-DCP)	[33]
8	$ZnFe_2O_4$@ZnO	Microwave synthesis and hydrothermal method	MO dye	[35]
9	N-doped TiO_2/$ZnFe_2O_4$ catalysts	One-pot vapour-thermal coupling	RhB dye	[36]
10	Ag/ZnO/$ZnFe_2O_4$ ternary composites	Calcination	MB dye	[37]
11	$NiFe_2O_4$/Bi_2O_3	Hydrothermal approach	TC antibiotic drug	[38]
12	$NiFe_2O_4$-graphene photocatalyst	Simple method	MB dye	[39]
13	$MgFe_2O_4$	Sol-gel method	MB dye	[40]
14	$CuFe_2O_4$ NPs	Sol-gel method	Sulfanilamide	[41]
15	$MnFe_2O_4$	Auto combustion approach	MB dye	[42]
16	$MnFe_2O_4$	Sol-gel method	MO dye	[44]
17	Inverse spinel cobalt ferrite $CoFe_2O_4$	Co-precipitation method	MB dye	[50]
18	$Mg_{1-x}Ni_xFe_2O_4$	Co-precipitation method	MB dye	[54]
19	MFe_2O_4	Co-precipitat	MB dye	[51]

		ion method		
20	Cobalt-substituted magnesium-zinc ferrites	Co-precipitation method	Benzimidazole and MB dye	[55]
21	Meso-$ZnFe_2O_4$	Hydrothermal method	Acid Orange II (AOII)	[56]
22	$CuFe_2O_4$ nanospheres (CFNS)	Hydrothermal method	Phenol	[58]
23	Spinel $NiFe_2O_4$	Template method	Acid orange 7 (AO7)	[69]
24	$MgFe_2O_4$ nanorod catalyst	Template method	CR dye	[70]
25	La^{3+} doped $ZnFe_2O_4$ clusters	Template method	MO dye	[74]
26	$NiFe_2O_4$ NPs	Sonochemical method	Paracetamol	[80]
27	$ZnFe_2O_4$	Electrochemical method	MB dye	[90]

4. Classification of spinel ferrites based on the number of metals present:

4.1 Mono metal spinel ferrites:

Due to their unique properties, spinel ferrite NPs (SFNPs) are highly suitable for various applications, including use as photocatalysts, biosensors, and wastewater treatment. The crystallite sizes of the produced samples, excluding $ZnFe_2O_4$, range from 33 to 36 nm. Among these, $CoFe_2O_4$ exhibits the highest saturation magnetization at approximately 60 emu/g. Further research involving various doses, cell lines, and organisms is essential to fully understand the effects and potential applications of SNPs in industrial, environmental, and medical fields. This will also aid in evaluating their overall environmental impact.[116] Recent studies highlight a growing interest in porous magnetic materials for water pollutant detoxification. These materials are effective due to their enhanced efficiency and ease of separation post-treatment. Reddy et al. developed a three-dimensional porous $NiFe_2O_4$ adsorbent (PNA) with notable magnetic properties, used to detoxify an aqueous Pb (II) solution. The PNA was synthesized using chitosan as a precursor through a sol-gel process. The PNA's surface appearance as seen in SEM scans revealed its three-dimensional porous structure, with many interconnected pores. The $NiFe_2O_4$ adsorbent with a 3D porous structure shows remarkable adsorption characteristics for the elimination of Pb (II) from water-based solutions. It takes less than 60 minutes to achieve equilibrium due to the rapid adsorption rate. Lastly, it was shown that the adsorbent PNA has exceptional capability for handling wastewater containing Pb (II).[117] Sharma et al. synthesized spinel ferrites with the formula MFe_2O_4 (where M represents Ni, Cu, Zn, and Co) to explore their effectiveness in degrading the reactive azo dye RB5, a model pollutant, through Fenton and photo-Fenton systems. $CuFe_2O_4$ demonstrated high efficiency due to the involvement of Cu^{2+} ions in Fenton's reaction, leading to the production of more hydroxyl radicals. All the catalysts remained stable, magnetically separable, and recyclable even after four cycles, making them promising materials for wastewater treatment in the textile industry.[118] In the current study, $SnFe_2O_4$ NPs have been created and studied by Singh, Sunanda, et al. by utilizing three distinct capping agents, including starch, PVP, and PEG (polyethylene glycol). The arsenic removal process involved two key components: $SnFe_2O_4$ NPs, synthesized through chemical precipitation, and a carbon foam, made by carbonizing polyurethane foam and then treating it with a phenol-formaldehyde solution. The NPs were incorporated into the carbon foam before it was used to treat As contaminated water.[119] This study presents the synthesis of magnetic mesoporous spinel $NiFe_2O_4$, which possesses a high surface area of up to 301.6 m^2/g and a well-defined distribution of pore sizes ranging from 2.5 to 16.2 nm. The synthesis was achieved by the simple oxalate decomposition process using a one-phase, multi-component precursor. This method effectively generates the material without the use of any templates to create pores. This mesoporous material has shown great potential in adsorbing acid orange 7 (AO7) and might be utilized as a magnetically distinguishable adsorbent for wastewater treatment that contains AO7. In their study, Gao et al. successfully manufactured mesoporous $NiFe_2O_4$, which exhibits excellent adsorption properties and can be conveniently recycled without any loss in its effectiveness. In addition, the adsorbed AO7 on the adsorbent can be quickly eliminated through heat breakdown.[69] Sujata, et al. created $ZnFe_2O_4$ MNPs and used them against gram-positive and gram-negative bacterial strains, it had a respectable antibacterial efficacy. The findings show that these magnetic ferrites, in their pristine and calcined forms, made by a soft chemical route and synthesized in ambient conditions, can be used successfully as a magnetically recyclable material to

remove biological and chemical contaminants from water and waste.[120]

In a study by Vinosha et al., $CoFe_2O_4$ NPs were synthesized using a co-precipitation method, with the pH during the process adjusted between 9 and 12. The resulting nanocatalyst was then employed to degrade MB dye, a common organic pollutant in textile wastewater. Notably, the research suggests that the catalyst exhibits good reusability, making it a promising option for industrial wastewater treatment applications.[50] The hydrothermal (ZFO-H) and citrate sol-gel (ZFO-C) methods were used by Zhang et al. to produce the $ZnFe_2O_4$ catalysts. Their findings revealed that the ZFO-H catalyst significantly enhanced phenol oxidation compared to uncatalyzed ozonation, with a roughly 1.5-fold increase in reaction rate. This superior performance of ZFO-H was attributed to its larger contact surface area and higher density of surface hydroxyl groups, facilitating more effective phenol degradation compared to ZFO-C. Additionally, ZFO-H's ability to decompose ozone and generate hydroxyl radicals (•OH) further supports its increased catalytic activity.[121] $ZnSFe_2O_4$ NPs were made by Patil, S. B., et al. using a combustion process with sugar cane juice as the fuel to create their spinel-like cubic shape. The degradation of combined organic dyes (MB and RB) carried out the photocatalytic activity. In the presence of a mixture of organic dyes, it exhibits excellent photocatalytic activity comparable to the destruction of individual dyes. In the field of industrial wastewater effluent treatment for environmental protection, it can be anticipated that $ZnSFe_2O_4$ is a viable photocatalyst. Additionally, $ZnSFe_2O_4$ NPs were chosen for their antibacterial efficacy against strains of gram-negative bacteria. Different microorganisms, including Escherichia coli, Bacillus subtilis, Pseudomonas aeruginosa, and Staphylococcus aureus were used to test the $ZnSFe_2O_4$ NP's antibacterial activity.[122]

Jadhav et al. used urea and glycine as a combination fuel and the sol-gel auto-combustion method to produce $NiFe_2O_4$ NPs. Based on the degradation of the model component, the dye MB, the photocatalytic activity of the NPs was investigated. The obtained NPs showed high photocatalytic activity against MB dye degradation, according to the results.[123] Gerbaldo and colleagues investigated a heterogeneous Photo-Fenton approach using $CoFe_2O_4$, H_2O_2, and UV light (254 nm) to remove sodium diclofenac, a common non-steroidal anti-inflammatory drug. $CoFe_2O_4$ were synthesized via the Pechini process and then calcined at temperatures between 600^0 to 800^0 C. The resulting inverse spinel structure exhibited good performance in the photo-Fenton reaction. The degradation process is suggested to involve the formation of •OH radicals. Using $CoFe_2O_4$ calcined at 800°C, 86% TOC mineralization and complete degradation of sodium diclofenac were achieved. The catalyst showed minimal activity loss and low Fe leaching after three cycles.[124] Udhaya et al. implemented an eco-friendly approach to synthesize $CuFe_2O_4$ NPs using egg white as a precursor. Notably, egg white albumin, a component of egg white, is a potential biofuel. The resulting $CuFe_2O_4$ NPs exhibit promising photocatalytic properties, as evidenced by their energy band structure. Significantly, these NPs outperform chemically synthesized $CuFe_2O_4$ NPs in degrading RhB dye under visible light, achieving an impressive degradation efficiency of 94%.[125] To degrade the antibiotics TC and MNZ in the "$MgFe_2O_4/H_2C_2O_4$/vis" system Qiu, et al. have identified an effective Fenton-like catalyst. This catalyst consists of metal-doped $MgFe_2O_4$ derived from saprolite laterite nickel ore. The formation of $[Fe(C_2O_4)_3]^{3-}$ complex ions due to the reaction of octahedral Fe^{3+} with oxalate ions on the surface of $MgFe_2O_4$ leads to the creation of •OH radicals and ultimately enhances the catalyst's degrading activity, as per the TC degradation mechanism. The fresh catalyst's degrading performance can be maintained at over 90% even after five cycles, demonstrating its great cycling stability and applicability.[126]

The MFe_2O_4 nano ferrites (M = Co, Ni, and Zn) were created by Dehghani et al. The ability of spinel-type NPs to adsorb Bromo Phenol Red (BPR) dye from aqueous solutions. The outcomes demonstrated that $NiFe_2O_4$ had the greatest BPR adsorption capacity. Both the Freundlich isotherm equation and the Langmuir equation were employed to analyze adsorption behaviour. The $NiFe_2O_4$ nano spinel is a highly promising candidate for the adsorption of triphenylmethane dyes derived from wastewater.[127] Mohammed A. et al. determined whether $CoFe_2O_4$ NPs were suitable for removing chromium and other pollutants from tannery wastewater. By annealing the $CoFe_2O_4$ NPs at 300, 500, and 900 °C, the co-precipitation approach was successful in producing the desired results. The wastewater from the tannery was treated using $CoFe_2O_4$ NPs. TDS, BOD, COD, and chromium removal were each removed with 90.83, 52.72, 48.07, and 23.75% efficiency, respectively.[128] De la Torre and colleagues used nitrate salts of cobalt, copper, and iron as precursors to synthesize cobalt and copper ferrites via the precipitation method. The molar ratio of Co:Fe or Cu:Fe was maintained at 1:2, with NaOH serving as the precipitant. After 8 hours of agitation, the

$CoFe_2O_4$ soaked on activated carbon achieved 98% cyanide oxidation and could be recycled five times with an 18% reduction in catalytic activity. Iron dissolved more readily in $CoFe_2O_4$ compared to cobalt, while the dissolution rate of copper was higher in $CuFe_2O_4$. These results suggest that ferrite and activated carbon composites are promising alternatives for cyanide treatment in mining effluents.[129] Frolova et al. used the co-precipitation approach and low-temperature contact

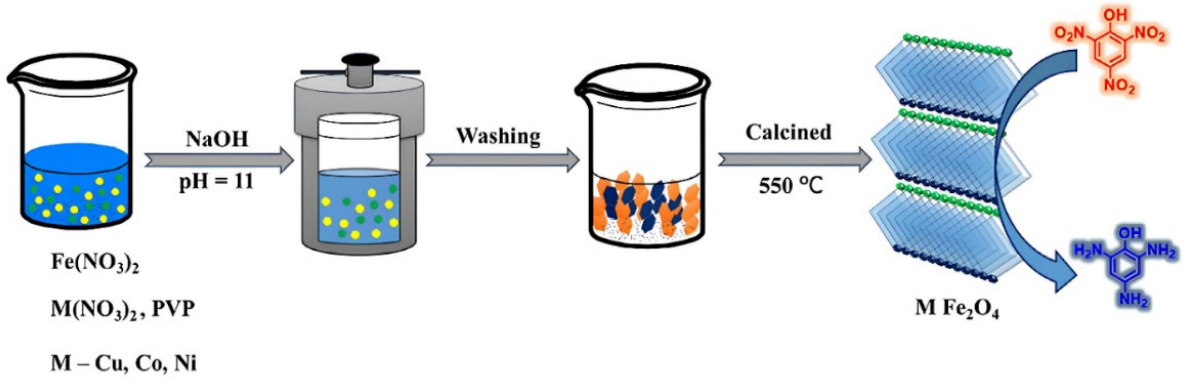

Figure 4. Graphical representation of MFO NPs preparation and nitro compound removal (NP, DNP, TNP) using MFO NPs. (Reprinted with permission from Dongjin et al. (2021). Copyright 2021 Elsevier).

nonequilibrium plasma treatment to synthesize nanocrystalline powder of $Co_xFe_{3x}O_4$ spinel ferrite. The objective of the research was to investigate the impact of cobalt ferrite composition on the rate of the photocatalytic breakdown reaction of 4-nitrophenol (4-NP) under UV light. The findings indicate that the photocatalytic activity in the breakdown process of 4-NP diminishes with increasing.[130] Tatarchuk et al. to make $CoFe_2O_4$ Fenton catalysts. Crystallites in the samples that were annealed at 400 and 600°C measured 16 and 18 nm, respectively. The catalyst for the oxidation of caffeine and the breakdown of H_2O_2 that demonstrated the greatest improvement in catalytic activity was $CoFe_2O_4$ which had been annealed at 400°C. The rate of caffeine breakdown increased by 85% as a result of electromagnetic heating, which more than doubled the catalytic reaction rate. $CoFe_2O_4$ heated by an electromagnetic field can act as a controlled catalyst in the water purification process.[131]

Wang and colleagues synthesized $MnFe_2O_4$ nanospheres using a solvothermal process, with oleic acid employed for hydrophobic modification. The resulting $MnFe_2O_4$ nanospheres exhibited superparamagnetic properties, high saturation magnetization, a rough surface, and a well-defined mesostructure. These unique features make the $MnFe_2O_4$ nanospheres suitable for integration into magnetorheological (MR) fluids and efficient oil removal.[132] Using magnetic $CuFe_2O_4$, $CoFe_2O_4$, and $NiFe_2O_4$ material systems, the harmful nitro compounds (4-NP, 2,4-dinitrophenol, and 2,4,6-trinitrophenol) were eliminated by Ramu, A. G., et al. The hydrothermal approach was used to create the metal ferrites, and the calcination procedure is shown in Figure 4. The obtained results support the idea that a material system based on $CuFe_2O_4$ NPs can be one of the potential catalysts for the process of removing nitro compounds.[133]

Table 2. Mono metal spinel ferrites synthesis techniques and effective removal of toxic contaminants from wastewater.

S. No	*Material*	*Synthesis method*	*Contaminant*	*Ref*
1	Porous $NiFe_2O_4$ adsorbent (PNA)	Sol-gel procedure	Detoxify aqueous Pb (II) solution	[117]
2	MFe_2O_4 (M = Co, Ni, Cu, and Zn)	Sol-gel technique	Azo dye RB5	[118]
3	$SnFe_2O_4$ NPs	Chemical precipitation procedure	As from water	[119]
4	Mesoporous spinel $NiFe_2O_4$	Simple oxalate decomposition process	Acid orange 7 (AO7)	[69]

5	$ZnFe_2O_4$ NPs	Soft chemical methods	Biological and chemical contaminants from water	[120]
6	Inverse spinel $CoFe_2O_4$ NPs	Co-precipitation method	MB dye	[50]
7	$ZnFe_2O_4$ catalysts	Hydrothermal (ZFO-H) and citrate sol-gel (ZFO-C) methods	Phenol	[121]
8	$ZnFe_2O_4$ NPs	Combustion process	MB and RB dye	[122]
9	$NiFe_2O_4$ NPs	Sol-gel auto-combustion technique	MB dye	[123]
10	$CoFe_2O_4$	Heterogeneous Photo-Fenton method	Diclofenac sodium	[124]
11	$CuFe_2O_4$ NPs	Combustion process	RhB dye	[125]
12	$MgFe_2O_4/H_2C_2O_4$	Fenton's method	Antibiotics TC and MNZ	[126]
13	MFe_2O_4 nano ferrites (M = Co, Ni, and Zn)	Coprecipitation method	BPR dye	[127]
14	Cobalt and Copper ferrites	Precipitation method	Cyanide oxidation	[129]
15.	$Co_xFe_{3x}O_4$	Co-precipitation technique	4-Nitrophenol	[130]
16	Cobalt ferrite Fenton catalysts	Co-precipitation approach	Caffeine oxidation and H_2O_2 breakdown	[131]
17	$CuFe_2O_4$, $CoFe_2O_4$, and $NiFe_2O_4$	Hydrothermal approach	P-nitrophenol, Dinitrophenol, and picric acid	[133]

4.2 Bi-metal spinel ferrites:

Dojcinovic, et al. used a combustion process to create $Co_xMg_{1-x}Fe_2O_4$ spinel ferrites using citric acid as fuel. Different values of x (0.0, 0.1, 0.3, 0.5, 0.7, 0.9, and 1) were used, and the amorphous particles were calcined for three hours at 700°C The presence of an excessive amount of cobalt resulted in a decrease in the photocatalytic activity, both under visible light and natural light conditions. Interestingly, $Co_{0.9}Mg_{0.1}Fe_2O_4$ had a very high activity level of 74.5% throughout 4 hours. $MgFe_2O_4$ had the most significant photocatalytic efficiency when exposed to natural sunlight, achieving an 82% degradation rate after 4 hours. In contrast, $Co_{0.1}Mg_{0.9}Fe_2O_4$ demonstrated the greatest photocatalytic activity when subjected to visible light, achieving a degradation rate of 79% after 4 hours.[134] In a study by Mondal et al., a chemical co-precipitation process was used to synthesize $Zn_{0.3}Ni_{0.7}Fe_2O_4$ (ZNFO) NPs samples with varying particle sizes. X-ray diffraction analysis confirmed the crystalline phase purity and spinel cubic structure formation in all samples. Testing the photocatalytic activity of each nanocatalyst with MB dye revealed that the smallest ZNFO NPs demonstrated the highest efficiency in degrading the dye under light irradiation. Additionally, ZNFO displayed the strongest ability to eliminate free radicals compared to other samples. These results suggest that tailoring the physical properties of Ni-Zn spinel ferrites, particularly by reducing their size, can enhance their functionality. This makes them promising candidates for applications in photocatalysis and as antioxidants.[135] Shukrullah, Shazia, and other researchers created Ni-$ZnFe_2O_4$ NPs by the co-precipitation technique to eliminate chromium metal from industrial wastewater. The synthesized NZF NPs hold great promise for wastewater treatment. Their effectiveness stems from a combination of factors: an extensive surface area, precisely controlled size, and a well-organized internal structure. In the experiment, the industrial wastewater was mixed with the described NPs

continuously for 20 mins, and the photocatalytic behavior of NZF NPs was investigated using UV-vis spectrophotometry on the suspension of the NPs. The study found that Zn doping in NZF plays a crucial role in enhancing the efficiency of Cr removal from wastewater, particularly under visible light irradiation.[136] Jesudoss, S. K., et al. successfully created Spinel magnetic ferrite $Mn_{1-x}Ni_xFe_2O_4$ NPs using a microwave combustion method. They found that $Mn_{0.5}Ni_{0.5}Fe_2O_4$ NPs had the best photocatalytic activity in breaking down synthetic indigo carmine dye. The researchers also observed that the NPs had antibacterial effects comparable to that of the antibiotic streptomycin. These results suggest that these NPs could be a promising low-cost photocatalyst for wastewater treatment and environmental remediation.[137] Deepika, et al. used the citrate precursor approach to create cobalt-zinc ferrite with the chemical formula $Co_xZn_{1-x}Fe_2O_4$. It was shown that a rise in cobalt concentration accelerated the breakdown of MB. Under visible light irradiation, the degradation efficiency increased to a maximum of 77% and a minimum of 65% in 1 hour. As a result, they conclude that cobalt-zinc ferrite is a viable material for water filtration and that its degradation efficiency increases with increased cobalt concentration.[138] Researchers investigated spinel NPs ($Mg_{1-x}Ni_xFe_2O_4$) synthesized using a chemical co-precipitation method. The study explored their structural, magnetic, optical, and photocatalytic properties. Notably, the materials exhibited light absorption in the visible region, indicating their potential for photocatalytic applications. Furthermore, increasing the nickel content narrowed the band gap energy, enhancing their photocatalytic activity for degrading MB dye. These findings suggest these NPs hold promise for wastewater treatment. [54]

Table 3. Hazardous contaminant removal from wastewater using different bimetal spinel ferrites prepared by different synthesizing methodologies.

S. No	*Material*	*Synthesis method*	*Contaminant*	*Ref*
1	$Co_xMg_{1-x}Fe_2O_4$	Sol-gel combustion process	MB dye	[134]
2	$Zn_{0.3}Ni_{0.7}Fe_2O_4$	Chemical co-precipitation technique	MB dye	[135]
3	Ni-$ZnFe_2O_4$ NPs	Co-precipitation method	Chromium metal	[136]
4	$Mn_{1-x}Ni_xFe_2O_4$	Microwave combustion method	Indigo carmine (IC) dye	[137]
5	$Co_xZn_{1-x}Fe_2O_4$	Citrate precursor approach	MB dye	[138]
6	$Mg_{1-x}Ni_xFe_2O_4$	Chemical co-precipitation method	MB dye	[54]
7	$Cu_{0.5}Mg_{0.5}Fe_2O_4$-TiO_2	Coprecipitation and sol-gel techniques	RhB dye	[139]
8	Cobalt-substituted magnesium-zinc ferrites	Co-precipitation method	Benzimidazole and MB dye	[55]
9	Magnetically recoverable ferrite catalysts	Reverse microemulsion, sol-gel, and combustion	CPX and CBZ	[140]
10	$Zn_{1-x}Ni_xFe_2O_4$	Solvothermal reflux method	MB dye	[141]
11	$Al_xZnFe_{2-x}O_4$	Co-precipitation method	MB dye	[142]
12	$Mn_{0.5}Zn_{0.5}Fe_2O_4$	Hydrothermal technique	MB dye	[143]
13	Cu-$MgFe_2O_4$	Chemical co-precipitation technique	MB dye	[144]
14	$MRu_xFe_{2x}O_4$	Sol-gel method	Antibiotic CPX and the Remazol deep red dye	[145]
15	$MnNiFe_2O_4$	Co-precipitation process	Adsorbs Cr from wastewater	[146]
16	Ag/CFO NPs, Ag NPs	Hydrothermal synthesis	MO, MB and RhB dyes adsorpti	[147]

		on, 4-NP reductio n		
17	$Co_{1x}Sr_xFe_2O_4$	Sol-gel combustio n method	MB dye	[148]

A study investigated the use of coprecipitation and sol-gel techniques to synthesize a novel hybrid material, $Cu_{0.5}Mg_{0.5}Fe_2O_4$-TiO_2. This material was designed to target the breakdown of organic dyes present in wastewater. The experiment achieved a successful synthesis of the composite material, with the TiO_2 and $Cu_{0.5}Mg_{0.5}Fe_2O_4$-TiO_2 components averaging around 40.1 nm and 27.9 nm in size, respectively. Importantly, the $Cu_{0.5}Mg_{0.5}Fe_2O_4$-TiO_2hybrid exhibited superior photocatalytic activity in degrading RhB dye compared to its counterparts, $Cu_{0.5}Mg_{0.5}Fe_2O_4$ and TiO_2. This finding suggests promising potential for this material in wastewater treatment applications.[139]

A study investigated the photocatalytic activity of cobalt-substituted magnesium-zinc ferrites synthesized using a coprecipitation method. The research aimed to assess their ability to degrade coloured and colourless pollutants, including harmful substances like benzimidazole and MB dye, under sunlight irradiation. The results revealed a significant improvement in photocatalytic activity with increasing cobalt content. Notably, MZF3, with the highest cobalt level, demonstrated the most effective MB degradation. These findings suggest that $Mg_{0.5}Zn_{0.5}Co_xFe_2O_4$ holds promise as a potential catalyst for wastewater treatment applications.[55] Researchers investigated using Fenton chemistry to treat wastewater containing pollutants that resist biodegradation. Their approach involved developing environmentally friendly recoverable ferrites as catalysts. These catalysts were then used in a solar photo-Fenton process under slightly acidic conditions to break down ciprofloxacin (CPX) and carbamazepine (CBZ). The study successfully degraded both pollutants, identifying the degradation pathways. For CPX, the breakdown targeted specific molecular structures within the molecule. CBZ degradation involved the formation of intermediate compounds, which were further transformed through a series of reactions.[140] A study successfully synthesized high-quality ZNF NPs with a narrow size distribution and small diameter. These NPs exhibited significantly improved magnetic properties, making them suitable for applications in photocatalysis and localized magnetic hyperthermia treatments. This enhancement was attributed to the specific positioning of nickel ions within the NP structure. The researchers further evaluated the photocatalytic activity of each NP by measuring its effectiveness in degrading MB dye under visible light irradiation. The results revealed a clear correlation between the concentration of nickel ions and the degradation efficiency, with higher nickel content leading to faster dye degradation. The study demonstrates that incorporating nickel into these spinel ferrites significantly increases their catalytic activity under visible light.[141] Gul, et al. used a quick and inexpensive chemical process called co-precipitation to create $Al_xZnFe_{2-x}O_4$ NPs. The material was found to have significant resistance values after an electrical investigation. The synthetic NPs' optical characteristics demonstrated that they were suitable for photocatalysis and could break down the organic chemicals in the water.[142] Zhang, B. B. et al. used a hydrothermal technique to attach $Mn_{0.5}Zn_{0.5}Fe_2O_4$ (MZFO) into AC, producing AC NCs with outstanding magnetic response for wastewater treatment. [143]

George, et al. prepared Cu-$MgFe_2O_4$ (CMFO) NPs using a simple chemical co-precipitation technique, as these NPs can act as effective photocatalysts to remove dye contaminants from wastewater. The antibacterial activity of CMFO NPs was investigated using the agar well diffusion method. Among the samples tested against the Gram-negative and Gram-positive bacteria Escherichia coli and Micrococcus luteus, CMFO-2 and CMFO-3 NPs demonstrated the most excellent antibacterial activity, while CMFO-1 NPs showed minimal activity. To test the effectiveness of spinel CMFO NPs at removing dye, organic MB was used in a photo-Fenton operation.[144] Singh et al. conducted a comprehensive study on the effects of adding Ru to sol-gel-prepared $MRu_xFe_{2x}O_4$ (MRFO) (M = Ni, Cu: x = 0.0, 0.02, 0.06, 0.1, and 0.4) spinel nanoferrites. The study assessed the photocatalytic activity of MRFO NPs for the degradation of the antibiotic CPX and the Remazol deep red dye. The results showed that Ru-doped nanoferrites were highly effective in degrading both substances. $CuRu_{0.1}Fe_{1.9}O_4$ degraded the drug in 90 mins, while $NiRu_{0.4}Fe_{1.6}O_4$ degraded the dye in just 5 mins. The high degrading efficiency of Ru-doped nanoferrites demonstrates their potential in photocatalysis applications.[145] Chromium absorption from textile effluent was studied by Jemal Fito et al. using Mn-Ni ferrite NC. The NC showed promising results in eliminating chromium from industrial wastewater, and its adsorption mechanism was found to be chemical sorption and monolayer.[146]
Hoa et al. used Hydrothermal synthesis to create $CoFe_2O_4$ NPs. They then added Ag NPs to the $CoFe_2O_4$ NPs with jasmine extract serving as the reducing agent for Ag^+ ions to create Ag/$CoFe_2O_4$ NPs. The catalytic results demonstrated that Ag/ $CoFe_2O_4$ NPs could activate peroxymonosulfate

(PMS), producing sulfate radicals that can oxidize several dyes, including MB, MO, and RhB. The Ag NPs in the Ag/$CoFe_2O_4$ sample were validated to have functions in dye adsorption, 4-nitrophenol reduction, and enhanced antibacterial behaviour. Ag/$CoFe_2O_4$ NPs were found to have growth suppression activity against P. aeruginosa and S. aureus. After three consecutive runs, Ag/$CoFe_2O_4$ NPs also showed good reusability. These results suggest that Ag/$CoFe_2O_4$ material is a viable multifunctional catalyst for the treatment of wastewater.[147] $Co_{1x}Sr_xFe_2O_4$ NPs synthesized by M.K. Shobana et al. through sol-gel combustion, with Sr^{2+} ions affecting structural variations. The NPs have a crystalline size of 34.07-36.32 nm, a pure phase, and decreased magnetic values with increased temperature fluctuation. The sample heated to 200°C had the highest Ms value. These $Co_{1x}Sr_xFe_2O_4$ NPs exhibited diminishing effectiveness in removing MB dye, with the sample subjected to a temperature of 500°C for 45 minutes showing the maximum efficacy at 72%.[148]

4.3 Tri-metal spinel ferrites:

Huixin et al. found a mesoporous magnet made of $NiFe_2O_4$ and ZnCuCr-LDH that was easily hydrothermally created from saccharin wastewater and its potential for use in wastewater treatment by practical adsorption. During the procedure, iron was completely recirculated and about 83% COD of the saccharin effluent was eliminated. It may be inferred that electrostatic attraction and anion exchange accounted for most of the adsorption mechanism. The porous magnet composite as-prepared exhibits excellent adsorption capability and a straightforward synthesis and separation method, indicating good potential to recirculate the waste metal for use in realistic wastewater treatment applications. [149] Scientists addressed two challenges in wastewater treatment with photocatalysis: reducing the catalyst's energy requirement and simplifying its removal after treatment. Their solution involved designing magnetic NCs that can be easily separated. These catalysts were made by combining magnetic NPs ($Co_{0.5}Zn_{0.25}M_{0.25}Fe_2O_4$, where M varied by Mg, Mn, Cu and Ni) with a specific sugar molecule (carboxymethyl cellulose) and then co-precipitating them with a base. Next, the magnetic NPs were integrated with titanium dioxide using a template and a titanium source. A key feature of these NCs is that the magnetic NPs allow the titanium dioxide to be activated by visible light, enabling them to function under sunlight. [150] Jianping et al. explored a novel class of high-entropy (HE) spinel ferrites for wastewater treatment applications. Their research focused on $(Mg_{0.2}Co_{0.2}Ni_{0.2}Cu_{0.2}Zn_{0.2})Fe_2O_4$ a newly developed ferrite material synthesized using the solution combustion method followed by heat treatment (500-1500 °C). This study marks the first application of these HE spinel ferrites as catalysts in a heterogeneous peroxodisulfate reaction for wastewater treatment. The results revealed that the HE spinel ferrite/PDS system exhibited superior efficiency in removing organic pollutants, such as RhB and tetracycline (TC), compared to the baseline reaction conditions. The degradation process was found to be significantly influenced by both hydroxyl and sulfate radicals generated during the reaction. Notably, this catalyst demonstrated remarkable catalytic activity and excellent stability throughout the study, highlighting its potential as a promising candidate for real-world wastewater treatment applications.[151] Dongmei et al. investigated the potential of ceramic membranes (CMs) for removing heavy metal contaminants. Their study focused on creating a cost-effective and durable CM from readily available waste materials. This innovative approach involved sintering a matrix of iron-sulfur-rich gold tailings and silicon-rich marine mussel powder, combined with copper/cobalt-rich precursors. The resulting waste-to-resource conversion material, designated CM-(Cu-Co)Fe_2O_4, demonstrated exceptional efficiency in removing heavy metal iron ions from water, achieving a removal rate exceeding 94%. This remarkable performance is attributed to a combination of electrostatic attraction and adsorption mechanisms.

Dongmei et al.'s research highlights the feasibility of using common solid waste as a source material for the development of multifunctional ceramic membranes.[152] Researchers employed a solution-combustion technique to synthesize indium-doped cobalt-zinc spinel nano-ferrites ($Co_{0.9}Zn_{0.1}In_xFe_{2-x}O_4$). The study investigated the electrical properties of these materials, focusing on their dielectric constant and loss tangent. Interestingly, both parameters decreased with increasing frequency but increased with rising temperatures. Importantly, the research achieved low dielectric loss tangent values, making these nano-ferrites promising candidates for applications involving microwave frequencies.[153] A new approach to wastewater treatment utilizes biochar derived from banana peels. The biochar is first created using a molten salt technique. Then, a one-pot hydrothermal process incorporates Mn, Zn, and Fe trimetallic spinel onto the biochar, forming a composite named MZF-BC. This MZF-BC demonstrates exceptional tetracycline adsorption, reaching a maximum capacity of 142.4 mg/g.

Researchers believe pore filling, coordination with TC functional groups, and interactions within the biochar structure contribute to this high adsorption. Additionally, MZF-BC exhibits promising reusability, retaining over 70% of its adsorption capacity after five regeneration cycles.[154] In a study by Ahmed et al., flash auto combustion was employed to synthesize single-phase spinel nanoferrites containing rare earth elements (Sm, Pr, Ce, and La). These nanoferrites exhibited potential for colored wastewater treatment. Notably, lanthanum (La)-doped ferrites demonstrated the highest dye removal efficiency (92%), followed by praseodymium (Pr) at 85%. Conversely, ferrites doped with Sm) and Ce exhibited lower efficiencies (80% and 72%, respectively). Doping ferrites with La and Pr resulted in the formation of nanowires, leading to improved conductivity. This discovery represents a major leap forward in utilizing nanomaterials for wastewater treatment applications.[155] A study explored the potential of cadmium (Cd) and cobalt (Co) doped zinc ferrites for wastewater treatment applications. These catalysts were synthesized using a simple sol-gel method. Their photocatalytic activity was evaluated by measuring the degradation of MO dye in the presence of visible light. The research identified a specific composition ($Cd_{0.75}Zn_{0.25}Co_{0.25}Fe_{1.75}O_4$) that exhibited the highest degradation rate (82%) in 2 hours of visible light irradiation. This superior performance is likely due to the presence of favourable atomic arrangements within the material's structure and its ability to minimize the recombination of electrons and holes, which can hinder photocatalytic activity.[156] $Cd_{0.5}Cu_{0.5x}Ag_xFe_2O_4$ ferrites were studied by Ahmed H., et al. and made using a straightforward co-precipitation process. The standard organic impurity indigo carmine dye (IC), a byproduct of dyeing indigo, was oxidatively broken down using the samples as catalysts. In the pH range of 2–11, $Cd_{0.5}Cu_{0.5-x}Ag_xFe_2O_4$ showed good catalytic activity, making them promising, stable, and effective materials for Fenton-based alkaline wastewater treatment.[157] Researchers investigated a rapid and cost-effective method (sol-gel and self-combustion) to synthesize scandium (Sc)-doped nickel-cobalt ferrite NPs ($Ni_{0.5}Co_{0.5}Sc_xFe_{2x}O_4$). The resulting materials exhibited nanoscale crystallinity (ranging from 35 to 42 nm). The study explored the impact of Sc substitution on the catalytic activity of these ferrites. This was evaluated by analyzing the flameless combustion of acetone, propane, and benzene in the presence of the different samples. The findings revealed a clear benefit of replacing some iron (Fe^{3+}) ions with Sc^{3+} ions within the ferrite structure. Notably, the Sc-doped catalysts achieved conversion rates exceeding 90% for acetone or propane at a temperature of 400°C. This enhanced catalytic activity compared to pure Ni-Co ferrites is likely due to a combination of factors, including smaller crystallite size, larger specific surface area, and the incorporation of Sc cations within the material's structure.[158] Researchers investigated magnesium-zinc nanoferrites doped with cobalt for wastewater treatment. A simple combustion method produced $Mg_{0.5}Zn_{0.4}Co_{0.1}Fe_2O_4$, $Mg_{0.4}Zn_{0.5}Co_{0.1}Fe_2O_4$, and $Mg_{0.5}Zn_{0.5}Co_{0.1}Fe_{1.9}O_4$. The synthesized catalysts underwent structural, optical, and magnetic characterization. Notably, the Z5C1 catalyst achieved impressive photocatalytic activity under UV-visible light, degrading 97.76% of CV dye in 90 minutes. This efficiency is attributed to the Z5C1's low charge carrier recombination and suitable band gap. Scavenger studies suggest holes play a key role in breaking down CV dye. The Z5C1 catalyst's reusability and magnetic separation potential highlight its promise for degrading organic pollutants.[159]

Table 4. Tri-metal spinel ferrite materials are used to remove harmful substances from wastewater.

S. No	*Material*	*Synthesis method*	*Contaminant*	*Ref*
1	$NiFe_2O_4$ and ZnCuCr-LDH	Hydrothermal Method	Wastewater treatment	[149]
2	$Co_{0.5}Zn_{0.25}M_{0.25}Fe_2O_4$	Template Method	MO and MB dye	[150]
3	$(Mg_{0.2}Co_{0.2}Ni_{0.2}Cu_{0.2}Zn_{0.2})Fe_2O_4$	Combustion synthesis approach	RhB dye and TC antibiotic drug	[151]
4	$Co_{0.9}Zn_{0.1}In_xFe_{2-x}O_4$	Solution-combustion (SC) method	Microwave frequency applications	[153]

5	MZF-BC (Mn, Zn, and Fe trimetallic spinel on biochar)	One-pot hydrothermal synthesis	TC antibiotic drug	[154]
6	$Zn_{0.5}Co_{0.5}Al_{0.5}R_{0.04}Fe_{1.46}O_4$	Flash auto combustion	Dye removal	[155]
7	$Cd_xZn_{1-x}Co_{0.25}Fe_{1.75}O_4$	Sol-gel process	MO dye	[156]
8	$Cd_{0.5}Cu_{0.5x}Ag_xFe_2O_4$	Co-precipitation process	IC dye	[157]
9	$Ni_{0.5}Co_{0.5}Sc_xFe_{2x}O_4$	Sol-gel and self-combustion approach	Catalytic combustion of propane or acetone at moderate temperatures	[158]
10	$Mg_{0.5}Zn_{0.4}Co_{0.1}Fe_2O_4$	Combustion approach	CV dye	[159]

4.4 Rare earth doped metal ferrites:

Researchers used the citrate combustion method to create Co-Cu-Sm nano ferrites, effectively removing RhB dye from polluted water. The band gaps of these nanoferrites decrease when Sm^{3+} ions are added. The nano ferrite with x = 0.15 achieved a 94.36% degradation rate within 270 minutes, indicating their potential application in wastewater treatment.[160] Singh, Sneha, and colleagues have discovered that magnetically recoverable spinel nanoferrites doped with samarium (Sm) can effectively be photocatalysts for removing organic contaminants from wastewater. They produced a series of Sm-doped spinel nano ferrites, $MSm_xFe_{2ex}O_4$ (M= Ni, Co), using the sol-gel method and systematically studied the influence of Sm doping on the pure nanoferrites structural, morphological, optical, and magnetic properties. The synthesized materials were subsequently evaluated as photocatalysts to facilitate the oxidative decomposition of dyes (MO and safranin O) and antibiotics (ofloxacin and norfloxacin). The increased surface area of Sm-doped nanoferrites, Sm ions' affinity for the octahedral location, and their smaller band gap contributed to their remarkable catalytic efficacy. These nanoferrites are highly recyclable, making them ideal for wastewater treatment photocatalysts.[161] A study investigated the use of a non-toxic sol-gel process to create nickel-zinc ferrite nanostructures ($Ni_{0.6}Zn_{0.4}Fe_2O_4$ and $Ni_{0.6}Zn_{0.2}Ce_{0.2}Fe_2O_4$) with cubic shapes. These NPs exhibited remarkable effectiveness in eliminating harmful bacteria present in sewage samples. The results suggest that magnetic NPs (MNPs) hold promise as powerful tools for sewage treatment by eliminating harmful bacteria. Notably, the nickel-zinc-cerium ferrite demonstrated superior performance compared to the other two ferrite types in suppressing microbial growth.[162] Basfer, N.M et al. synthesized cobalt-magnesium ferrites doped with the rare earth element cerium (Ce) with the chemical formula $Co_{0.7}Mg_{0.3}Ce_xFe_{2-x}O_4$ (abbreviated as CMCF) by a combustion technique to generate a highly efficient nano-photocatalyst capable of removing harmful dyes. Although the CMCF nanoferrites used a bigger ion (Ce) instead of a smaller ion (Fe), the lattice parameter and crystallite size exhibited an unexpected pattern, reducing from 8.4077 to 8.3922 and 34.66 to 20.76 nm, respectively. The CMCF (x = 0.1) photocatalyst was used to induce four distinct stages in the MB degradation process. The CMCF NPs hold great potential as efficient photocatalysts for eliminating harmful MB in wastewater treatment processes.[163] Irfan, M. et al. produced a wide variety of $Co_{0.5}Cd_{0.5}Fe_{2-x}Ce_xO_4$ (CoCdCeFO) nanoferrites using the sol-gel method. The presence of Ce^{3+} in the Co-Cd photocatalyst did not have a substantial impact on its photocatalytic activity throughout the range of x = 0 to 0.04. However, the photocatalytic activity of Co-Cd exhibited a noticeable decrease as the Ce^{3+} concentration increased. Hence, the incorporation of a small quantity of Ce^{3+} in Co-Cd samples enhances the photocatalytic activity under visible light.[164]

Table 5. Exploring various synthesis methods for incorporating rare earth metals into spinel ferrites to effectively remove virulent chemicals from wastewater.

S. No	*Material*	*Synthesis method*	*Contaminant*	*Ref*
1	$Co_{0.5}Cu_{0.5}Sm_xFe_{2x}O_4$	Citrate combustion method	RhB dye	[160]
2	$MSm_xFe_2exO_4$	Sol-gel process	MO, safranin O dyes and ofloxacin, norfloxacin antibiotics	[161]
3	$Ni_{0.6}Zn_{0.4}Fe_2O_4$	Non-toxic sol-gel method and citrate	Microbial growth inhibition	[162]
4	$Co_{0.7}Mg_{0.3}Ce_xFe_{2-x}O_4$	Combustion method	MB dye	[163]
5	$Co_{0.5}Cd_{0.5}Fe_{2-x}Ce_xO_4$	Sol-gel technique	photocatalytic activity	[164]
6	Dy^{3+} doped and undoped Zn-Mg nano photocatalysts	Sol-gel auto-combustion method	MG dye	[165]
7	Ce-doped copper ferrite	Hydrothermal production	RhB dye	[166]
8	Yttrium-doped cobalt ferrite ($CoFe_2O_4$)	Photo-Fenton reaction	H_2O_2 and PMS	[167]
9	Sm doped $ZnFe_2O_4$	Co-precipitation process	MB dye	[168]
10	Ce substituted Zn-Mn ferrite $Zn_{0.5}Mn_{0.5}Ce_xFe_{2-x}O_4$	Combustion approach	RhB dye	[169]
11	p-lanthanum ferrite and n-ceria (n-CeO_2@p-$LaFeO_3$/3DOM SiO_2)		Bisphenol A (BPA)	[170]
12	Magnesium ferrites doped with lanthanide ions.	Fenton process	MB dye	[171]
13	Ce doped $MnFe_2O_4$	Solution combustion technique	D-glucose and paracetamol	[172]

Researchers investigated a sol-gel auto-combustion technique to synthesize undoped and dysprosium (Dy^{3+})-doped zinc-magnesium (Zn-Mg) NCs. The effectiveness of these NCs for degrading a model organic dye (MG dye) under sunlight irradiation was evaluated. The study revealed that ZM3, a specific composition of the doped NCs, exhibited the highest degradation efficiency, reaching 94.23%. An additional advantage of these NCs is their ease of separation from the treated water using an external magnet due to their magnetic properties.[165] Keerthana, et al. prepared two photocatalysts for degrading dye components. Ce-doped $CuFe_2O_4$ and Sm-loaded $ZnFe_2O_4$ NPs prepared successfully. The created Ce-doped $CuFe_2O_4$ substance demonstrated photocatalytic activity and promoted RhB degradation. The outcomes showed that adding a catalyst significantly increased the effectiveness of RhB degradation. The dye solution with no $CuFe_2O_4$ added the dye solution with 1% Ce and 2% Ce doped $CuFe_2O_4$ added, and the dye solution with $CuFe_2O_4$ added were 48%, 50%, 66%, and 88%, respectively, after two hours of irradiation UV light. The samples produced were pure, with 1% and 2% Samarium-doped $ZnFe_2O_4$. The cationic dye MB underwent degradation when it was exposed to visible light. In a few hours, the Sm-doped $ZnFe_2O_4$ NPs, with a 2% concentration, successfully eliminated 65% of the dye. This indicates that the sample exhibits resistance to the degradation of MB cationic dye. These Sm-loaded $ZnFe_2O_4$ NPs were stable for a period above three cycles. These findings proved

that these two photocatalysts effectively degrade the RhB and MB dyes. [166, 168] Sharma et al. successfully created yttrium-doped $CoFe_2O_4$, a magnetic photocatalyst with the chemical formula $CoY_xFe_{2-x}O_4$ with outstanding catalytic activity. The primary goal of the current research is to change the catalytic activity of $CoFe_2O_4$; as a result, the photo-Fenton reaction with H_2O_2 and PMS two various inorganic oxidants was chosen. Regardless of the inorganic oxidant used, the data showed that Y^{3+} doping increased catalytic activity compared to pure $CoFe_2O_4$.[167] M.A. Abdo et al. prepared Ce-substituted Zn-Mn ferrite NPs using a straightforward combustion method. The nano ferrite $Zn_{0.5}Mn_{0.5}Ce_{0.08}Fe_{1.92}O_4$ demonstrated moderate magnetism (36.94 emu/g) and the lowest coercivity, making it highly suitable for soft ferrite applications in high-frequency technology and communication. The $Zn_{0.5}Mn_{0.5}Ce_{0.08}Fe_{1.92}O_4$ photocatalyst demonstrated excellent photocatalytic efficacy for RhB and superior stability. It's simple synthesis method, superior magnetic characteristics, and excellent stability make it a promising candidate for high-frequency applications and large-scale pollution treatment.[169] Li et al. created a photocatalyst (figure-5) supported by three-dimensional ordered microporous silica to activate PMS and degrade BPA using visible light. The photocatalyst, n-CeO_2@p-$LaFeO_3$/3DOM SiO_2, demonstrated exceptional photocatalytic efficiency due to the catalysts' pore confinement effects and the combined influence of $LaFeO_3$ and CeO_2. The researchers have shown that the breakdown of BPA occurs via the generation and identification of reactive oxygen species (ROS), as well as through adsorption and diffusion processes. The researchers determined that n-CeO_2@p-$LaFeO_3$/3DOM SiO_2 has great potential as a sustainable material for effective sewage treatment.[170]

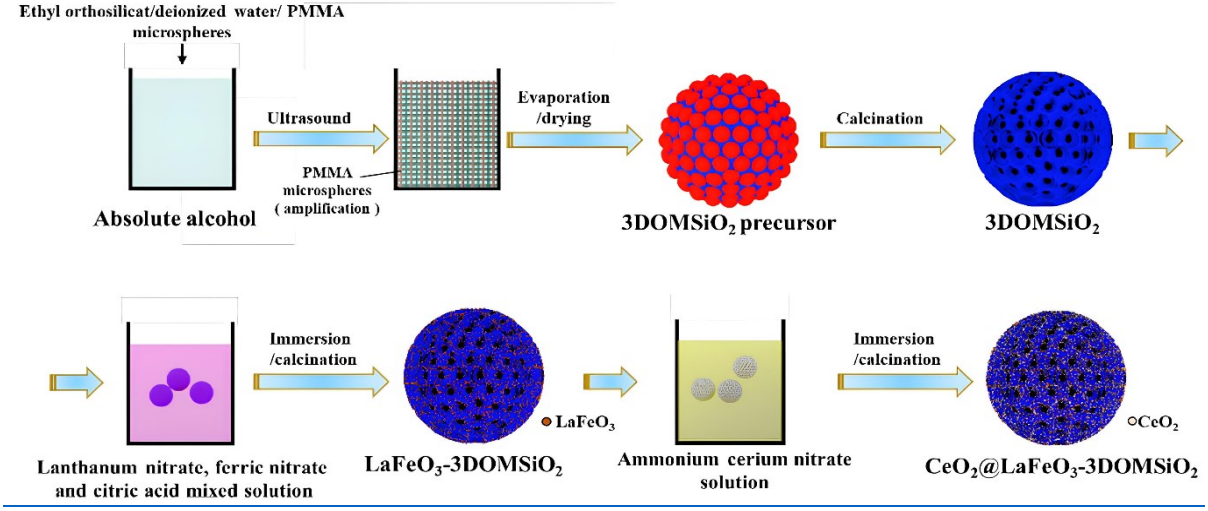

Figure 5. Fabrication of n-CeO_2@p-$LaFeO_3$/3DOM SiO_2 composite as photocatalyst. (Reprinted with permission from Chao et al. (2023). Copyright 2023 Elsevier).

Andrei et al. did research where they used the Fenton method to examine the catalytic activity of lanthanide-doped magnesium ferrites. The lanthanide ions used for doping were La^{3+}, Ce^{3+}, Sm^{3+}, Gd^{3+}, and Dy^{3+}. Under the study, the catalytic efficacy of the catalysts, as measured by the maximum appearance rate constant k, declined in the following sequence when exposed to UV irradiation: $Ce^{3+} > Dy^{3+} > La^{3+}$ $MgFe_2O_4 > Sm^{3+} > Gd^{3+}$. The ferrites demonstrated excellent efficiency, achieving a degradation rate of up to 99% for MB within 60 minutes for visible-driven Fenton reactions, and within 20 mins for UV-driven Fenton reactions. Also, the investigation demonstrated that the outcomes were similar to those of other heterogeneous Fenton catalysts.[171] A study explored Ce-doped manganese ferrite ($MnFe_2O_4$) for wastewater treatment and sensing. A simple solution combustion method synthesized Ce-doped

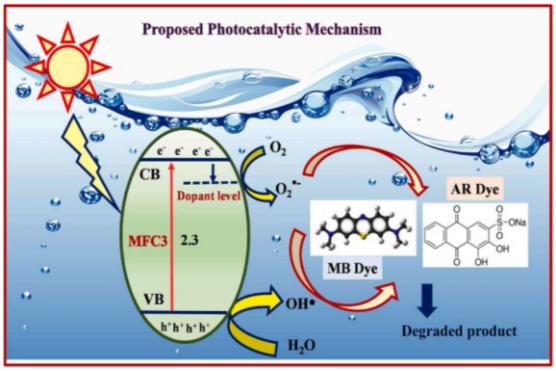

Figure 6. Solution combustion methodologically synthesized MFC3 material photocatalytic mechanism for degradation of MB and AR dye in the presence of sunlight. (Reprinted with permission from Vidya et al. (2021). Copyright 2021 Elsevier).

$MnFe_2O_4$ (MFC3). This magnetic photocatalyst demonstrated excellent performance, degrading 98% and 89% of MB and AR dyes in the presence of sunlight (Figure 6). MFC3 also showed promise in sensing D-glucose and paracetamol from water. Utilizing magnetic properties facilitated MFC3's fabrication and characterization. These findings suggest that MFC3 has the potential as a multifunctional material for wastewater treatment (photocatalysis), biomedicine (soft magnetism), and sensor technology (detecting specific molecules).[172]

5. Based on different materials

5.1. Polymer-based ferrites:

According to Kumar M. et al., magnetic biopolymer beads consisting of zinc ferrite and alginate (ZFN-Alg) are an affordable alternative for eliminating Pb (II) and Cu (II) metal ions from both single and binary systems, as found in the current work. When Pb (II) and Cu (II) ions were investigated for adsorption on ZFN-Alg beads in batch mode, the results revealed that these beads still had a regeneration effectiveness of about 80% even after five cycles. This study highlights the promise of magnetic biopolymer beads as a practical and cost-effective solution for removing lead (Pb(II)) and copper (Cu(II)) ions from contaminated water.[173] Atul Sharma, et al. produced a magnetic NC made of cobalt ferrite and occimum sanctum. The analysis revealed that the NC has strong magnetic characteristics and could be an economical adsorbent for wastewater treatment technologies. It was examined for its capability to adsorb MB and CV, two cationic dyes, and both tests revealed a high capacity. As a result of these findings, the Cobalt ferrite-Occimum sanctum NC is a promising contender for wastewater treatment applications.[174] Chitosan beads entrapping magnetic cobalt ferrite with amine functionalization (NH_2-CF-CB) are a cost-effective and highly efficient adsorbent. These beads possess exceptional adsorption capabilities, making them ideal for reducing water pollution. They can effectively remove MG, an organic pollutant, as well as Cu (II) ions, an inorganic contaminant. In addition, these beads are reusable and can be easily separated from the water. The Langmuir adsorption isotherm model was used to evaluate the maximum adsorption capacities of MG and Cu (II) ions on NH_2-CF-CB. The maximum adsorption capacity for MG was found to be 357.16 mg/g, while for Cu (II) ions, it was 158.73 mg/g.[175] Joshi et al. made PANI and $Mn_{0.25}Co_{0.75}Fe_2O_4$ (MCF) NCs with 0, 10, 20, 50, and 100 weight percentages of MCF to break down CV dye under sun radiation. PANI/MCF NCs were made by in-situ chemical oxidative polymerization of aniline. XRD and FTIR showed pure phase development in all samples. MCF and PANI/MCF crystallite diameters were 20–30 nm. PANI/MCF NCs with 10 and 20 wt% MCF degrade CV dye efficiently. The degradation efficiency of 10 and 20 wt% PANI/MCF NCs was 77% and 89% in 75 mins. The research showed that heterogeneous photocatalysts with reduced optical band gaps work. Maximum degradation rate constants were 0.5 and 0.7 min-1 for PANI/MCF NCs with 10 and 20 wt% MCF.[176] Hosseini et al. synthesized $CoFe_2O_4$ NPs by a simple chemical precipitation technique. The dialytic rate of the magnetic PVC-$CoFe_2O_4$ membrane was superior to that of the pristine PVC membrane in removing chromium ions. The considerable affinity of NPs with magnetic properties for heavy metal ion adsorption is the main reason for this effect.[177] Kaur, et al. explained the ES technique used to create a novel nanofiber membrane consisting of $Co_{0.5}Ni_{0.5}Fe_2O_4$-PVDF. The $Co_{0.5}Ni_{0.5}Fe_2O_4$ NPs were synthesized using the sol-gel combustion method. The results of their comprehensive analysis suggest that spintronics devices, magnetic sensors, and ferrite-based nanofiber membranes have a high potential for competition.[100] A.R. Sadrolhosseini et al. produced composite layers of polypyrrole, chitosan, and nickel-ferrite NPs at varied times using the electrochemical method. The surface plasmon resonance technique was then used to analyze the PPy-Chi/$NiFe_2O_4$-NPs to find heavy metal ions in aqueous solutions, such as Ni, Fe, Co, Al, Mn, Hg, and Pb. Comparing the sensing layer to other sensing layers, including polypyrrole and polypyrrole chitosan, it showed a better capacity to detect paramagnetic substances and was proven to be more sensitive.[178] Abou Hammad, A.B. et al. produced a biodegradable, semiconducting, and antibacterial cellulosic composite that in-situ polymerizes PANI in the presence of cellulose. This composite magnetic property was obtained by adding cobalt ferrite NPs (CFO-NPs) during the polymerization process. The CFO-NPs produced by the sol-gel method had an average particle size of less than 50 nm. Because of its exceptional biodegradability and antibacterial efficacy against Candida albicans, Escherichia coli, and Bacillus subtilis, the electromagnetic NC was generated. [179] Tatarchuk, et al. developed a magnetic core-shell adsorbent by immobilizing TiO_2 nanoclusters on the cobalt ferrite NPs. Ethylene glycol and citric acid were used as chelating agents in a modified Pechini sol-gel synthesis. They conducted a detailed analysis of the shape and structure of pure $CoFe_2O_4$, reference TiO_2, and the resulting $CoFe_2O_4$@TiO_2 NC shown in Figure 7. The $CoFe_2O_4$@TiO_2 NC was

found to have an adsorption efficacy that was more than twice as high as that of TiO_2 and $CoFe_2O_4$ alone. The observed synergistic effect can only be attributed to the formation of deformed titania nanocrystals. The magnetic nano adsorbents that were found were successful in eliminating dichromate anions (83% removal) and CR dye (61% removal) from water.[180]

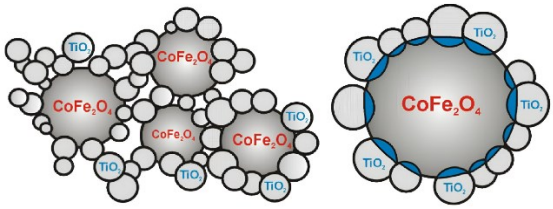

Figure 7. The suggested configurations of (a) $CoFe_2O_4$@TiO_2 NC and (b) a surface layer of titanium enrichment on cobalt ferrite NPs. (Reprinted with permission from Tetiana et al. (2020). Copyright 2020 Elsevier).

Giri et al. have researched the biomedical applications of substituted ferrites [$Fe_{1-x}B_xFe_2O_4$, B=Mn, Co]. Superparamagnetic ferrites and ferrofluids containing fatty acids have been synthesized by use of the co-precipitation process. $Fe_{1-x}Mn_xFe_2O_4$ may have uses in biological applications, such as MRI contrast agents and cancer therapy for hyperthermia. They also studied GO-manganese ferrite (GMF) to remove As (V) ions through adsorption-filtration. The newly created adsorptive MMMs have the potential to be used as a single treatment approach for the removal of As (V) ions.[181] Polymer bimetal complexes were utilised to synthesise nitrogen-doped mesoporous carbon embedded with $NiFe_2O_4$-NC, which was then employed to extract Hg^{2+} from aqueous medium. The proposed method employs a single-source precursor to create $NiFe_2O_4$ nanocrystals incorporated into a nitrogen-doped graphitised carbon matrix. This technique can produce an extremely effective magnetic adsorbent to eliminate harmful pollutants from contaminated water.[182]

Table 6. Polymer-based spinel metal ferrite NC materials for efficient removal of harmful substances from water.

S. No	*Material*	*Synthesis method*	*Contaminant*	*Ref*
1	Beads made of zinc ferrite & alginate (ZFN-Alg beads)	Batch mode	Pb (II) and Cu (II) metal ions	[173]
2	Cobalt ferrite-Ocimum sanctum magnetic NC	Co-precipitation	MB and CV dye	[174]
3	Chitosan beads embedded with magnetic cobalt ferrite	Hydrothermal Method	MG and copper (II) ions	[175]
4	Polyaniline/$Mn_{0.25}Co_{0.75}Fe_2O_4$ (PANI/MCF) NCs	In-situ chemical oxidative polymerisation	CV dye	[176]
5	$CoFe_2O_4$ NPs	Chemical precipitation process	Chromium (Cr) ions	[177]
6	$Co_{0.5}Ni_{0.5}Fe_2O_4$-Polyvinylidene Fluoride (PVDF)	Electrospinning process	Spintronics devices, magnetic sensors	[100]
7	Polypyrrole, chitosan, and $NiFe_2O_4$ NPs	Electrochemical approach	Heavy metals such as Ni, Fe, Co, Al, Mn, Hg, and Pb in an aqueous solution	[178]
8	$CoFe_2O_4$@TiO_2	Sol-gel method	CR dye & dichromate anions from water.	[180]
9	$Fe_{1x}Mn_xFe_2O_4$	Co-precipitation technique	Removal of As (V) ions	[181]
10	Nickel ferrite containing nitrogen-doped mesoporous carbon ($NiFe_2O_4$-NC)	Thermal treatment	Hg^{2+} from the aqueous medium.	[182]
11	Aluminium doped nano manganese copper ferrite	Chemical co-precipitation method	Arsenic from aqueous solutions	[183]
12	Composite $CoFe_2O_4$/CuO NPs	Chemical precipitation	Cu^{2+}, Ni^{2+}, and Pb^{2+} rejection	[184]
13	$BiFeO_3$ (BFO) NPs	Non-aqueous wet chemical methods	Influencing the mud's properties	
14	Alginate-cobalt ferrite NC	Ex-situ polymerisation method	Binary dyes (Reactive Red 195 and Reactive Yellow 145)	[185]

15	Chitosan (CS), $CoFe_2O_4$ NPs, and Poly(Pyrrole-co-O-Toluidine) matrix (P(Py-coOT)) NCs	In situ chemical oxidation method	Proposed Co^{2+} ion sensor	[186]
16	Ni-$ZnFe_2O_4$ NPs	Chelation reaction	Basic Blue 9, Basic Blue 41, and Basic Red 18	[187]

Malana, M.A. et al. used the chemical co-precipitation technique to synthesize a 13 nm-sized aluminium-doped nano manganese copper ferrite. The ferrite was then impregnated with methacrylate, vinyl acetate, and acrylic acid polymer by a gradual heating process to produce NC. An NC was used to extract arsenic from aqueous solutions.[183] Zareei, F et al. utilised Composite $CoFe_2O_4$/CuO NPs to produce nanofiltration membranes based on mixed matrix polyethersulfone (PES). The blended [PES-0.5 wt% $CoFe_2O_4$/CuO] membrane exhibited a rejection rate of 98%, 92%, and 88% for Cu^{2+}, Ni^{2+}, and Pb^{2+} respectively, whereas the pure PES membrane exhibited a rejection rate of 85%, 80%, and 78% for the same metal ions. The blended membrane exhibited superior reusability with a marginal decline of less than 4.9% in average performance.[184] In a fixed bed column, binary dyes were removed using an alginate-cobalt ferrite (ACF) as a nanosorbent. The bed depth and flow rate caused the binary adsorption. The study showed that a considerable bed depth and a reduced flow rate were needed to effectively sequestrate binary dyes. The characteristics of the ACF in powder form are ideal candidates: easy preparation, cheap cost, biocompatibility, renewable, mechanical separability, no formation of secondary pollutants, and environmental friendliness. The outcomes demonstrated ACF's efficiency when applied to eliminate binary dyes.[185] Researchers employed nitrilotriacetic acid (NA) as a chelating agent to coordinate with iron (Fe(II)) and manganese (Mn(II)) ions in various ratios during the thermal decomposition synthesis of porous magnetic ferrite nanowires. Two distinct types of nanowires were successfully produced: one containing pure $MnFe_2O_4$ and another containing manganese-doped Fe_3O_4. These porous nanowires demonstrate a remarkable ability to remove heavy metal ions and organic pollutants from wastewater. The research suggests that these magnetic ferrites have broader applicability in fields beyond water treatment, potentially extending to areas like biotechnology and lithium-ion battery technology.[188] Martins, et al. focused on creating novel magnetoelectric (ME) material polymer NCs that display a customised ME response at room temperature. The three distinct ferrite NPs, $Zn_{0.2}Mn_{0.8}Fe_2O_4$ (ZMFO), $CoFe_2O_4$ (CFO), and Fe_3O_4 (FO), are the basis for the multiferroic NCs, which are disseminated in a matrix of the piezoelectric copolymer poly (vinylidene fluoridetrifluoroethylene, or P(VDF-TrFE)). The ME response of ZMFO/P(VDF-TrFE), on the other hand, revealed little hysteresis and a strong dependency on the ZMFO filler content. Potential novel uses have been discussed for these ferrite/PVDF NCs, including memories and information storage, signal processing, ME sensors, and oscillators.[189] An in situ chemical oxidation method was used by Katowah, D. F., et al. to create nanostructured ternary NCs made up of chitosan (CS), $CoFe_2O_4$ (CF) NPs and a Poly (Pyrrole-co-O-Toluidine) matrix (P(Py-coOT)). A Co^{2+} ion detection electrochemical sensor was made using P(Py-co-OT)/CF/CS NCs. The CS and P(Py-co-OT) layers are applied uniformly to the CF NPs. The P(Py-co-OT)/CF/CS NCs are promising Co^{2+} ion sensors due to their excellent detection limit, sensitivity, and electrical interaction. For values between 0.1 nM and 0.1 mM, the Co^{2+} sensor responded to Co^{2+} linearly. The performance and response times of the proposed Co^{2+} ion sensor are satisfactory and repeatable. [186] Jayalakshmi, R. et al. researched the structural characterization of the ex-situ produced alginate-cobalt ferrite NC ($CoFe_2O_4$-ANa NC), the current communication's primary focus. $CoFe_2O_4$ NPs stabilisation of sodium alginate has been demonstrated by the characterisation results. As a result, the alginate-cobalt ferrite NC was shown to have enhanced particle distribution, fewer and smaller particle agglomerates, increased crystallinity, and increased surface area. [190] Researchers investigated the potential of a composite material, MFN-alginate, for removing dyes from wastewater. MFN-alginate is comprised of magnetic ferrite NPs and alginate. The study assessed its ability to remove model dyes (Basic Blue 9, Basic Blue 41, and Basic Red 18) from both individual dye solutions (single systems) and mixtures of these dyes (binary systems).[187]

5.2 Carbon-based metal ferrites composites

Researchers investigated the influence of metal ferrite NPs (MFNPs) on biohydrogen production through thermophilic dark fermentation of milk processing wastewater (MPWW). The MFNPs consist of $NiFe_2O_4$, $CoFe_2O_4$, and $CuFe_2O_4$ NPs. Chemical coprecipitation was used to create the MFNPs, which were then characterised. The characterisation results showed that the average nanocrystallite diameters of the $NiFe_2O_4$, $CoFe_2O_4$, and $CuFe_2O_4$ spinels were 25.8 nm, 33 nm, and 20.7 nm, respectively. The prepared NPs were pure and exhibited ferromagnetic properties.[191] Mona

Moradi et al. aimed to improve wastewater treatment by using spinel cobalt ferrite (SCF) NPs coupled with g-C_3N_4 in their UVC/persulfate technique. As a model recalcitrant pollutant, they examined the breakdown of BPA to assess how well their strategy worked. The team's investigations revealed that SCF@g-C_3N_4 produced practically, had more excellent photocatalytic activity and superior PS activation capabilities than either pure SCF or g-C_3N_4. The novel technique was also successful in treating wastewater samples that were BPA-contaminated. After five catalyst reuse cycles, the system removed more than 95% of the BPA, demonstrating the potential for SCF@g-C_3N_4 to be a cost-effective wastewater treatment method. The results indicate that this method can potentially intensify wastewater treatment through synergy.[192]

Wu et al. have shown that electro-peroxone, a combination of ozonation and electrolysis utilizing a carbon-polytetrafluoroethylene cathode, is an effective method for treating the growing contaminant diatrizoate (DTZ) in water. The researchers synthesized cathodic catalysts by modifying carbon nanotubes with ferrite (MFe_2O_4/CNTs, M: Fe, Mn). They determined that these catalysts were well-suited and showed great promise for this specific method. These results indicate that using electro-peroxide with cathodic materials and MFe_2O_4/CNTs catalysts is a feasible approach for breaking down DTZ in an aqueous solution.[193] Yao et al. conducted a study on the enhancement of crystallinity, thermostability, and magnetization of γ-Fe_2O_3 and ferrites NCs by co-modifying them with carbon nanotubes (γ-Fe_2O_3/MFe_2O_4/CNTs, M: Co, Cu, and Mn). The purpose of this modification was to improve the capacity of the NCs to adsorb and eliminate CPX from wastewater. The presence of γ-Fe_2O_3 changed the way CPX is adsorbed on MFe_2O_4/CNTs and γ-Fe_2O_3/MFe_2O_4/CNTs. The investigation revealed that the adsorption interaction and capacity of the copper and manganese ferrite systems were governed by CNTs and γ-hematite (γ-Fe_2O_3). The study's results highlight the role of magnetic materials, which may be used to create identical adsorbents for environmental applications.[194] Nadeem et al. used coal fly ash (CFA) to manufacture copper ferrite NCs. These NCs were specifically designed for photocatalytic degradation of MO dye. The researchers used hydrothermal synthesis to produce NPs of pure copper ferrite and copper ferrite NC of CFA. The NC photocatalyst demonstrated improved physicochemical properties, facilitating the effective degradation of MO, reaching a maximum of 98% under optimum conditions.[195] Jelokhani et al. effectively produced cobalt ferrite (CF) NCs containing rGO and CNT by using the simple co-precipitation method at low temperatures. The CF-CNT NC exhibited the greatest dark adsorption capacity and best effectiveness in decomposing MB at all concentrations. The CF-CNT NC exhibited a photocatalytic efficiency of 97% under visible light, resulting in the decomposition of a 10 mg/L MB solution during a 180-minute reaction period. This effectiveness was 1.8 times higher than that of the CF-rGO NC and up to 2.5 times higher than that of pure CF NPs.[196]

Cobalt hexaferrite NPs were made by Ansari, F et al. for the first time utilising the sol-gel process and organic reducing agents (carbohydrates and pigments). According to the band gap estimate made by DRS, these goods can function as active photocatalysts. Therefore, MO degradation was examined under UV irradiation in the presence of the finished goods. The findings indicate that the graphene-based NC exhibits higher photocatalytic activity compared to both the CNT-based NC and the pure NPs.[197]

Table 7. Spinel metal ferrites with carbon composite-based materials are used for an effective photocatalytic and adsorption of hazardous contaminants from water.

S. No	*Material*	*Synthesis method*	*Contaminant*	*Ref*
1	$CoFe_2O_4$ NPs anchoring g-C_3N_4	UVC/persulfate technique	BPA	[192]
2	MFe_2O_4/CNTs	Combined ozonation with electrolysis process	Diatrizoate (DTZ) in aqueous solution	[193]
3	(c-Fe_2O_3/MFe_2O_4/CNTs		CPX antibiotic drug	[194]
4	$CuFe_2O_4$ NCs	Hydrothermal synthesis	MO dye	[195]

5	Cobalt ferrite (CF)-rGO and CF-CNT NCs	Simple co-precipitation process	MB dye	[196]
6	Cobalt hexaferrite NPs	Sol-gel process	MO dye	[197]
7	MnFMC and CoFMC nanohybrid composites	One-pot solvothermal synthetic approach	Pb (II) ions	[198]
8	(CNZF/CNTs) NC	Inverse co-precipitation	As (V) contaminated anions	[199]
9	$MgFe_2O_4$ NPs	Sol-gel process	Cr (VI) ions	[200]
10	Mn or Co-modified magnetic ferrite CNT	Hydrothermal method	Bezafibrate (BZF) from aqueous solution	[201]
11	$CuFe_2O_4$ NPs	Hydrothermal technique	Arsenite [As (III)] from drinking water	[202]
12	Nanosheets of BFO with functionalized carbon nanofiber.	Hydrothermal method	Detection of catechol (CC).	[203]

Wang et al. synthesized nanohybrid composite [MFe_2O_4 (M = Co, Mn)–MoS_2–Carbon dots (CD)] mentioned samples named at MnFMC and CoFMC with highly efficient removal of Pb (II) from water. In this study synthesized composites showed strong Pb (II) adsorption performances at 588.24 mg/g for MnFMC composite and 660.67 mg/g for CoFMC composite. These composites also showed a preference for Pb (II) sorption despite the presence of strong competition from Ca (II) and Mg (II) cations. The nanohybrid adsorbents' remarkable reusability makes them attractive choices for water filtration. They can lower effluent Pb (II) values to the ppb level, which satisfies the WHO drinking water standard recommendation.[198] Ahangari, A. et al. created two magnetic adsorbents, $Ni_{0.5}Zn_{0.5}Fe_2O_4$ Ferrite (NZF) and $Ni_{0.5}Zn_{0.5}Fe_2O_4$/CNTs (CNZF/CNTs) NC, via inverse co-precipitation. These two adsorbents have a fast magnetic response that may be separated from the solution using a magnetic field. From the experimental results of As (V) adsorption CNZF/CNTs shows higher maximum adsorption capacity than NZF. These two NCs used to remove the As (V) from the industrial effluent.[199] Verma et al. developed magnetic $MgFe_2O_4$ NPs (MMFNPs) using the sol-gel method. Ultrasonography coated MWCNTs with these NPs to form MMF composites. Prepared materials were tested for heavy metal wastewater remediation. Cr (VI) adsorption onto as-produced MMFNC suited the Langmuir model best. MMFNC are cheap because their magnetic properties make them easy to extract from aqueous solutions. The MMFNC removed Cr (VI) ions with less than 20% efficiency loss after seven adsorption-desorption cycles.[200] Wu et al. constructed magnetic ferrite-modified carbon nanotubes (MFe_2O_4/CNTs, M: Mn or Co) to remove bezafibrate (BZF) from water. From these experiments, Wu et al. observed that $MnFe_2O_4$/CNTs adsorb BZF better than $CoFe_2O_4$/CNTs. Results reveal that MFe_2O_4/CNTs might adsorb BZF from aqueous solutions.[201] Luan, et al. made $CuFe_2O_4$ particles hydrothermally. These particles were added to stacked CNT membranes to remove arsenite [As (III)] from drinking water. Drinking water treatment conditions were used to evaluate the composite membrane. $CuFe_2O_4$ particles were retained by the CNT membrane and did not enter the filtered water. The composite membrane eliminated over 90% of As (III) under different solution chemical conditions. As (III) removal from drinking water is promising via the novel composite membrane.[202] Ramaraj et al. proposed a simple hydrothermal approach for making BFO nanosheets with functionalized carbon nanofiber. Electrochemical catechol detection was also performed on the BFO NS/F-CNF NC-modified glassy carbon electrode (GCE). As projected, $BiFeO_3$ NS/F-CNF/GCE has strong electrocatalytic activity and electrochemical redox responses 3.44 and 7.92 fold higher for catechol sensing.[203]

5.3 agricultural waste based spinel ferrites

Guo et al. developed amine-functionalized rice bran biochar/$MgFeAlO_4$ ($RB@MgFeAlO_4$-NH_2) magnetic composites using a one-step solvothermal method. They found that the $RB@MgFeAlO_4$-NH_2 magnetic composite could remove hazardous Ni (II) from wastewater. Experimental results show the composite can accept 201.62 mg g^{-1} Ni (II). Due to its environmental friendliness, inexpensive cost, magnetic separation ease, and high sorption capacity, $RB@MgFeAlO_4$-NH_2 may be used to remove Ni(II) from aqueous solutions at a low cost.[204] In treating organic wastewater, adsorbent/ferrite composites can adsorb and decompose organics. Ying et al. used microwave radiation to treat organic wastewater using a rice hull/$MnFe_2O_4$ composite (RHM) created through calcination in a nitrogen atmosphere. This is believed because $MnFe_2O_4$ is present, which increases RHM's catalytic activity. Water washing can renew RHM. However, RHM's surface area and maximal COD removal rate decline for each regeneration cycle. This innovative rice hull/$MnFe_2O_4$ composite has the benefits of low cost and quick processing, and it may find promising use as a wastewater treatment agent.[205] A new NC adsorbent known as ALW/$CoFe_2O_4$ was produced by Suba et al. by auto-combusting Apocynaceae leaf waste-activated carbon (ALW) and $CoFe_2O_4$. This compound's antibacterial and dye-elimination properties were examined against S. aureus, E. coli, and C. albicans. The outcomes demonstrated that the synthetic ALW/$CoFe_2O_4$ has antimicrobial activity comparable to that of the common antibacterial (Streptomycin) and antifungal (Amphotericin B) medications, with a zone of inhibition spanning from 11 to 17.56 mm. With varying concentrations (100-500 mg), the good diffusion method was used to evaluate the antibacterial activity against S. aureus and E. coli and the antifungal static efficacy against C. albicans.[206] Saleh et al. generated activated carbon (AC) from willow catkins using chemical modification techniques. Using a one-step hydrothermal process, they loaded the AC with nickel ferrite NCs. The researchers found that the 45NFAC photocatalyst was the most efficient, degrading 99.7% of RhB dye in just 90 mins under simulated sunshine. The NFAC NCs are dependable, efficient, and reusable, making them a viable photocatalyst for water environmental remediation.[207] A new type of biochar was developed by Bai et al. (figure-8) In this study, spinel ferrite was loaded onto straw using the sol-gel technique. This study examined the impact of various environmental factors and preparation methods on biochar's adsorption characteristics. Additionally, ion-competitive adsorption tests examined ion interference and preference. To maximize biochar recovery and reuse, magnetic determination and recycling tests were done. This research contributes to straw-based biochar adsorption for heavy metal wastewater treatment.[208]

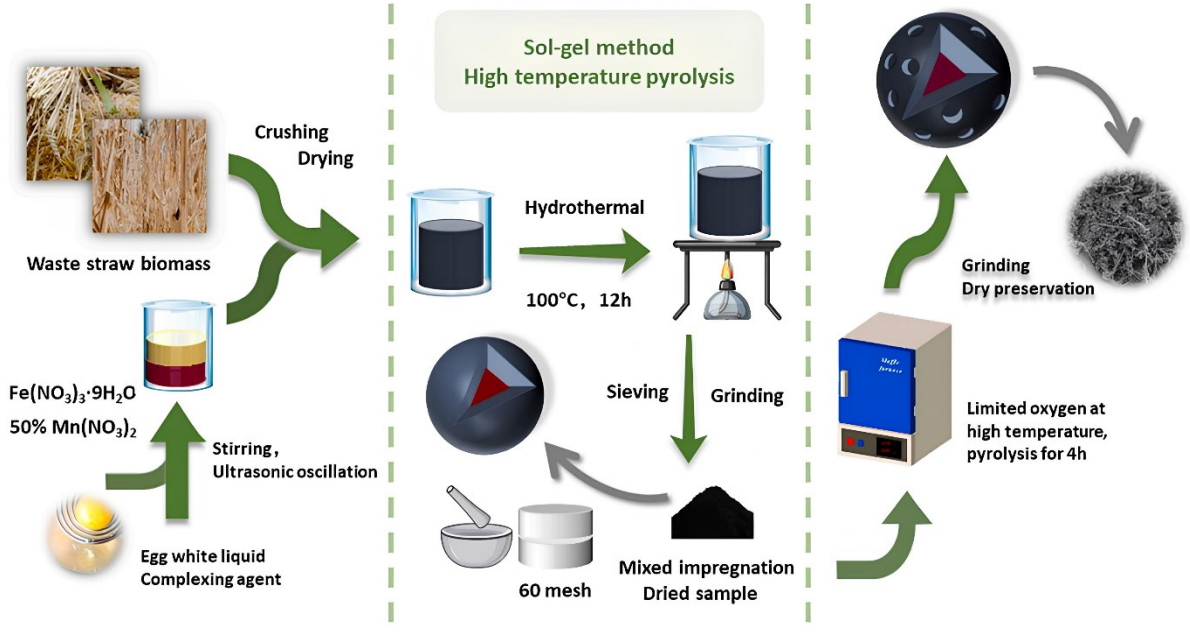

Figure 8. Schematic illustration of biochar modified bimetallic spinel ferrite synthesis by using sol-gel method with high-temperature pyrolysis. (Reprinted with permission from Chen et al. (2023). Copyright 2023 Elsevier).

Carbon quantum dots (CQDs) can be synthesised from agricultural waste, such as sugarcane bagasse, to maximise the value of manure. Grewal J. et al. used an ultrasonication method to create a trimetallic strontium-titanium ferrite NC of CQDs. The NC was researched to determine its photocatalytic

effectiveness and was compared to NPs and CQDs to investigate the degradation of nitroaromatic pollutants (namely p-nitrophenol, Martius yellow, and pendimethalin) when exposed to visible light. The findings indicated that NC including CQDs and $Sr_{0.4}Ti_{0.6}Fe_2O_{4.6}$ in a weight-to-volume ratio of 2:1 had excellent photocatalytic activity. The degradation efficiencies ranged from 91.2% to 97.4%, surpassing the range of 65.0% to 88.3% seen for pure NPs and CQDs.[209] Zirconium ferrite NCs (BC-$ZrFe_2O_5$ NCs) mediated by biochar were created by Perveen, Shazia, and colleagues with biochar derived from wheat straw. These NCs were employed to remove Tartrazine dye from textile effluent through adsorption. The study indicates that nano adsorbents can be created effectively and used as affordable and practical materials for real-world industrial engineering applications. It's worth noting that the NCs were recovered in five cycles and still retained an impressive adsorption efficiency, with only a marginal reduction from 89% to 63%.[210] Algethami et al. used butchered cow bones from the Najran region of Saudi Arabia to generate a manganese ferrite and hydroxyapatite composite. Their research sought to develop new composites that can aid in water filtration using animal bone waste, notably that from cows, in an economical and environmentally responsible manner. The composite they produced, which demonstrated excellent photocatalytic activity against the industrial waste pollutant MB dye, was made using the synthesised hydroxyapatite ($Ca_{10}(PO_4)_6(OH)_2$). In addition, the synthetic composite exhibited exceptional bacteriostatic activity against the pathogens that cause acute waterborne illnesses, S. aureus and E. coli.[211]

Researchers have found a simple technique to create composite materials by utilizing biochar made from various agricultural waste. The procedure entails synthesizing cobalt (II) ferrite onto the charcoal surface and using chelate complexes of transition metal cations with citric acid to produce composite materials. These materials efficiently eliminate chromium (VI) ions from water-based solutions, making them valuable for the treatment of industrial effluent.[212]

Table 8. Spinel metal ferrites with Agriculture waste material-based composite are used for an effective photocatalytic and adsorption of dangerous pollutants from water.

S. No	*Material*	*Synthesis method*	*Contaminant*	*Ref*
1	Magnetic rice bran biochar/$MgFeAlO_4$-NH_2 composites	One-step solvothermal method	Harmful Ni (II) from wastewater	[204]
2	Rice hull/$MnFe_2O_4$ composite (RHM)	Calcination in a nitrogen atmosphere	Maximal COD removal rate decline	[213]
3	Activated carbon from Apocynaceae leaf materials was mixed with CoFe2O4.	Auto combustion process	Reactive Red 141 dye and microorganism removal	[206]
4	Willow catkin-derived activated carbon (AC)	Chemical modification techniques	RhB dye	[207]
5	New biochar loading spinel ferrite onto the straw	Sol-gel technique	Heavy metal removal from wastewater via adsorption	[208]
6	Sugarcane bagasse-derived CQDs. trimetallic strontium-titanium ferrite CQD NC. ($Sr_{0.4}Ti_{0.6}Fe_2O_{4.6}$)	Ultrasonication method	Pendimethalin, Martius yellow, and p-nitrophenol	[209]
7	Zirconium ferrite NCs with biochar	Co-precipitation method	Tartrazine dye	[210]
8	Cobalt (II) ferrite ($CoFe_2O_4$)	Straightforward one-stage synthesis	Chromium (VI) ions from aqueous solutions	[211]
9	Hydrolyzed Luffa Cylindrica HLC/$CoFe_2O_4$ magnetic composite	Chemical co-precipitation method	Divalent nickel ion removal from water	[214]
10	A magnetic NC of $CoFe_2O_4$@SiO_2@$Dy_2Ce_2O_7$	Combustion method	MB, CV and RhB dyes	[215]

Alizadeh, Mehran et al. created a magnetic adsorbent using chemical co-precipitation and hydrolysed Luffa Cylindrica (HLC). This adsorbent was tested for divalent nickel ion removal from water. According to the study, adsorption effectiveness declined as Ca^{2+} and Na^{+} cation concentrations rose in the aqueous medium. The synthesised adsorbents, however, continued to work well even after eight reuse cycles. Furthermore, during real wastewater treatment, the HLC/$CoFe_2O_4$ magnetic composite was discovered to be incredibly successful at eliminating heavy metal contaminants from shipbuilding effluent.[214] Zinatloo-Ajabshir, S et al. have successfully developed a recyclable photocatalyst called $CoFe_2O_4$@SiO_2@$Dy_2Ce_2O_7$ (CFO@SiO_2@DCO), an MNC. The compound 2,2-dimethyl-1,3-propanediamine was used as a novel pH regulator in the synthesis of the $Dy_2Ce_2O_7$ component and as a new crucial agent in the manufacture of the silica component. The cobalt ferrite was synthesized by combustion using grape juice as an innovative and eco-friendly fuel source (Synthesized steps given in Figure 10). This is the first endeavour to evaluate the photocatalytic efficiency of nanostructures composed of (CFO@SiO_2@DCO). In this study synthesized nanostructure composite was used to effectively degrade the MB, CV and RhB dyes in the presence of UV irradiation. The results indicated that the synthesized (CFO@SiO_2@DCO) might serve as a promising and beneficial photocatalyst for the efficient removal of water contaminants, with an additional advantage of being recyclable.[215] The study focuses on examining and documenting the effects of NC formulations, which consist of carbon materials with high conductivity, metal enzyme cofactors, and DIET activators, on enhancing the generation of biogas from anaerobically incubated cow dung in the context of anaerobic digestion (AD). The three distinct formulations of NCs created and manufactured by Fatma Y., et al. consist of zinc ferrite (ZnFe), zinc ferrite blended with 10% carbon nanotubes (ZFCNTs), and zinc ferrite combined with 10% C76 fullerene (ZFC76). ZnFe exhibited a methane production increase of 185.3% compared to all other materials, making it the most significant improvement. The use of ZFCNTs and ZFC76 resulted in a significant increase in methane production, with boosts of 162% and 145.9%, respectively, compared to the performance of the control reactors. Also, the presence of these substances increased the hydraulic retention time.[216]

5.4 Fullerene-based spinel ferrites:

Hydrothermal synthesis of magnetic $CoFe_2O_4$/GO adsorbents is simple. GO and magnetic $CoFe_2O_4$ adsorbents are produced by Chang, et al. using a simple hydrothermal process. Here, a clear selective adsorption behaviour can be shown, with MB > RhB > MO being the order of adsorption capacity. Theoretical simulations indicate that the primary factors contributing to the adsorption of dye on GO are electrostatic interaction and stacking interaction. In addition, they conduct a theoretical investigation on the notable impacts of GO defects and oxygen-containing functional groups on the efficacy of its adsorption of organic dyes.[217] A one-step hydrothermal method created new $NiFe_2O_4$/MWCNTs hybrids with varying MWCNT content. These hybrids are magnetically recyclable and were used to examine the photocatalytic activity of $NiFe_2O_4$/MWCNTs hybrids by Zhu, H-Y. et al. The photocatalytic activity was determined by measuring the rate of CR decolorisation in an aqueous solution under simulated solar light irradiation.[24] Dhiman et al. created a combination of mixed-spinel ferrite and g-C_3N_4 to remove antibiotic pollutants from wastewater. The procedure consisted of three continuous steps: pyrolysis, solution combustion, mechanical grinding, and annealing, which were used to produce a Z-scheme g-C_3N_4/$Ni_{0.5}Zn_{0.5}Fe_2O_4$ nano

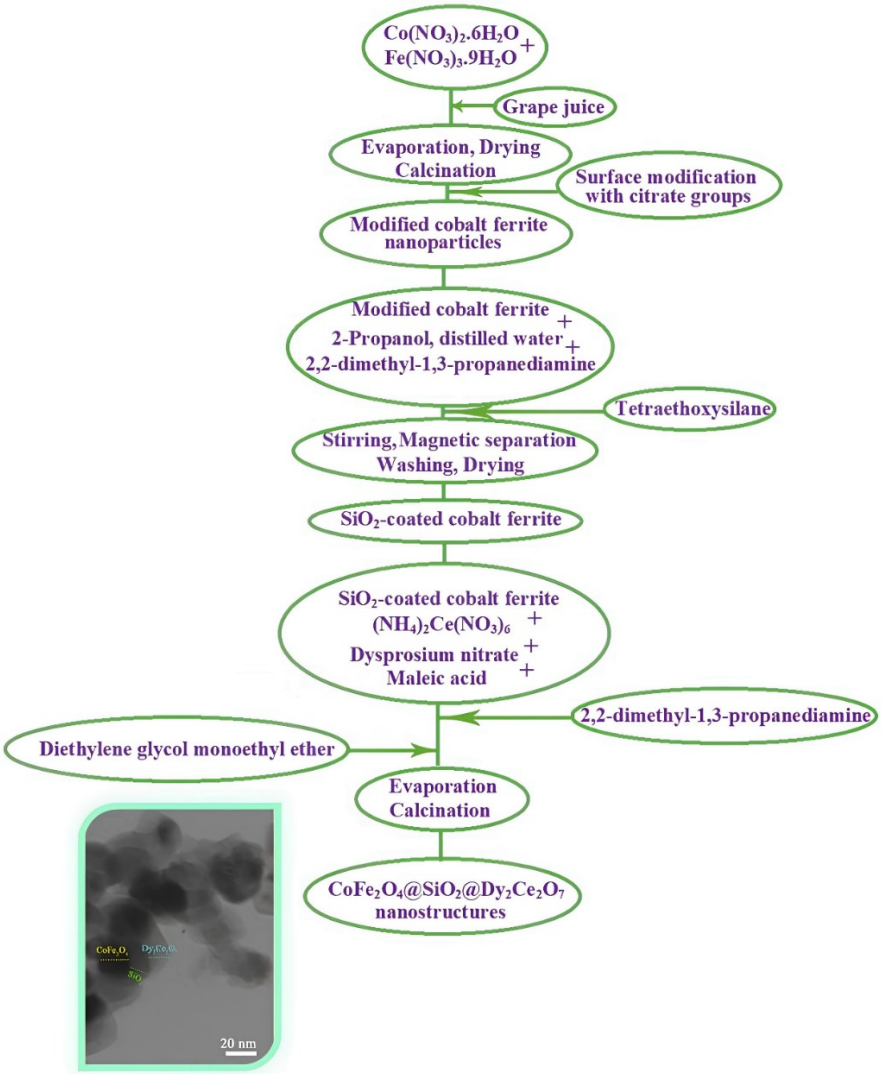

Figure 10. Step-by-step synthesis approach of $CoFe_2O_4@SiO_2@Dy_2Ce_2O_7$ MNCs. (Reprinted with permission from Sahar et al. (2019). Copyright 2019 Elsevier).

heterojunction. The photocatalyst that was created was assessed for its capacity to break down the Doxycycline medication using natural sunlight. The heterojunction had a peak deterioration efficiency of 97.10% during a 60-minute evaluation. The higher photodegradation efficiency was a result of the greater redox capacity and separation of photoinduced charges facilitated by the Z-scheme heterojunction between g-C_3N_4 and Ni-Zn ferrite.[218] Wabaidur et al. have developed a new NC that effectively eliminates cationic MB and celestine blue (CB) dyes from water. The NC, consisting of silica-coated $CuFe_2O_4$-decorated oxidised MWCNTs ($CuFe_2O_4$/oMWCNTs), was synthesized via co-precipitation and hydrothermal processes. The regeneration studies showed that the highest recovery of CB was obtained using acetonitrile (ACN), while complete recovery of MB was accomplished using methanol (MeOH). The $CuFe_2O_4$/oMWCNTs NC is an exceptionally excellent adsorbent for rapidly and effectively decolorizing wastewater that contains cationic dyes.[219]

Table 9. Spinel metal ferrites with fullerene-based compounds and carbon composite-based materials are used for the efficient removal of toxic pollutants from wastewater.

S. No	*Material*	*Synthesis method*	*Contaminant*	*Ref*
1	$CoFe_2O_4$/GO	Hydrothermal synthesis	MB, MO and RhB dyes	[217]
2	MWCNT/$NiFe_2O_4$ hybrids	One-step hydrothermal approach	CR dye	[24]
3	g-C_3N_4 /$Ni_{0.5}Zn_{0.5}Fe_2O_4$ nano heterojunction	Pyrolysis, solution combustion, mechanical grinding, and annealing	Doxycycline drug	[218]
4	Novel NC of $CuFe_2O_4$/oMWCNTs with silica-coated $CuFe_2O_4$.	Co-precipitation and hydrothermal synthesis	MB and Celestine Blue dyes	[219]
5	Composites of magnetic bronze F-TiO_2 with carbon nanostructures	Hydrothermal procedure	MG dye	[220]
6	TiO_2/$CoFe_2O_4$/rGO NCs	Hydrothermal method	MO, RhB, and MB dyes	[221]
7	$CuFe_2O_4$-GO catalyst	Photo-Fenton-like oxidation	Reactive Black 5 (RB5)	[222]
8	($ZnFe_2O_4$/rGO).	One-pot approach	Decompose ammonia and nitrogen gas from an organic pollutant-ammonia mixed solution	[223]

Titanium tetraisopropoxide (TTIP) and carbon nanostructures (MWCNT or Fullerene (C60)) were hydrothermally processed to make magnetic bronze F-TiO_2/carbon nanostructure NCs.

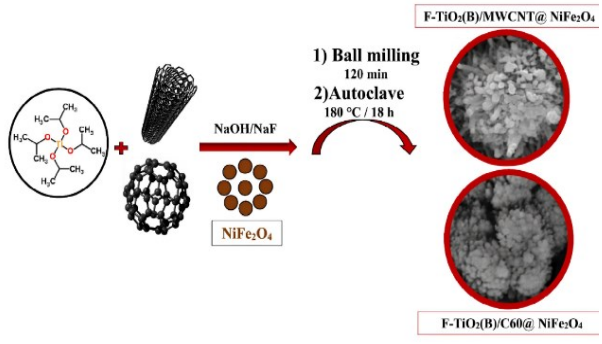

Figure 11. Synthesis of F-TiO_2(B)/MWCNT @$NiFe_2O_4$ and F-TiO_2(B)/C60@$NiFe_2O_4$ magnetic composites (Schematic representation). (Reprinted with permission from Arsalani et al. (2019). Copyright 2019 Elsevier).

MG was utilized as a contaminant to test magnetic catalyst photocatalysis. The study found that the F-TiO_2(B)/ MWCNT@$NiFe_2O_4$ and F-TiO_2(B)/Fullerene@$NiFe_2O_4$ NCs photo catalytically degrade MG dye at 93% and 98% after 120 mins of visible irradiation. F-TiO_2(B)/carbon nanostructure@$NiFe_2O_4$ NCs degrade well and may be reused four times without losing efficacy.[220] Ghosh, B.K. et al. developed a non-hydrothermal synthesis for producing TiO_2/$CoFe_2O_4$/rGO NCs, which are effective catalysts for breaking down hazardous organic dyes.[221] Kodasma, et al. conducted a study on the photocatalytic efficiency of $CuFe_2O_4$XGO, which is a hybrid catalyst consisting of $CuFe_2O_4$ and GO, to remove dyes. The findings indicated that catalysts with varying weight ratios of GO have great potential as practical options for environmentally friendly wastewater treatment methods.[222] Liu, Shou-Qing, and colleagues used a single-location method to synthesize catalysts of $ZnFe_2O_4$ and $ZnFe_2O_4$ with rGO ($ZnFe_2O_4$/rGO). The researchers found that the interaction between Zn cations on $ZnFe_2O_4$ and ammonia in solution led

to the selective breakdown of ammonia and nitrogen gas from a mixture of organic contaminant and ammonia solution using the $ZnFe_2O_4$/rGO catalyst. Under visible light exposure, the surface photovoltage spectra indicated that the photo-generated holes migrated towards the surface of $ZnFe_2O_4$ particles, resulting in the removal of ammonia adsorbed on the catalyst surface.[223]

5.5 Semiconductor-based spinel ferrites:

Through their research, Saputra et al. explored the potential of a hybrid semiconductor known as CTF-$ZnFe_2O_4$ catalysts to enhance the effectiveness of visible-light-driven photocatalytic degradation of pollutants. Their study discovered that a certain proportion of CTF-$ZnFe_2O_4$, with a ratio of 90:10, was successful in breaking down MB. The degradation process achieved an efficiency rate of 95.4% and a k_{obs} value of 0.421 min1. This was achieved by utilizing 0.5 g/L dosages of CTF-$ZnFe_2O_4$ to degrade 50 mg/L of MB over 120 mins, using a UV-vis light photocatalytic technique.[224] Shu, Ruiwen, and colleagues fabricated hybrid composites of nitrogen-doped MWCNT and cobalt-zinc ferrite (NMWCNTs/$Co_{0.5}Zn_{0.5}Fe_2O_4$) by a one-step solvothermal process given in figure-12. The microspheres were uniformly dispersed on the surface of NMWCNTs, and the interconnecting of NMWCNTs in the hybrid composites facilitated the formation of 3D conductive networks in situ. The research examined how the number of NMWCNTs affected the electromagnetic properties and microwave absorption behaviour of composites made of NMWCNTs, $Co_{0.5}Zn_{0.5}Fe_2O_4$, and paraffin wax. The observations indicated that the materials could be easily manufactured, and the research findings helped design highly effective microwave absorbers based on MWCNTs and the structural design of these materials.[225]

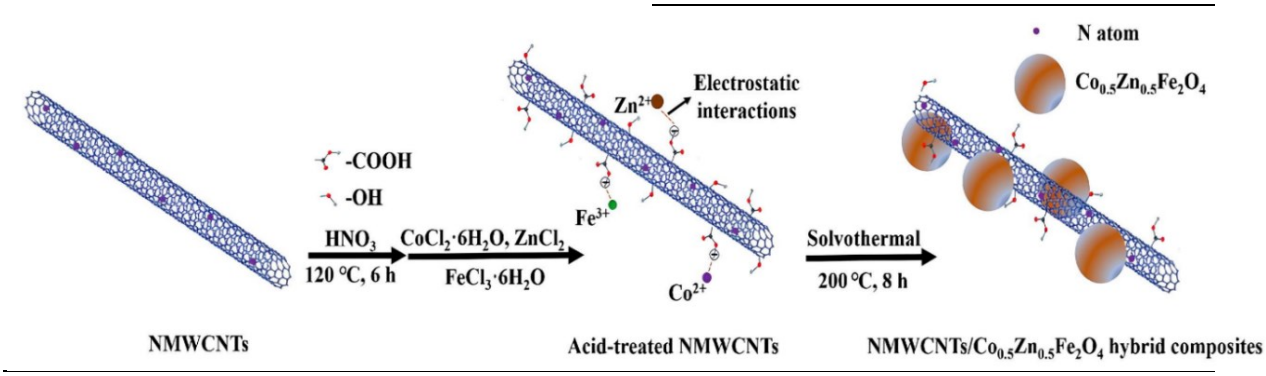

Figure 12. Graphical Illustration of NMWCNTs/$Co_{0.5}Zn_{0.5}Fe_2O_4$ hybrid composite synthesis procedure. This image is reprinted from the Journal of Composites Science and Technology ref. [225].

Table 10. Semiconductor-combined spinel ferrite materials are used for the highly efficient removal of poisonous pollutants from wastewater.

S. No	*Material*	*Synthesis method*	*Contaminant*	*Ref*
1	CTF-$ZnFe_2O_4$ catalysts	One-pot ionothermal method.	Degradation of MB	[224]
2	MWCNT doped $Co_{0.5}Zn_{0.5}Fe_2O_4$	One-step solvothermal method	Highly effective microwave absorbers	[225]
3	($MnFe_2O_4$-G)	One-pot solvothermal method	Remove glyphosate from contaminated water for water treatment	[226]

Yamaguchi invented the $MnFe_2O_4$-G hybrid composite. N.U. et al. immobilized $MnFe_2O_4$ microspheres on graphene nanosheets using a one-pot solvothermal technique and rGO with microspheres. Single-layer GO and $MnFe_2O_4$ magnetic microspheres removed glyphosate from water. Analytical methods tested the graphene manganese ferrite composite for glyphosate adsorption in several experimental settings. This research's $MnFe_2O_4$-G hybrids may be suitable adsorbents for glyphosate removal from

contaminated water for water treatment and purification.[226]

5.6 Composite material-based spinel ferrites:

Tran, N.B.T., et al. utilised simple hydrothermal procedures to produce a magnetic NC called Fe_3O_4/zeolite NaA (Fe_3O_4/ZA), Fe_3O_4 NPs and zeolite NaA. This NC helps remove MB from the aqueous solution through adsorption. The adsorption mechanism of MB molecules on the Fe_3O_4/ZA is the result of the interaction between the active sites on the surfaces and edges of inversion spinel ferrite Fe_3O_4 NPs and zeolite NaA with MB molecules. This method provides a simple, effective, and scalable process to synthesise the magnetic Fe_3O_4/ZA NC, which can be used as an inexpensive adsorbent for wastewater treatment.[227] In a study by Raghavendra, N. et al., $CoFe_2O_4$ and clay/$CoFe_2O_4$ were effectively produced and analysed. Results showed that the combination of clay and $CoFe_2O_4$ is a promising material for detecting heavy metals in industrial wastewater treatments using various chemicals and biosensors. This can aid in environmental remediation efforts.[228] Magnetic composite photocatalysts (Ag_2O/MFe_2O_4) were developed using three magnetic carriers, namely $ZnFe_2O_4$, $CoFe_2O_4$, and $NiFe_2O_4$. The amount of silver utilised was reduced, which improved the separation efficiency and lowered the operational cost for practical applications. The outcomes of the study demonstrate the excellent photocatalytic performance and superior magnetic recovery rate of the developed three magnetic composite photocatalysts. These composites can photodegrade common organic contaminants such as MO, MB, RhB, and phenol. However, evaluating the silver content, photocatalytic activity and stability, and magnetic recovery rate following recycling testing shows that Ag_2O/$ZnFe_2O_4$ (60%) is the best composite.[229] Zhang used the hydrothermal (ZFO-H) and citrate sol-gel (ZFO-C) methods, to produce the zinc ferrite ($ZnFe_2O_4$, ZFO) catalysts. This study compares the effectiveness of catalysts and non-catalytic ozonation in the oxidation of contaminants and phenol in biologically treated coking wastewater (BTCW), as well as to assess the kinetics of the ozonation reaction. [121]

Table 11. Spinel ferrite with composite-based materials produced by various methods is used to treat wastewater.

S. No	*Material*	*Synthesis method*	*Contaminant*	*Ref*
1	Magnetic Fe_3O_4 /zeolite NaA NC	Simple hydrothermal method	MB dye from aqueous solution	[227]
2	$CoFe_2O_4$ and clay/$CoFe_2O_4$	Chemical method	Electrochemical heavy metal detection of industrial wastewater treatments	[228]
3	Ag_2O/MFe_2O_4 magnetic composite	Hydrothermal method	MO, MB, RhB dyes and phenol	[229]
4	$ZnFe_2O_4$ catalysts	Sol-gel method	Oxidation of contaminants and phenol	[121]
5	mZVAl/MFe_2O_4 composites (M = Mn, Zn, Ni)	The simple ball milling procedure	Removal of Cr (VI)	[230]
6	$CoFe_2O_4$@MXene nanohybrid	Liquid self-assembly approach	NPX in an aqueous environment	[231]
7	Magnetic $CoFe_2O_4$/GO adsorbents	Simple hydrothermal process	MB, RhB, and MO dyes	[217]
8	$ZnFe_2O_4$ MNPs	Soft chemical methods	Breakdown of the azo dye Acid Blue 113	[120]
9	$CoFe_2O_4$ NPs	Co-precipitation process	Ampicillin antibiotic drug	[232]
10	$NiFe_2O_4$@SiO_2 magnetic catalyst	Hydrothermal	RhB dye	[233]
11	$ZnFe_2O_4$	Co-precipitation procedure	Diclofenac sodium	[234]
12	1-D ZnO-$ZnFe_2O_4$ nanofiber	In-situ synthesis	CR dye	[235]
13	$ZnFe_2O_4$ NPs	Thermal annealing	Organic dye degradation	[236]
14	$NiFe_2O_4$ NPs	Co-precipitation approach	Efficient and magnetically releasable photocatalyst	[237]

ZVAl is a promising substance for removing heavy metals since it is a cost-effective addition with great reducibility. However, thick surface oxide layers reduce ZVAl's reactivity. Li et al. developed mZVAl/MFe_2O_4 composites (M = Mn, Zn, Ni) using a simple ball milling procedure, and they verified their successful adsorption-reduction capability for the removal of Cr (VI). The oxide coating was removed, and the lattice spacing of mZVAl increased due to ball milling with MFe_2O_4, according to direct spectroscopic investigations and density functional theory calculations. The improvement in Cr (VI) removal was primarily due to ZVAl's improved adsorption and reduction capabilities following ball milling. To remove heavy metals from wastewater, a new route for the synthesis of reductive materials is presented in this study.[230] The catalytic degradation of NPX in water was carried out using a unique magnetically recoverable $CoFe_2O_4$@MXene nanohybrid with a multilayer structure and accordion-like morphology. This hybrid was created by Fayyaz et al. using a liquid self-assembly approach. Overall, it was demonstrated that the $CoFe_2O_4$@MXene could function as a nanohybrid catalyst for the NPX in an aqueous media and other organic pollutants. It was shown that the $CoFe_2O_4$@MXene could act as a nanohybrid catalyst for the NPX in an aqueous environment to be degraded.[231] Magnetic adsorbents are produced using a simple hydrothermal procedure including $CoFe_2O_4$ and GO. $CoFe_2O_4$/GO composites are utilised to extract MB, RhB, and MO. This study provides a thorough insight into the mechanism of adsorption in $CoFe_2O_4$/GO composites. It proposes a novel design strategy for employing GO-based composites as magnetic adsorbents to remove wastewater pigments.[217] Mandal, et al. used soft chemical methods to create zinc ferrite magnetic NPs. In the presence of trace amounts of H_2O_2, the zinc ferrite spinel, in its natural and calcined forms, exhibited excellent photocatalytic activity to break down the azo dye Acid Blue 113. After several operation cycles, the catalyst maintained its initial action, demonstrating a natural photocatalytic reaction. The antibacterial activity of zinc ferrite NPs was shown to be effective against both gram-positive and gram-negative bacterial strains.[120] $CoFe_2O_4$ NPs were synthesized by the coprecipitation technique. They were used to initiate the oxidizing agent PMS in the breakdown of the antibiotic ampicillin. The analysis revealed that the NPs have a cubic spinel structure and a crystallite size of 10.10 nm. The study investigated the impact of several parameters of operation, including pH, PMS concentration, presence or absence of catalyst, and length of time, on the degradation of ampicillin. Under conditions of neutral pH, 90.1% of the ampicillin completed degradation over a 25-minute duration when exposed to a catalyst concentration of 0.1 g/L and a PMS concentration of 0.2 mM.[232] The study involved the fabrication of heterogeneous Fenton catalysts using a new core-shell modified $NiFe_2O_4$@SiO_2 magnetic catalyst. The study looked at how dispersants, precipitants, and hydrothermal temperatures affected the structure, surface morphology, magnetism, and catalytic activity of magnetic nanoparticle catalysts before and after coating with SiO_2. The catalytic activity of the materials was assessed utilising the RhB degradation detection analysis.[233] ZnO and $ZnFe_2O_4$ were synthesised by Latif, et al. using a co-precipitation procedure, and they were then evaluated using various analytical methods. In contrast to ZnO, which destroyed only 48.9% of the drug in the photocatalytic study against diclofenac sodium, $ZnFe_2O_4$ had a greater degradation efficiency of 61.4% in just 120 mins. Additionally, zinc ferrite demonstrated good recyclability and remained stable after five photodegradation cycles with only a slight (3.9% loss) in photocatalytic activity. According to a study of two catalysts, $ZnFe_2O_4$ has a promising role in wastewater cleanup to get rid of dangerous pharmaceuticals.[234] Ntiamoah, et al. successfully showed, for the first time, that the synthesis of 1-D ZnO-$ZnFe_2O_4$ nanofiber at its original position leads to a strong contact at the interface and a well-suited heterojunction for the chemisorption of CR. As a result, 1-D ZnO-$ZnFe_2O_4$ has the highest recorded adsorption capacity for $ZnFe_2O_4$-based adsorbent, at 263 mg/g. Additionally, even after multiple uses, the used adsorbent is easily regenerable and retains 75% of its adsorption capability. The recent findings offer a method for creating inexpensive but efficient ZnO-$ZnFe_2O_4$-based adsorbents to eliminate harmful dyes. [235] Al-Najar et al. have described a simple yet highly efficient thermal annealing method for controlling defects related to oxygen vacancies in $ZnFe_2O_4$ NPs. This method enhances the efficacy of the NPs in wastewater treatment. The photocatalytic performances of each sample were evaluated, and the $ZnFe_2O_4$ samples subjected to annealing at 500°C exhibited the highest photocatalytic efficiencies. Under conditions of high salinity, this particular sample's organic dye breakdown efficiency remained the highest. $ZnFe_2O_4$ samples possess remarkable dye degradation capabilities as a result of the high concentration of oxygen vacancies within their crystal lattice. This leads to a significant reduction in the recombination rate during the photocatalytic process.[236] In their study, Shah et al.

utilised the co-precipitation method to generate $NiFe_2O_4$ while also creating composites of $NiFe_2O_4$ and TiO_2 with varying concentrations of TiO_2. The primary benefit of these composites lies in their enhanced ability to absorb visible light and effectively separate electron-hole pairs, which is attributed to the various energy band positions in $NiFe_2O_4$ and TiO_2. The findings of our study indicate that NCs based on $NiFe_2O_4$ can serve as a highly efficient photocatalyst that can be easily recovered using magnetic attraction.[237]

6. Applications

6.1. Dye degradation using spinel ferrites:

$MnFe_2O_4$/rGO (MrGO) was created by Adel M et al. to remove a variety of cationic dyes efficiently. MG and MB dye have strong adsorption capacities for removal in the produced NCs, reaching 156 and 105 mg/g at 30°C, respectively. Electrostatic contact, π-π interaction, and the produced adsorbent's high surface area of 95 m^2/g made removing dyes from $MnFe_2O_4$/rGO easier. After being reused for five consecutive cycles, the as-synthesized adsorbent exhibited good stability.[238] The self-combustion method was used by Andrei et al. to create the magnesium ferrite adsorbents, which were then tested for MB adsorption. The effects of dye, adsorbent concentrations, and pH were established on the kinetic adsorption and magnesium ferrite performance. As a result, during the MB adsorption-desorption process, the produced adsorbents showed structure stability and reusability. The characteristics of the magnesium ferrite. It is suited for practical application due to its high adsorption capacity, regeneration abilities, and structural stability.[239] Wang et al. researched to examine how well various hydrothermally synthesized MFe_2O_4 (M = Mn, Fe, Co, Ni) ferrite nanocrystals can adsorb CR from wastewater. The MFe_2O_4 NPs exhibited significant ferromagnetic characteristics when subjected to a magnetic field, allowing them to be efficiently separated using magnetic methods. Acetone was discovered to be a proficient desorption agent for MFe_2O_4 NPs that were loaded with CR. Among the spinel ferrite nanocrystals, the $CoFe_2O_4$ nanocrystals showed exceptional CR adsorption ability and a greater saturation magnetisation of 86.1 emu g^{-1}.[240] A study by Jadhav et al. evaluated the physical, chemical, magnetic, and photocatalytic properties of Ni-Zn nanoferrites using the auto-combustion sol-gel method. The photocatalytic activity of RhB was assessed under sunlight irradiation, showing an increase in degradation efficiency up to 98% with an increase in Ni^{2+} concentration.[241] Imran Hasan, along with colleagues, looked into the environmentally friendly production of $NiFe_2O_4$ (NIFE) spinel MNPs using chemical coprecipitation of a Ni^{2+}/Fe^{3+} solution in the presence of a biopolymer combination of chitosan (CT) and ascorbic acid (AS). In the presence of visible light and ultrasonic vibrations, the material was also studied as a potential photocatalyst for MG photocatalytic degradation. Unlike adsorption, photodegradation using sonochemistry produces 99% MG mineralisation without changing the material's structure.[242] Semi-conductive photocatalysts for water treatment are popular due to their effectiveness and affordability. Muhammad Rashid and his team developed nanostructured Mn-doped cobalt ferrite. The material is a photocatalyst with excellent electrical conductivity, magnetic recyclability, and visible light activity. The photocatalyst efficiently eliminated CV dye, which is driven by visible light, from water and retained 97.2% of its original photocatalytic activity even after four consecutive cycles. This study demonstrates the potential of combining the surface characteristics of a semi-conductive catalyst with its magnetically charged, mechanical, and optical features to efficiently and economically clean wastewater.[243] Zulhumar Musajan et al. created nano-$CoFe_2O_4$@MC, a catalyst to degrade CR in wastewater treatment. It addresses issues of low activation performance, secondary pollution, and challenging recovery of nanometal catalysts. The catalyst's efficient degradation of CR was through both radical and nonradical routes. The catalyst exhibits exceptional catalytic efficiency, stability, reusability, and very little release of ions, making it highly suitable for the remediation of antimicrobial wastewater.[244] Researchers explored using spherical (28 nm) nickel ferrite crystals to remove crystal violet dye from water. Detailed analysis suggests the crystals physically attract the dye, forming multiple layers on their surface, rather than creating a chemical bond. This method achieved a high capacity (19.6 mg/g of dye removed per gram of crystals) but with a moderate rate of adsorption. Further investigation revealed the process aligns with a scientific model describing physical adsorption on surfaces.[245] Ramadevi et al. synthesised $NiFe_2O_4$ and $NiFe_2O_4$ doped with aluminium using hydrothermal synthesis. The NPs were characterised by different techniques. The material demonstrated strong photocatalytic performance in degrading MB and MO dyes when irradiated with visible light.[246]

Table 11. Dyes removal from industrial wastewater using spinel metal ferrites as a photocatalyst and adsorbents.

S. No	*Material*	*Synthesis method*	*Contaminant*	*Ref*
1	$MnFe_2O_4$/rGO NPs	Sol-gel method	MB and MG dyes	[238]
2	Magnesium ferrite adsorbents	Self-combustion method	MB dye	[239]
3	MFe_2O_4 (M = Fe, Mn, Ni, Co) ferrite	Hydrothermal	CR dye	[240]
4	Mixed spinel Ni-Zn nano ferrites	Auto-combustion sol-gel method	RhB dye	[241]
5	Nickel ferrite spinel MNPs	Chemical coprecipitation	MG dye	[242]
6	Undoped and Mn-doped cobalt ferrite materials	Co-precipitation method	CV dye	[243]
7	Cobalt ferrite NCs with carbon mesopores	Hydrothermal method	CR dye	[244]
8	Nickel ferrite NPs	Thermal heat treatment	CV dye	[245]
9	Nickel ferrite and nickel ferrite doped with aluminium ($NiAl_{0.6}Fe_{1.4}O_4$)	Hydrothermal synthesis	MB and MO dyes	[246]
10	$NiFe_2O_4$ NPs	Microwave-assisted technique	Cationic MB and anionic Alizarin Red S dyes	[247]
11	$NiFe_2O_4$ spinel NPs doped with copper	Simple microwave combustion	RhB dye	[248]

Naik, M. et al. used Tamarindus indica seeds to create magnetic $NiFe_2O_4$ NPs (NFNPs) through a microwave-assisted technique with a green reducing agent. The NFNPs were identified through various techniques. The NFNPs exhibited a spinel structure that was proven to be single-phase using XRD analysis. The average size of the crystallites was determined to be 21 nm. The FTIR analysis determined the specific positions of the NFNPs, both in tetrahedral and octahedral arrangements. The NFNPs possess a noticeable band gap of 1.92 eV. Under visible light irradiation, NFNPs exhibit strong photocatalytic activity for the adsorption of cationic MB and anionic Alizarin Red S dyes. VSM investigations demonstrate that NFNPs exhibit good magnetic properties. NFNPs can be used for wastewater treatment.[247] Microwave combustion was used to synthesize Copper-doped $NiFe_2O_4$ spinel NPs. The X-ray diffraction patterns revealed that the introduction of Cu resulted in the emergence of the secondary -Fe_2O_3 phase, alongside the pre-existing cubic structure. The Cu-doped $NiFe_2O_4$ spinel NPs, in their original state, demonstrated exceptional photocatalytic destruction of RhB when exposed to visible light. The photocatalytic performance of bulk $NiFe_2O_4$ was greatly improved by Cu-doping. The highest photocatalytic activity was achieved when the ratio of Cu-doping reached x = 0.4, up to an ideal value.[248]

6.2. Pharma waste removal using spinel ferrites:

Co-precipitation was used by Latif et al. to create the ZnO and $ZnFe_2O_4$ NPs. The breakdown of diclofenac sodium during 120 minutes of UV light irradiation was shown to be more successfully catalyzed by synthetic $ZnFe_2O_4$ (61.4%) than by ZnO (48.9%) without the need for an oxidizing agent. Furthermore, zinc ferrite exhibited excellent recyclability even after undergoing five distinct photocatalytic activity tests, indicating a promising level of catalyst stability.[234] Tetracycline hydrochloride (TCH) is degraded 90% and 86% of the time by strong MW synthesized adsorbers, the highly crystalline spinel $NiFe_2O_4$ and $ZnFe_2O_4$, which are formed by coprecipitation. The catalyst is reusable, as shown by the fact that the whole reaction is completed in less than 15 minutes.[249] Researchers employed a microwave-assisted process with K_2CO_3 chemical activation under optimized conditions to produce activated carbon

from lentil waste (LW). The LWAC was later used as a matrix for the production of spinel ferrite composites due to its significant surface area of 1875 m^2/g. The combination of $CuFe_2O_4$ NPs with LWAC resulted in the creation of a new magnetic composite material called M-LWAC. The wastewater containing Tetracycline (TC) was efficiently eliminated using M-LWAC, which had an adsorption capacity of 384.62 mg/g.[250] A study investigated spinel ferrite NPs (MFe_2O_4, where M represents iron, cobalt, nickel, or zinc) as potential carriers for the anticancer drugs doxorubicin (DOX) and methotrexate (MTX). Among the different MFe_2O_4 NPs tested, cobalt ferrite (CFO) emerged as the most promising candidate for targeted cancer therapy due to its superior magnetic properties, colloidal stability, cytotoxicity towards cancer cells, and biocompatibility.[251] Sol-gel auto-combustion was used by Jasrotia et al. to create nickel-modified Co single bond Mg magnetic nano photocatalysts with the following chemical formula: $Co_{0.65}Mg_{0.35-x}Ni_xFe_2O_4$. The produced NPs were employed to photodegrade the pharmaceutical effluent from amoxicillin using sunlight.[252] Xiao S. et al. used sonochemical methods to synthesize $SnFe_2O_4/BiFeO_3$ NCs, which were then employed as photocatalysts. NCs consisting of $SnFe_2O_4/BiFeO_3$ exhibit superior photocatalytic activity compared to individual $SnFe_2O4$ or $BiFeO_3$ NPs. The $^{\cdot}OH$ radical had a predominant role in the photocatalytic degradation method. The $SnFe_2O_4$-$BiFeO_3$ NCs completely eradicated the malachite green dye under visible light exposure, achieving 100% degradation over 60 mins. The anticancer medicine doxorubicin was put into NCs consisting of $SnFe_2O_4$ and $BiFeO_3$. The survival capacity of human liver cancer cells was assessed by subjecting them to doxorubicin, $SnFe_2O_4$, $BiFeO_3$, and folic acid. The potential features of $SnFe_2O_4/BiFeO_3$ NCs are proven in their applications for ecological remediation, antibacterial activities, and drug delivery.[253] Researchers developed a photocatalyst, $ZrFe_2O_4$@ZIF-8, by combining $ZrFe_2O_4$ with zeolitic imidazolate framework-8 (ZIF-8). This novel material proved highly effective in eliminating dopamine (DOP) and sulfamethoxazole (SMX) from water. Notably, $ZrFe_2O_4$@ZIF-8 achieved complete degradation (100%) of both DOP and SMX, surpassing the performance of $ZrFe_2O_4$ alone.[254]

Table 12. Pharmaceutical drug removal from industrial wastewater using spinel ferrites

S. No	*Material*	*Synthesis method*	*Contaminant*	*Ref*
1	ZnO and $ZnFe_2O_4$ NPs	Co-precipitation	Removal of dangerous environmental pollutants	[234]
2	Spinel $NiFe_2O_4$ and $ZnFe_2O_4$ NPs	Co-precipitation	TCH antibiotic drug	[249]
3	LWAC with $CuFe_2O_4$ NPs	Microwave-assisted synthesis	TC antibiotic drug	[250]
4	MFe_2O_4, where M = Fe, Co, Ni, or Zn) NPs	Sonochemical technique	Doxorubicin (DOX) and methotrexate (MTX)	[251]
5	$Co_{0.65}Mg_{0.35-x}Ni_xFe_2O_4$	Sol-gel auto-combustion	Amoxicillin	[252]
6	$SnFe_2O_4/BiFeO_3$ NCs	Sonochemical method	MG dye	[253]
7	$ZrFe_2O_4$ with zeolitic imidazolate framework-8 (ZIF-8)	Sonochemical method	DOP and SMX	[254]
8	g-$C_3N_4/Ni_{0.5}Zn_{0.5}Fe_2O_4$	Pyrolysis, solution combustion, mechanical grinding, and annealing	Doxycycline drug	[218]
9	$CoFe_2O_4$ NPs enhanced activated carbon (AC-$CoFe_2O_4$)	Simple refluxing route	Promazine	[255]
10	$Zn_xNi_{1-x}Fe_2O_4$	Sol-gel auto combustion method	RhB dye	[256]
11	$CoFe_2O_4$ NPs	Co-precipitation method	CR dye	[257]
12	SrFe@Dop@M	Chemical coprecipitation method	Levofloxacin and SMX	[258]

13	Mg-substituted Zn nano-ferrite ($Zn_{1-x}Mg_xFe_2O_4$)	Sol-gel method	Sulfadiazine	[259]
14	$ZnFe_2O_4$ NPs	Hydrothermal route	MB dye	[260]
15	$CoFe_2O_4$ NPs	Coprecipitation method	Degradation of ampicillin	[232]

Researchers developed a method to create an NC material combining spinel ferrite with g-C_3N_4 for eliminating antibiotic pollutants from wastewater. This synthesis involved a four-step process: pyrolysis, solution combustion, mechanical grinding, and annealing. The created photocatalyst was evaluated for its capacity to decompose the drug Doxycycline in sunlight. Based on the results, the experiment resulted in a maximum degradation efficiency of 97.10% for the pollutant in a created heterojunction. The experiment lasted for 60 mins.[218] Promazine was eliminated from wastewater using a magnetic nano adsorbent composed of AC that was modified with $CoFe_2O_4$ NPs, a kind of metal ferrite (AC-$CoFe_2O_4$). Al-Hetlani et al. exhibited remarkable stability, showed efficacy in eliminating both acidic and alkaline pharmaceuticals from wastewater, and could be regenerated and reused by the application of a magnetic field.[255] The sol-gel auto-combustion method was utilised by Jadhav et al.to generate the NPs of $Zn_xNi_{1-x}Fe_2O_4$, which were also employed to eliminate RhB from the industrial wastewater. Under 180 mins of exposure to sunshine, the produced NPs' photocatalytic activity showed maximal degradation rates of 90%, 94%, and 98%, respectively.[256] Behura, R. et al. effectively synthesized $CoFe_2O_4$ NPs by using iron recovered from waste iron ore tailings and cobalt recovered from wasted lithium-ion batteries. Subsequently, they were characterized and used for photo/sono-catalytic degradation of CR.[257] Kaur, P. et al. developed a novel hexagonal ferrite-based core-shell-shell nanostructure, namely SrFe@Dop@M, for the combined electrochemical detection and photocatalytic degradation of medical drugs. M represents the elements Cr, Mn, Fe, Co, Ni, Cu, and Zn. The degradation of levofloxacin and SMX was assessed using a comparative photocatalytic assessment of SrFe, SrFe@Dop, and SrFe@Dop@M.[258] Dhiman et al. observed the synthesis of Mg-substituted Zn nano-ferrite ($Zn_{1-x}Mg_xFe_2O_4$) with varying levels of Mg. The purpose of this synthesis was to investigate its effectiveness in degrading sulfadiazine. The objective of the project is to create cost-effective photocatalysts that are solar-active and tunable, to efficiently degrade and mineralize pharmaceutical pollutants using photochemical processes.[259] Makofane, A. et al. used an extract derived from the Monsonia burkeana plant to synthesize $ZnFe_2O_4$ NPs. The optimal conditions for achieving a 99.8% elimination of MB were a pH of 12, a reaction time of 45 minutes, and a catalyst dose of 25 mg. The ability of the $ZnFe_2O_4$ NPs to be easily separated and recycled, as well as their continued effectiveness even after five reuses, demonstrate the material's great stability. The ROS tests also showed that the key elements causing MB to deteriorate are electrons. Sulfisoxazole in water degraded by 67% when the photocatalytic efficiency of the sulfonamide antibiotic was tested. This study has demonstrated that these materials can be utilised to target water contaminated by textiles and drugs.[260] $CoFe_2O_4$ NPs that were synthesized by Balakrishnan, et al. were produced using the Coprecipitation method. Analyses were conducted on the degradation of ampicillin caused by the cooperative action of $CoFe_2O_4$ and PMS NPs. The estimated optimisation of the impacting parameters during deterioration.[232]

6.3. Spinel ferrites anti-bacterial and anti-microbial studies

A new NC adsorbent, ALW/$CoFe_2O_4$, was made by combining Apocynaceae leaf waste-AC (ALW) with $CoFe_2O_4$ using an auto-combustion technique. This adsorbent was developed to eliminate Reactive Red 141 dye and bacteria, namely S. aureus, E. coli, and C. albicans.[206] The hydrothermal method at 180°C for 15, 20, and 25 hours was effectively used by Sarang R et al. to prepare the spinel ferrite NPs (SFNPs) of $Mg_{0.2}Zn_{0.5}Mn_{0.3}Fe_2O_4$. Through the use of Zone of Influence (ZOI), the antibacterial effectiveness of SFNPs against several harmful bacteria was demonstrated.[261] Kumari et al. described the production of Ca-doped Mg-Zn ferrite $Mg_{0.4}Zn_{(0.6-x)}Ca_xFe_2O_4$ nanomaterials using a citrate precursor method, and they conducted a thorough analysis of their structural, morphological, optical, photocatalytic, and antibacterial properties. The RhB dye solution was degraded by photocatalysis under UV light. On the fungus Candida albicans, every one of the produced nano ferrites showed a promising antibacterial activity. RhB dye may be degraded by $Mg_{0.4}Zn_{0.1}Ca_{0.5}Fe_2O_4$ NPs more effectively (99.5%) and they exhibit greater antibacterial activity (96.1%) when it comes to inhibiting the Candida albicans fungus.[262] Silver-magnetite NPs were combined by El-Bassuony et al. with several magnetic materials, including spinel copper and cobalt nanoferrites, to create NC that was made easily, cheaply, and quickly using auto-combustion. Finally, against the evaluated Gram-positive and Gram-negative species, both samples demonstrated excellent antibacterial effectiveness. As a result, their prospective use as antibacterial NPs in biomedical applications is suggested.[263] The

structural characteristics of combustion-produced nanocrystalline spinel ferrites have the chemical formula $Mg_{0.8x}Cd_xFe_2O_4$ (x = 0.2, 0.4, and 0.6). Using the produced nanocatalysts, the photocatalytic reduction of MB and CR was also studied by Bessy, T. C., et al. When compared to MB, CR deteriorated more successfully. According to antibacterial test results, Pseudomonas aeruginosa, Staphylococcus aureus, Candida albicans, and Aspergillus flavus were all susceptible. To all chosen pathogens, all ferrite NPs displayed antibacterial activity. The most effective of these had a zone of inhibition of 32 mm against P. aeruginosa and was $Cd_{0.2}Mg_{0.6}Fe_2O_4$.[264] The citrate gel method is used by Mordekar, Rajashri Karmali et al. to create the silver-substituted cobalt zinc ferrite series, $Co_xAg_{0.5-x}Zn_{0.5}Fe_2O_4$, with ferrite formation occurring at 600 °C. As silver concentration rises, antimicrobial activity increases before further declining. The material $Co_{0.4}Ag_{0.1}Zn_{0.5}Fe_2O_4$ demonstrates magnetic and antibacterial properties. The creation of removable antimicrobial agents for water filtration and medicine delivery systems may benefit from using these materials.[265] Dhanda et al. used the auto-combustion method, using aloe vera extract as a fuel, to produce nickel-doped cobalt nano ferrites ($Ni_xCo_{1-x}Fe_2O_4$, where x ranges from 0.0 to 1.0 with an increment of 0.2). In addition, the antibacterial capabilities of ferrite NPs were evaluated on the C. albicans fungus, and it was discovered that nickel-doped cobalt ferrite exhibits inhibitory characteristics. The component x = 1.0 had a maximum inhibition of 0.43, corresponding to a 67% reduction in growth. Consequently, these ferrite NPs may be used to treat fungal infections.[266] The sol-gel process was used by Nigam et al. to create the Fe_3O_4 NPs. The antibacterial experiment against E. coli and S.aureus bacteria showed a sizable zone of inhibition.[267] El-Khawaga et al. used co-precipitation to synthesize $CoFe_2O_4$ NPs, which were then subjected to surface modification using Capsaicin derived from Capsicum annuum ssp. The antibacterial potential and photocatalytic degradation efficacy of the generated compounds were evaluated using Fuchsine basic. This study investigated the effectiveness of a substance against two types of bacteria, Staphylococcus aureus (Gram-positive) and Escherichia coli (Gram-negative). The disk diffusion and broth dilution methods were employed to assess the extent of bacterial growth inhibition (zones of inhibition) and the minimum concentration required to completely suppress bacterial growth. The synthesised CPCF NPs showed substantial antibacterial activity against both Gram-positive and Gram-negative bacteria. Additionally, they exhibited exceptional efficacy in removing FB, making them promising for applications in both medicinal and biological environments.[268]
Wendari, et al. used a hydrothermal technique to produce $CuFe_2O_4$/hydroxyapatite magnetic composites. The capping agent employed was betel leaf extract, while Pensi clam shells were used as the source of calcium. The degradation rate of Direct Red 81 was 99.8% after a 2-hour exposure. The combination exhibited antimicrobial activity against both S. aureus and E. coli, resulting in an inhibition zone of 11.9 mm.[269] Blessy and their colleagues documented the synthesis of a range of ferrofluids composed of magnetite (Fe_3O_4) with chromium (Cr) substitution. The amounts of chromium varied from x = 0 to 0.8. The synthesis employs a cost-effective and simple co-precipitation method that stabilizes the product using tetramethylammonium hydroxide (TMOAH). This study focuses on the effectiveness of chromium-substituted ferrofluids in killing Escherichia coli and Staphylococcus aureus bacteria.[270] The coprecipitation approach was used by Hatami Kahkesh et al. to synthesize $CuFe_2O_4$ and $ZnFe_2O_4$ NPs. A study of their antioxidant and antibacterial characteristics was conducted. The $CuFe_2O_4$ NPs have an antioxidant activity of 71%, whereas the $ZnFe_2O_4$ NPs show an antioxidant activity of 80%. Moreover, the study demonstrated that $CuFe_2O_4$ and $ZnFe_2O_4$ NPs had a potent antibacterial impact on Escherichia coli and Staphylococcus aureus.[271]

Table 13. Anti-bacterial activity of spinel ferrites synthesized by different techniques.

S. No	*Material*	*Synthesis method*	*Contaminant*	*Ref*
1	Novel (ALW/$CoFe_2O_4$)	Auto combustion process	Elimination of Reactive Red 141 dye	[206]
2	$Mg_{0.2}Zn_{0.5}Mn_{0.3}Fe_2O_4$	Hydrothermal method	Antibacterial activity against E. coli, B. subtilis, S. aureus and P. aeruginosa bacteria	[261]
3	Ca-doped Mg-Zn ferrite $Mg_{0.4}ZnCa_xFe_2O_4$ nanomaterials	Citrate precursor method	RhB dye	[262]
4	$Mg_{0.8x}Cd_xFe_2O_4$	Combustion	MB and CR	[264]

5	$Co_xAg_{0.5-x}Zn_{0.5}Fe_2O_4$	Citrate gel method	Antimicrobial agents for water purification and drug delivery systems.	[265]
6	$Ni_xCo_{1-x}Fe_2O_4$ nano ferrite	Auto combustion process	Drug against fungus infection.	[266]
7	Fe_3O_4 NPs	Sol-gel process	Good antimicrobial activity	[267]
8	$CoFe_2O_4$ NPs	Co-precipitation	Fuchsine basic	[268]
9	$CuFe_2O$/hydroxyapatite magnetic composites	Hydrothermal method	Direct Red 81 degradation	[269]
10	Chromium-substituted magnetite ($Cr_xFe_{1x}Fe_2O_4$)	Co-precipitation approach	Application in the medical field	[270]
11	$CuFe_2O_4$ and $ZnFe_2O_4$ NPs	Co-precipitation process	Strong bacterial activity	[271]
12	$Mg_xCd_{1-x}Fe_2O_4$ Cd-doped Mg nano ferrites	Citrate gel auto combustion process	Anti-bacterial activity	[272]
13	CS-$NiFe_2O_4$ NPs	Co-precipitation technique	Biomedical applications	[273]
14	Gd-doped $CoFe_2O_4$ nano powder	Auto-combustion process	Anti-microbial and anti-fungal	[274]

The citrate gel auto-combustion method was used by Goud et al. to create $Mg_xCd_{1-x}Fe_2O_4$ (MgCdFO). Mg-Cd nano ferrites exhibit a significant antibacterial activity against both Gram-positive and -negative Klebsiella pneumonia. As a result, the MgCdFO nano ferrite particles might be thought of as potential candidates for use as antimicrobials in the field of medicine due to their substantial growth inhibition against bacteria.[272] Shokri et al. used the co-precipitation process to fabricate an innovative nanomagnet modified with $NiFe_2O_4$ NPs and coated with hybrid chitosan (CS-$NiFe_2O_4$). The antibacterial activities of CS-$NiFe_2O_4$ NPs were more effective than $NiFe_2O_4$ NPs and CS. The CS-$NiFe_2O_4$ NPs exhibited minimum inhibitory concentrations of 128 and 256 mg/mL against S. aureus and E. coli, respectively.[273] Reddy et al. synthesised samples of $CoFe_2O_4$ nano powder doped with gadolinium (Gd) using an easy auto-combustion procedure. The combustion agent used in this process was citric acid. The samples were then subjected to structural, magnetic, and antimicrobial analyses. Both pure $CoFe_2O_4$ and $CoFe_2O_4$ replaced with Gd have antibacterial action against many diseases, including the fungal strain Aspergillus niger, as well as the Gram-positive bacteria Bacillus subtilis and the Gram-negative bacteria Escherichia coli and Pseudomonas aeruginosa. These findings indicate that the replacement of Gd greatly enhances the activity of cobalt ferrite nanopowders. [274]

6.4. Photocatalytic performance enhancement:

The photocatalyst produces electron and hole pairs via the absorption of energy from photons. However, in its pristine form, the catalyst exhibits a substantial rate of electron-hole recombination, resulting in a restricted photocatalytic efficiency. The improved photocatalytic activity observed in CuO/$ZnFe_2O_4$ NCs can be attributed to a synergistic effect that enhances the separation of photo-generated carriers. This effect is facilitated by the internal electric field, which promotes effective charge separation by facilitating the interaction between electrons in the conduction band of CuO and holes concentrated in the valence band of $ZnFe_2O_4$. The decrease in recombination rate prolongs the lifetime of charge carriers. In addition, in proximity to the conduction band edge of $ZnFe_2O_4$, oxygen that is dissolved in a solution utilizes available electrons to initiate oxidation reactions, leading to the generation of a significant quantity of superoxide radicals. Additionally, hydroxyl ions and water molecules trap vacancies in the valence band of CuO, leading to the production of hydroxyl radicals via oxidation reactions. The primary reactive species, $O_2^{\bullet -}$, together with additional species, $OH^{\bullet}$ and h^+, collectively facilitate the effective degradation of the target pollutant, CR, into smaller intermediate compounds.[275] The D-CNFO@G photocatalyst produces free electrons and holes via an electron transition process upon exposure to light. Superoxide $O_2^{\bullet -}$ and hydrogen oxide $HO^{\bullet}$ radicals form because of the interaction between electrons, holes, oxygen molecules, and water on the surface of graphene.[276] RhB may be destroyed via two main mechanisms: direct oxidation by photogenerated holes or by interaction with superoxide or hydroxyl radicals generated by photocatalysts.[277] Azo dyes have aromatic rings that possess an azo bond, which serves as a chromophore. The number of azo bonds may range from one to many. Their aromatic structure provided stability against light and oxidation to these pigments. However, Anthraquinone dyes persist in the effluent for an extended period because they are more resistant to degradation owing to their fused aromatic structure. In addition, the anthraquinone structure has two carbonyl groups, which act as electron acceptors. The

degradation of these dyes takes place via the acceptance of electron donors.[278] When light interacts with the surface of the photocatalyst $Mg_{0.6}Zn_{0.2}Co_{0.2}Fe_2O_4$, charges are produced. MXene sheets function as acceptors by effectively capturing electrons and enhancing the separation of charge carriers. Electrons reduce adsorbed oxygen (O_2) to make superoxide radicals ($O_2^{\bullet-}$), whereas holes oxidize water molecules to produce hydroxyl radical ions ($OH^{\bullet-}$). These species engage with the contaminants and decompose them in the catalytic solution, resulting in the production of not harmful degradation byproducts such as water and carbon dioxide.[279] When the dye solution containing the resultant catalysts is exposed to UV irradiation, electron transfer occurs. Electrons (e^-) move from the valence band of NZF and CO to the conduction band of NZF and CO, respectively. This transfer results in the generation of positively charged holes (h+). The degradation of the dye is attributed to the generation of electrons (e-) and holes (h+) induced by light. Electrons engage in a reaction with oxygen (O_2) to generate superoxide radicals ($O_2^{\bullet-}$) at a potential of -0.046 electron volts (compared to the conventional hydrogen electrode, NHE). On the other hand, the holes react with water (H_2O) to make hydroxyl radicals ($^{\bullet}OH$) at a potential of 2.4 electron volts (compared to NHE). The radicals induce the decomposition of the organic pigment into water (H_2O) and carbon dioxide (CO_2). The probability of superoxide radicals being formed is lower than the conduction band of NZF and CO, whereas the likelihood of hydroxyl radicals being generated is greater than the valence band of CO. The lack of reactivity between the valence band of NZF and H_2O, resulting in the absence of hydroxyl radicals, may be ascribed to the high position of the valence band in NZF. Therefore, both categories of radicals may coexist to participate in the photocatalytic process, and the Z-scheme heterojunction system can enhance the interaction between NZF and CO in the presence of UV light. Furthermore, the exceptional ability of MWCNT to transmit charges expeditiously enhances charge transfer and inhibits the recombination of excitons.[280] Barium hexaferrite ($BaFe_{12}O_{19}$) has a conduction band and valence band between TiO_2. TiO_2's conduction band is greater than barium hexaferrite's and Pt and Pd's Fermi energy levels. Therefore, two techniques are beneficial: Noble metals and barium hexaferrite promote separation as adsorbents. Light energizes TiO_2's valence band VB electrons, which move to the conduction band. Photoexcited electrons travel toward noble metals on titanium oxide and $BaFe_{12}O_{19}$'s conduction band after electron-hole pairs are created. Additionally, the holes created approach the barium hexaferrite valence band. (ii) Noble metals absorb visible light and donate electrons to TiO_2 via surface plasmon resonance (SPR). Electrons in the electric current rise. TiO_2 and $BaFe_{12}O_{19}$ may exchange photoexcited electrons. These reactions may separate electrons and holes, causing dyes to degrade by interacting with water and oxygen to create $O_2^{\bullet}$ and hydroxyl radicals.[281] Using the $CoFe_2O_4$@UiO-66 photocatalyst and the results and talk previously already had, researchers, have come up with a good reaction route for breaking down MB and MO directly through light. When excited by simulated direct sunshine, UiO-66 and $CoFe_2O_4$ create electrons (e^-) and holes (h^+) in their conduction band and valence band. The excited electrons may easily flow across the heterojunction interface channels to reach the LUMO of UiO-66 because $CoFe_2O_4$ has a higher negative CB potential (-0.56 V) than the LUMO (-0.44 V). This approach effectively blocks photogenerated carrier recombination. The electrons generated by photoinduction at the lowest unoccupied molecular orbital (LUMO) of UiO-66 may combine with dissolved oxygen, forming $^{\bullet}O_2^-$ radicals. Light-created gaps would move from UiO-66's valence band (VB) (+3.40 V) to $CoFe_2O_4$'s (+1.07 V). Photogenerated holes cannot oxidize H_2O and form $^{\bullet}OH$ radicals because $CoFe_2O_4$ has a lower VB potential (+1.07 V) than $^-OH/^{\bullet}OH$ (1.99 V versus NHE). However, dye molecules deteriorate fast due to their tremendous oxidation capabilities as holes increase. Alternatively, superoxide ($^{\bullet}O_2^-$) radicals may indirectly form hydroxyl ($^{\bullet}OH$) reactive radicals at the photocatalyst's conduction band.[282]

6.5. Heavy metals removal using spinel ferrites:

The objective of this work was to synthesise $MnFe_2O_4$ and $CoFe_2O_4$ spinel ferrite NPs using a co-precipitation method, to examine their effectiveness in removing zinc from water solutions. The thermodynamics investigations demonstrated that the adsorption of zinc (II) was both exothermic and spontaneous. Additionally, Asadi, Reza, et al. also examined the ability of the adsorbents to be reused and their capacity to release the adsorbed substances.[283] Lingamdinne et al. prepared a nanoscale hybrid material composed of GO and inverse spinel $NiFe_2O_4$ (GONF). Subsequently, this substance is used to extract toxic metals from aqueous solutions. The batch adsorption processes successfully used GONF for the elimination of Pb (II) and Cr (III). Hence, the process of Pb (II) and Cr (III) being attracted to GONF occurred by chemisorption, forming a single layer on the even surface of GONF. The adsorption of metal ions showed a direct relationship with temperature, suggesting that it is a chemisorption process that involves the formation of surface complexes in the inner layer. The results clearly show that GONF is a very efficient sorbent for the removal of Pb(II) and Cr(III) from wastewater.[284] Jung et al. showed the easy production of cubic spinel-type $MnFe_2O_4$ /biochar composites using a simple hydrothermal process. The biochar was coated with $MnFe_2O_4$ spinel NPs, resulting in magnetic separability due to superparamagnetic behaviour. Additionally, the treated biochar exhibited efficient adsorption capability for heavy metals such as Pb (II),

Cu (II), and Cd (II).[285] Sezgin et al. assess the effectiveness of $CuFe_2O_4$ and $NiFe_2O_4$ NPs in the removal of zinc, nickel, and copper heavy metals from synthetic wastewater. NPs of $CuFe_2O_4$ and $NiFe_2O_4$ were synthesized using the PEG-assisted hydrothermal method. Subsequently, the NPs ($CuFe_2O_4$ and $NiFe_2O_4$) were used to determine the extent to which they can effectively remove heavy metals and their capacity to adsorb these metals.[286] The synthesis of $NiFe_2O_4$ NPs (NFNs) was carried out by the co-precipitation technique from a research group. Subsequently, these NPs were used as an adsorbent to eliminate Cr(VI), Pb(II), and Cd(II) from wastewater.[287] $ZnFe_2O_4$-Alginate beads, referred to as ZFN-Alg beads, were created by Kumar et al. The results indicate the feasibility and cost-effectiveness of using magnetic biopolymer beads for the removal of Pb(II) and Cu(II) metal ions from both single and combined systems.[173] Ramadan et al. utilized the flash auto-combustion approach was used to synthesise different compositions of $CuFe_2O_4$, Zn-$CuFe_2O_4$, and Co-$CuFe_2O_4$. The samples that were created were tested to evaluate their effectiveness in eliminating the heavy metal Cr^{6+} from water. Optimal outcomes were achieved by adjusting the experimental parameters, namely by maintaining a pH level of 7 and allowing a contact period of 50 minutes. The $CuFe_2O_4$, Zn-$CuFe_2O_4$, and Co-$CuFe_2O_4$ NCs exhibited removal efficiencies of 54%, 90%, and 93% accordingly.[288] Camacho et al. produced zinc-copper ferrites ($Zn_{1-x}Cu_xFe_2O_4$) by the simple hydrothermal technique. After 24 hours, Z2C7 exhibited a relatively low efficacy in reducing Cr^{6+} compared to Pb^{2+} and Ni^{2+}. After 24 hours, Z2C7, Z5C5, and Z7C2 demonstrated a 100% efficacy in eliminating Ni^{2+} and Pb^{2+}, at a dosage of 0.5 g.[289] Lingamdinne et.al., synthesized biogenic MISFNPs from Cnidiummonnieri (L.) Cuss (CLC) seed extract. MISFNPs were utilized in batch tests to remove Pb (II) and Cr (III) from aqueous solutions and also showed that NPs adsorb Pb (II) and Cr (III) endothermically. Finally, green-synthesised MISFNPs can recycle and remove heavy metals without losing stability.[290] The process of microwave combustion was used by Al Yaqoob et al. to synthesize NPs of spinel ferrite MFe_2O_4. Metal nitrates were utilized as precursors, while urea served as the fuel. The MNPs, in their original state, exhibit enhanced efficacy in adsorbing Cd^{2+} and Pb^{2+} ions, with a maximum adsorption capacity of 69.4 mg/g and 47.1 mg/g, respectively. Remarkably, the presence of metal M influences selectivity: $CoFe_2O_4$ exhibits a preference for Cd^{2+} ions, while $ZnFe_2O_4$ exhibits a preference for Pb^{2+} ions.[291] A one-step solvothermal approach was used by Guo et al. to produce novel magnetic composites consisting of amino-modified rice bran biochar and $MgFeAlO_4$ (RB@$MgFeAlO_4$-NH_2). These composites were specifically designed to efficiently eliminate toxic Ni (II) from wastewater. The study investigated the removal and sorption of Ni (II) on RB@$MgFeAlO_4$-NH_2 using a combination of batch experiments and spectrum approaches. RB@$MgFeAlO_4$-NH_2 is a very efficient adsorbent for extracting Ni (II) from aqueous solutions due to its eco-friendliness, low cost, ease of magnetic separation, and high sorption capacity.[204] Narayana et al. prepared NC consisting of rGO-based inverse spinel $NiFe_2O_4$ (rGO-SNF) created to remove Pb (II). Lead (II) is a toxic heavy metal that is a significant pollutant in water pollution.[292] Tatarchuk et al. conducted a study to explore the capabilities of magnesium-zinc ferrites, namely $Mg_{1-x}Zn_xFe_2O_4$, as magnetic sorbents for environmental purposes. The research found that the adsorption processes of Cr (VI) and Ni (II) ions are mostly chemical. The produced magnesium-zinc ferrites have shown significant promise as magnetic adsorbents for the environmental removal of chromate and nickel ions.[293] The compound $Cu_{0.5}Mg_{0.5}Fe_2O_4$ was produced by a co-precipitation technique from Tran et al. and then subjected to calcination at a temperature of 900°C. The compound was then studied for its ability to adsorb Pb (II). The findings obtained have verified that the $Cu_{0.5}$ $Mg_{0.5}Fe_2O_4$ ternary oxides have a significant ability to adsorb Pb (II) due to the increased number of active adsorptive sites on the ferrite.[294] Tavares et al. examined the use of spinel ferrite particles (Fe_3O_4, $MnFe_2O_4$, and $CoFe_2O_4$) as magnetic nanosorbents to remove arsenic from water samples that were intentionally contaminated. Furthermore, these magnetic nano sorbents also show outstanding performance in sorbing As (V).[295] Iqbal et al. investigated the production, examination, and capacity to draw in molecules of spinel $CoFe_2O_4$ NPs that have been modified with rGO. The adsorption capabilities of the NC were assessed by examining its capacity to adsorb cationic CV, brilliant green (BG), anionic MO, and CR dyes. Hence, the NC exhibited remarkable adsorption properties for the removal of dyes and heavy metals.[296] Kumari et al. used the co-precipitation process to generate $NiFe_2O_4$ and $NiFe_2O_4$ doped with alkaline earth metals to effectively remove toxic components like Cd (II) and Pb (II). $NiFe_2O_4$ have removal efficiencies of 45% and 83% for Cd and Pb ions, respectively. Nevertheless, Pb (II) and Cd (II) clearance percentages improve to 97% and 80% respectively when $NiFe_2O_4$ are doped. The results suggest that mesoporous ferrites, as determined through BET analysis, demonstrate effective adsorption capabilities for the removal of heavy metals from wastewater. Furthermore, these ferrites exhibit a high level of recyclability and can be easily separated using an external magnetic field.[297]

7. Future research gaps:

Future research on spinel ferrites for dye degradation must address several critical gaps to enhance their efficiency and practical applicability. Achieving accurate manipulation of the size, shape, and surface characteristics of spinel ferrites, while also implementing scalable and cost-effective techniques,

remains a top priority in their synthesis. Enhancing surface area and porosity to improve interaction with dye molecules, and investigating the effects of doping and cation substitution to tailor catalytic properties, are crucial for optimization. Assessing the long-term stability and performance under various environmental conditions, and developing methods for regeneration and reuse without significant loss of catalytic activity, are vital for practical applications. Exploring the integration of spinel ferrites with other materials and technologies, such as photocatalysts and advanced oxidation processes, can enhance overall degradation efficiency. Identifying and characterizing by-products to ensure they are not harmful, and conducting comprehensive toxicity studies to assess the environmental impact of both the spinel ferrites and the degradation by-products, are also important. Pilot-scale studies to evaluate performance in real wastewater treatment scenarios, considering the presence of multiple contaminants, are necessary to bridge the gap between laboratory research and practical applications. Additionally, a cost-benefit analysis comparing spinel ferrites with existing dye degradation technologies will help assess their practical viability. Addressing these gaps will significantly enhance the understanding and effectiveness of spinel ferrites in dye degradation, leading to more efficient, sustainable, and economically viable solutions for treating dye-contaminated wastewater and contributing to environmental protection and public health.

The world's dye-based industries are now encountering significant obstacles, including intense rivalry, excess production capacity, declining profit margins, and heightened environmental concerns. This has led to a widespread reluctance to provide funds for overhead costs, such as research and development and wastewater treatment. Therefore, finding a cost-effective solution to remove colour and toxicity from effluents is still a significant challenge. The complexity of dye removal is further complicated by the wide range of structural variations among dyes that may be used in a single dyeing process, as well as by additional components present in wastewater that might hinder the treatment process.[298] The extensive use of synthetic dyes in the dyeing of textiles is leading to significant environmental contamination and damage to aquatic ecosystems. These dyes are derived from petrochemical sources and include possibly carcinogenic and poisonous substances.[299] By systematically addressing these research gaps, spinel ferrites can be further developed as a key material in environmental remediation technologies, ultimately providing more robust and versatile solutions for managing dye pollutants and contributing to environmental protection and public health.

8. Conclusion

This review focuses on the use of spinel ferrites in the treatment of wastewater contaminated with dyes. It highlights the potential of spinel ferrites as a cost-effective, efficient, and sustainable solution. Spinel ferrites, which have the general formula AB_2O_4, possess unique properties such as a high surface area, porosity, magnetic characteristics, chemical stability, and corrosion resistance. These properties make them highly effective in adsorbing and degrading dye pollutants. The catalytic properties of spinel ferrites enable advanced oxidation processes, leading to the efficient degradation of organic dyes. Moreover, the magnetic nature of spinel ferrites allows for easy separation from treated water, enabling their reuse and reducing operational costs. Research has shown that spinel ferrites can effectively remove a wide range of dye contaminants from real wastewater, and their ability to be regenerated ensures their long-term applicability. Spinel ferrites are environmentally friendly and scalable for industrial applications, making them versatile in treating various sources of dye-laden wastewater, including industrial effluents and textile wastewater. Despite their promise, there are challenges that need to be addressed, such as developing cost-effective synthesis methods, optimizing operational parameters for real wastewater conditions, and ensuring long-term stability and performance in continuous systems. Combining spinel ferrites with other technologies, such as membranes and biochar, could further enhance treatment efficiency. The integration of spinel ferrites into hybrid systems and their ability to function under diverse environmental conditions make them a promising solution for future innovations in dye degradation.

The review also discusses different synthesis methods for spinel ferrites, including sol-gel, coprecipitation, hydrothermal, microemulsion, template, sonochemical, electrochemical, flame spray pyrolysis, and electrospinning. Each method has an impact on the properties and performance of spinel ferrites in dye degradation, with specific advantages in terms of cost, scalability, and control over material characteristics. Sol-gel and coprecipitation methods are known for producing uniform and high-purity spinel ferrites, while hydrothermal synthesis and solid-state reactions offer simplicity and potential for large-scale production. Microemulsion and template methods provide precise control over particle size and morphology, sonochemical and electrochemical methods enable rapid synthesis, flame spray pyrolysis allows for large-scale production, and electrospinning creates fibrous structures with a high surface area. Additionally, the review discusses the classification of spinel ferrites based on the number and type of metal

ions involved, such as mono, bi, tri-metallic, or those incorporating noble metals. Mono-metallic spinel ferrites contain a single type of metal ion, while bi-metallic and tri-metallic variants include two or three different metal ions, respectively, enhancing their catalytic and adsorption properties. The inclusion of noble metals can further improve the efficiency and stability of spinel ferrites in dye degradation processes.

References:

1. Theron, J., J.A. Walker, and T.E. Cloete, *Nanotechnology and water treatment: applications and emerging opportunities.* Critical reviews in microbiology, 2008. **34**(1): p. 43-69.
2. Darling, S.B. and S.W. Snyder, *Water Is...: The Indispensability of Water in Society and Life*. 2018: World Scientific.
3. Ward, F.A., et al., *The economics of aquifer protection plans under climate water stress: New insights from hydroeconomic modeling.* Journal of Hydrology, 2019. **576**: p. 667-684.
4. Jiang, L., et al., *The effects of water stress on croplands in the Aral Sea basin.* Journal of Cleaner Production, 2020. **254**: p. 120114.
5. Lee, U., et al., *AWARE-US: Quantifying water stress impacts of energy systems in the United States.* Science of the total environment, 2019. **648**: p. 1313-1322.
6. McNabb, D.E., *Global pathways to water sustainability*. 2019: Springer.
7. Omer, A., et al., *Water scarcity in the Yellow River Basin under future climate change and human activities.* Science of the Total Environment, 2020. **749**: p. 141446.
8. Ram, S.A. and Z.B. Irfan, *Application of System Thinking Causal Loop Modelling in understanding water Crisis in India: A case for sustainable Integrated Water resources management across sectors.* HydroResearch, 2021. **4**: p. 1-10.
9. Shan, V., S. Singh, and A. Haritash, *Water Crisis in the Asian countries: status and future trends.* Resilience, Response, and Risk in Water Systems: Shifting Management and Natural Forcings Paradigms, 2020: p. 173-194.
10. Liu, J., Q. Liu, and H. Yang, *Assessing water scarcity by simultaneously considering environmental flow requirements, water quantity, and water quality.* Ecological indicators, 2016. **60**: p. 434-441.
11. Sharma, S.K., R. Sanghi, and A. Mudhoo, *Green practices to save our precious "water resource".* Advances in water treatment and pollution prevention, 2012: p. 1-36.
12. Inwald, J.F., et al., *Public Concern about Water Safety, Weather, and Climate: Insights from the World Risk Poll.* Environmental Science & Technology, 2023. **57**(5): p. 2075-2083.
13. Boholm, Å. and M. Prutzer, *Experts' understandings of drinking water risk management in a climate change scenario.* Climate Risk Management, 2017. **16**: p. 133-144.
14. Madhav, S., et al., *Water pollutants: sources and impact on the environment and human health.* Sensors in water pollutants monitoring: Role of material, 2020: p. 43-62.
15. Wasewar, K.L., S. Singh, and S.K. Kansal, *Process intensification of treatment of inorganic water pollutants*, in *Inorganic pollutants in water*. 2020, Elsevier. p. 245-271.
16. Liosis, C., et al., *Heavy metal adsorption using magnetic nanoparticles for water purification: A critical review.* Materials, 2021. **14**(24): p. 7500.
17. Vikrant, K., et al., *Recent advancements in bioremediation of dye: current status and challenges.* Bioresource technology, 2018. **253**: p. 355-367.
18. Bilal, M., et al., *Clean-green technologies for removal of emerging contaminants from industrial effluents*, in *Bioremediation for Environmental Sustainability*. 2021, Elsevier. p. 125-145.
19. Karri, R.R., G. Ravindran, and M.H. Dehghani, *Wastewater—sources, toxicity, and their consequences to human health*, in *Soft computing techniques in solid waste and wastewater management*. 2021, Elsevier. p. 3-33.
20. Mani, S. and R.N. Bharagava, *Textile industry wastewater: environmental and health hazards and treatment approaches*, in *Recent advances in environmental management*. 2018, CRC Press. p. 47-69.
21. Hunger, K., *Industrial dyes: chemistry, properties, applications*. 2007: John Wiley & Sons.
22. Liu, J., et al., *Adsorption of Congo red dye on FexCo3-xO4 nanoparticles.* Journal of environmental management, 2019. **238**: p. 473-483.
23. Zhang, D., et al., *One-step combustion synthesis of CoFe2O4–graphene hybrid materialsfor photodegradation of methylene blue.* Materials Letters, 2013. **113**: p. 179-181.
24. Zhu, H.-Y., et al., *Novel magnetic NiFe2O4/multi-walled carbon nanotubes hybrids: facile synthesis, characterization, and application to the treatment of dyeing wastewater.* Ceramics International, 2015. **41**(9): p. 11625-11631.
25. Bai, S., et al., *One-pot solvothermal preparation of magnetic reduced graphene oxide-ferrite hybrids for organic dye removal.* Carbon, 2012. **50**(6): p. 2337-2346.
26. Sun, J., et al., *A magnetically separable P25/CoFe 2 O 4/graphene catalyst with enhanced adsorption capacity and visible-light-driven photocatalytic activity.* RSC advances, 2013. **3**(44): p. 22490-22497.
27. Xiong, P., J. Zhu, and X. Wang, *Cadmium sulfide–ferrite nanocomposite as a magnetically recyclable photocatalyst with enhanced visible-light-driven photocatalytic activity and photostability.* Industrial & Engineering Chemistry Research, 2013. **52**(48): p. 17126-17133.
28. Fu, Y., et al., *Copper ferrite-graphene hybrid: a multifunctional heteroarchitecture for photocatalysis and energy storage.* Industrial & engineering chemistry research, 2012. **51**(36): p. 11700-11709.
29. Ji, H., et al., *Magnetic gC 3 N 4/NiFe 2 O 4 hybrids with enhanced photocatalytic activity.* RSC Advances, 2015. **5**(71): p. 57960-57967.
30. Zhang, W., et al., *Magnetic composite photocatalyst ZnFe 2 O 4/BiVO 4: synthesis, characterization, and visible-light photocatalytic activity.* Dalton Transactions, 2013. **42**(43): p. 15464-15474.
31. Yao, Y., et al., *Magnetic ZnFe2O4–C3N4 hybrid for photocatalytic degradation of aqueous organic pollutants by visible light.* Industrial & Engineering Chemistry Research, 2014. **53**(44): p. 17294-17302.
32. Wu, S., et al., *Reduced graphene oxide anchored magnetic ZnFe 2 O 4 nanoparticles with enhanced visible-light photocatalytic activity.* RSC Advances, 2015. **5**(12): p. 9069-9074.
33. Khadgi, N., et al., *Enhanced Photocatalytic Degradation of 17α-Ethinylestradiol Exhibited by Multifunctional ZnFe2O4–Ag/rGO Nanocomposite Under Visible Light.* Photochemistry and Photobiology, 2016. **92**(2): p. 238-246.
34. Chen, X., et al., *Novel magnetically separable reduced graphene oxide (RGO)/ZnFe2O4/Ag3PO4 nanocomposites for enhanced photocatalytic performance toward 2, 4-dichlorophenol under visible light.* Industrial & engineering chemistry research, 2016. **55**(3): p. 568-578.
35. Kulkarni, S.D., et al., *Magnetically separable core–shell ZnFe2O4@ ZnO nanoparticles for visible light photodegradation of methyl orange.* Materials Research Bulletin, 2016. **77**: p. 70-77.
36. Yao, Y., et al., *One-pot approach for synthesis of N-doped TiO2/ZnFe2O4 hybrid as an efficient photocatalyst for degradation of aqueous organic pollutants.* Journal of Hazardous Materials, 2015. **291**: p. 28-37.

37. Wu, S., et al., *Synthesis of ternary Ag/ZnO/ZnFe2O4 porous and hollow nanostructures with enhanced photocatalytic activity.* Applied Catalysis B: Environmental, 2016. **184**: p. 328-336.
38. Ren, A., et al., *Enhanced visible-light-driven photocatalytic activity for antibiotic degradation using magnetic NiFe2O4/Bi2O3 heterostructures.* Chemical engineering journal, 2014. **258**: p. 301-308.
39. Fu, Y., et al., *Graphene-supported nickel ferrite: A magnetically separable photocatalyst with high activity under visible light.* AIChE Journal, 2012. **58**(11): p. 3298-3305.
40. Ivanets, A., et al., *Effect of metal ions adsorption on the efficiency of methylene blue degradation onto MgFe2O4 as Fenton-like catalysts.* Colloids and Surfaces A: Physicochemical and Engineering Aspects, 2019. **571**: p. 17-26.
41. Feng, Y., C. Liao, and K. Shih, *Copper-promoted circumneutral activation of H2O2 by magnetic CuFe2O4 spinel nanoparticles: mechanism, stoichiometric efficiency, and pathway of degrading sulfanilamide.* Chemosphere, 2016. **154**: p. 573-582.
42. Desai, H.B., et al., *Synthesis and characterization of photocatalytic MnFe2O4 nanoparticles.* Materials Today: Proceedings, 2020. **21**: p. 1905-1910.
43. Trier, S.H. and M.S. Abdali, *The structural, magnetic, and optical properties of Cu1-xCoxFe2O4 spinel ferrite and its applications.* Al-Qadisiyah Journal Of Pure Science, 2020. **25**(3): p. 1-15.
44. Zhang, L. and Y. Wu, *Sol-gel synthesized magnetic MnFe2O4 spinel ferrite nanoparticles as novel catalyst for oxidative degradation of methyl orange.* Journal of Nanomaterials, 2013. **2013**: p. 2-2.
45. Jasrotia, R., et al., *Magnetic and electrical traits of sol-gel synthesized Ni-Cu-Zn nanosized spinel ferrites for multi-layer chip inductors application.* Journal of Solid State Chemistry, 2020. **289**: p. 121462.
46. Junaid, M., et al., *Structural, spectral, dielectric and magnetic properties of indium substituted copper spinel ferrites synthesized via sol gel technique.* Ceramics International, 2020. **46**(17): p. 27410-27418.
47. Khirade, P.P., et al., *Tuning of physical properties of multifunctional Mg-Zn spinel ferrite nanocrystals: a comparative investigations manufactured via conventional ceramic versus green approach sol-gel combustion route.* Materials Research Express, 2020. **7**(11): p. 116102.
48. Samoila, P., et al., *Nanosized spinel ferrites synthesized by sol-gel autocombustion for optimized removal of azo dye from aqueous solution.* Journal of Nanomaterials, 2015. **16**(1): p. 237-237.
49. Wu, R., et al., *Removal of azo-dye Acid Red B (ARB) by adsorption and catalytic combustion using magnetic CuFe2O4 powder.* Applied Catalysis B: Environmental, 2004. **48**(1): p. 49-56.
50. Vinosha, P.A. and S.J. Das, *Investigation on the role of pH for the structural, optical and magnetic properties of cobalt ferrite nanoparticles and its effect on the photo-fenton activity.* Materials Today: Proceedings, 2018. **5**(2): p. 8662-8671.
51. Vinosha, P.A., et al., *Nanocrystalline ferrite (MFe2O4, M= Ni, Cu, Mn and Sr) photocatalysts synthesized by homogeneous Co-precipitation technique.* Optik, 2018. **157**: p. 441-448.
52. Kaur, N. and M. Kaur, *Comparative studies on impact of synthesis methods on structural and magnetic properties of magnesium ferrite nanoparticles.* Processing and Application of Ceramics, 2014. **8**(3): p. 137-143.
53. Reyes-Rodríguez, P.Y., et al., *Structural and magnetic properties of Mg-Zn ferrites (Mg1− xZnxFe2O4) prepared by sol-gel method.* Journal of Magnetism and Magnetic Materials, 2017. **427**: p. 268-271.
54. Ajeesha, T., et al., *Nickel substituted MgFe2O4 nanoparticles via co-precipitation method for photocatalytic applications.* Physica B: Condensed Matter, 2021. **606**: p. 412660.
55. Irshad, A., et al., *Co-substituted Mg–Zn spinel nanocrystalline ferrites: Synthesis, characterization and evaluation of catalytic degradation efficiency for colored and colorless compounds.* Ceramics International, 2022. **48**(20): p. 29805-29815.
56. Su, M., et al., *Mesoporous zinc ferrite: synthesis, characterization, and photocatalytic activity with H2O2/visible light.* Journal of hazardous materials, 2012. **211**: p. 95-103.
57. Liu, S.-Q., et al., *Magnetic nickel ferrite as a heterogeneous photo-Fenton catalyst for the degradation of rhodamine B in the presence of oxalic acid.* Chemical Engineering Journal, 2012. **203**: p. 432-439.
58. Moreno-Castilla, C., et al., *Removal of phenolic compounds from water using copper ferrite nanosphere composites as fenton catalysts.* Nanomaterials, 2019. **9**(6): p. 901.
59. Kurian, J. and M.J. Mathew, *Structural, optical and magnetic studies of CuFe2O4, MgFe2O4 and ZnFe2O4 nanoparticles prepared by hydrothermal/solvothermal method.* Journal of Magnetism and Magnetic Materials, 2018. **451**: p. 121-130.
60. Fotukian, S.M., et al., *Solvothermal synthesis of CuFe2O4 and Fe3O4 nanoparticles with high heating efficiency for magnetic hyperthermia application.* Journal of Alloys and Compounds, 2020. **816**: p. 152548.
61. Rodríguez-Rodríguez, A.A., et al., *Spinel-type ferrite nanoparticles: Synthesis by the oil-in-water microemulsion reaction method and photocatalytic water-splitting evaluation.* international journal of hydrogen energy, 2019. **44**(24): p. 12421-12429.
62. Pemartin, K., et al., *Synthesis of Mn–Zn ferrite nanoparticles by the oil-in-water microemulsion reaction method.* Colloids and Surfaces A: Physicochemical and Engineering Aspects, 2014. **451**: p. 161-171.
63. Ali, R., et al., *Structural, magnetic and dielectric behavior of Mg1− xCaxNiyFe2− yO4 nano-ferrites synthesized by the micro-emulsion method.* Ceramics International, 2014. **40**(3): p. 3841-3846.
64. Ganure, K.A., et al., *Synthesis and characterization of lanthanum-doped Ni-Co-Zn spinel ferrites nanoparticles via normal micro-emulsion method.* Int. J. Nanotechnol. Appl, 2017. **11**(2): p. 189-195.
65. Gilani, Z.A., et al., *Impacts of neodymium on structural, spectral and dielectric properties of LiNi0. 5Fe2O4 nanocrystalline ferrites fabricated via micro-emulsion technique.* Physica E: Low-dimensional Systems and Nanostructures, 2015. **73**: p. 169-174.
66. Uskoković, V., M. Drofenik, and I. Ban, *The characterization of nanosized nickel-zinc ferrites synthesized within reverse micelles of CTAB/1–hexanol/water microemulsion.* Journal of Magnetism and Magnetic Materials, 2004. **284**: p. 294-302.
67. Misra, R., et al., *Synthesis of nanocrystalline nickel and zinc ferrites by microemulsion technique.* Materials science and technology, 2003. **19**(6): p. 826-830.
68. Gu, M., et al., *Template synthesis of magnetic one-dimensional nanostructured spinel MFe2O4 (M= Ni, Mg, Co).* Materials Research Bulletin, 2009. **44**(6): p. 1422-1427.
69. Gao, Z., et al., *A high surface area superparamagnetic mesoporous spinel ferrite synthesized by a template-free approach and its adsorptive property.* Microporous and mesoporous materials, 2010. **132**(1-2): p. 188-195.
70. Enlei, Z., et al., *Efficient Fenton oxidation of Congo red dye by magnetic MgFe2O4 nanorods.* Journal of Nanoscience and Nanotechnology, 2016. **16**(5): p. 4727-4732.
71. El-Sheikh, S.M., F.A. Harraz, and M.M. Hessien, *Magnetic behavior of cobalt ferrite nanowires prepared by template-assisted technique.* Materials Chemistry and Physics, 2010. **123**(1): p. 254-259.
72. Yu, B.Y. and S.-Y. Kwak, *Self-assembled mesoporous Co and Ni-ferrite spherical clusters consisting of spinel nanocrystals prepared using a template-free approach.* Dalton Transactions, 2011. **40**(39): p. 9989-9998.
73. Yourdkhani, A. and G. Caruntu, *Highly ordered transition metal ferrite nanotube arrays synthesized by template-assisted*

liquid phase deposition. Journal of Materials Chemistry, 2011. **21**(20): p. 7145-7153.
74. Zhao, B. and Z. Nan, *One-pot synthesis of ZnLa x Fe 2− x O 4 clusters without any template and their possible application in water treatment.* Journal of Materials Chemistry, 2012. **22**(14): p. 6581-6586.
75. Rajput, J.K., et al., *CuFe2O4 magnetic heterogeneous nanocatalyst: Low power sonochemical-coprecipitation preparation and applications in synthesis of 4H-chromene-3-carbonitrile scaffolds.* Ultrasonics sonochemistry, 2015. **26**: p. 229-240.
76. Almessiere, M.A., et al., *Sonochemical synthesis and physical properties of Co0. 3Ni0. 5Mn0. 2EuxFe2− xO4 nano-spinel ferrites.* Ultrasonics sonochemistry, 2019. **58**: p. 104654.
77. Yadav, R.S., et al., *Impact of sonochemical synthesis condition on the structural and physical properties of MnFe2O4 spinel ferrite nanoparticles.* Ultrasonics sonochemistry, 2020. **61**: p. 104839.
78. Yousefi, S.R., O. Amiri, and M. Salavati-Niasari, *Control sonochemical parameter to prepare pure Zn0. 35Fe2. 65O4 nanostructures and study their photocatalytic activity.* Ultrasonics sonochemistry, 2019. **58**: p. 104619.
79. Yadav, R.S., et al., *Sonochemical synthesis of Gd3+ doped CoFe2O4 spinel ferrite nanoparticles and its physical properties.* Ultrasonics sonochemistry, 2018. **40**: p. 773-783.
80. Amulya, M.S., et al., *Sonochemical synthesis of NiFe2O4 nanoparticles: Characterization and their photocatalytic and electrochemical applications.* Applied Surface Science Advances, 2020. **1**: p. 100023.
81. Ilosvai, A.M., et al., *Sonochemical combined synthesis of nickel ferrite and cobalt ferrite magnetic nanoparticles and their application in glycan analysis.* International journal of molecular sciences, 2022. **23**(9): p. 5081.
82. Goswami, P.P., et al., *Sonochemical synthesis of cobalt ferrite nanoparticles.* International Journal of Chemical Engineering, 2013. **2013**.
83. Almessiere, M.A., et al., *Synthesis of Dy-Y co-substituted manganese-zinc spinel nanoferrites induced anti-bacterial and anti-cancer activities: Comparison between sonochemical and sol-gel auto-combustion methods.* Materials Science and Engineering: C, 2020. **116**: p. 111186.
84. Goswami, P.P., et al., *Sonochemical synthesis and characterization of manganese ferrite nanoparticles.* Industrial & Engineering Chemistry Research, 2013. **52**(50): p. 17848-17855.
85. Mazarío, E., et al., *Synthesis and characterization of manganese ferrite nanoparticles obtained by electrochemical/chemical method.* Materials & Design, 2016. **111**: p. 646-650.
86. Mazarío, E., et al., *Synthesis and characterization of CoFe2O4 ferrite nanoparticles obtained by an electrochemical method.* Nanotechnology, 2012. **23**(35): p. 355708.
87. Es' haghzade, Z., et al., *Facile synthesis of Fe3O4 nanoparticles via aqueous based electro chemical route for heterogeneous electro-Fenton removal of azo dyes.* Journal of the Taiwan Institute of Chemical Engineers, 2017. **71**: p. 91-105.
88. Ovejero, J.G., et al., *Electrochemical synthesis and magnetic properties of MFe2O4 (M= Fe, Mn, Co, Ni) nanoparticles for potential biomedical applications.* Journal of Nanoscience and Nanotechnology, 2019. **19**(4): p. 2008-2015.
89. Mazario, E., et al., *Influence of the temperature in the electrochemical synthesis of cobalt ferrites nanoparticles.* Journal of alloys and compounds, 2012. **536**: p. S222-S225.
90. Lakshmi Ranganatha, V., et al., *Cost-effective and green approach for the synthesis of zinc ferrite nanoparticles using Aegle Marmelos extract as a fuel: catalytic, electrochemical, and microbial applications.* Journal of Materials Science: Materials in Electronics, 2020. **31**: p. 17386-17403.
91. Kotsikau, D., et al., *Structure and magnetic properties of manganese–zinc-ferrites prepared by spray pyrolysis method.* Solid State Sciences, 2015. **39**: p. 69-73.
92. Hong, D., et al., *Mesoporous nickel ferrites with spinel structure prepared by an aerosol spray pyrolysis method for photocatalytic hydrogen evolution.* ACS Sustainable Chemistry & Engineering, 2014. **2**(11): p. 2588-2594.
93. Chavan, A.R., et al., *Diverse physical characteristics of mixed Li–Mg spinel ferrite thin films fabricated by spray pyrolysis technique.* Physica B: Condensed Matter, 2021. **615**: p. 413075.
94. Li, Y., et al., *General flame approach to chainlike MFe2O4 spinel (M= Cu, Ni, Co, Zn) nanoaggregates for reduction of nitroaromatic compounds.* Industrial & Engineering Chemistry Research, 2015. **54**(40): p. 9750-9757.
95. Chavan, A.R., et al., *Cu2+ substituted NiFe2O4 thin films via spray pyrolysis technique and their high-frequency devices application.* Journal of Alloys and Compounds, 2018. **769**: p. 1132-1145.
96. Zheng, J., et al., *One step synthesis process for fabricating NiFe2O4 nanoparticle loaded porous carbon spheres by ultrasonic spray pyrolysis.* Advanced Powder Technology, 2018. **29**(6): p. 1474-1480.
97. Lorentzou, S., C.C. Agrafiotis, and A.G. Konstandopoulos, *Aerosol spray pyrolysis synthesis of water-splitting ferrites for solar hydrogen production.* Granular matter, 2008. **10**(2): p. 113-122.
98. Ozdemir, E.T., et al., *Effects of annealing on the structural and magnetic properties of flame spray pyrolyzed MnFe2O4 nanoparticles.* International Journal of Applied Ceramic Technology.
99. Maensiri, S., M. Sangmanee, and A. Wiengmoon, *Magnesium ferrite (MgFe 2 O 4) nanostructures fabricated by electrospinning.* Nanoscale research letters, 2009. **4**: p. 221-228.
100.Kaur, G.A., et al., *Modification of structural and magnetic properties of Co0. 5Ni0. 5Fe2O4 nanoparticles embedded Polyvinylidene Fluoride nanofiber membrane via electrospinning method.* Nano-Structures & Nano-Objects, 2020. **22**: p. 100428.
101.El-Rafei, A., A.S. El-Kalliny, and T.A. Gad-Allah, *Electrospun magnetically separable calcium ferrite nanofibers for photocatalytic water purification.* Journal of Magnetism and Magnetic Materials, 2017. **428**: p. 92-98.
102.Na, K.-H., et al., *Fabrication and characterization of the magnetic ferrite nanofibers by electrospinning process.* Thin Solid Films, 2018. **660**: p. 358-364.
103.Alahmari, F., et al., *Electrical and optical properties of Ni0· 5Co0. 5-xCdxNd0. 02Fe1· 78O4 (x≤ 0.25) spinel ferrite nanofibers.* Ceramics International, 2020. **46**(15): p. 24605-24614.
104.Dorneanu, P.P., et al., *Electrospun PVDF fibers and a novel PVDF/CoFe2O4 fibrous composite as nanostructured sorbent materials for oil spill cleanup.* Applied Surface Science, 2017. **424**: p. 389-396.
105.Nilmoung, S., et al., *Fabrication, structure, and magnetic properties of electrospun carbon/cobalt ferrite (C/CoFe 2 O 4) composite nanofibers.* Applied Physics A, 2015. **119**: p. 141-154.
106.Sertkol, M., et al., *Effect of Bi3+ ions substitution on the structure, morphology, and magnetic properties of Co–Ni spinel ferrite nanofibers.* Materials Chemistry and Physics, 2022. **284**: p. 126071.
107.Jun, X., et al., *Fabrication and magnetic properties of Ni0. 5Zn0. 5Fe2O4 nanofibres by electrospinning.* Chinese Physics B, 2009. **18**(11): p. 4960.
108.Li, J., et al., *Synthesis, characterization and magnetic properties of NiFe2− xCexO4 nanoribbons by electrospinning.* Journal of Magnetism and Magnetic Materials, 2017. **425**: p. 37-42.
109.Almessiere, M.A., et al., *Structural and magnetic properties of Co0. 5Ni0. 5Ga0. 01Gd0. 01Fe1. 98O4/ZnFe2O4 spinel ferrite nanocomposites: Comparative study between sol-gel and pulsed laser ablation in liquid approaches.* Nanomaterials, 2021. **11**(9): p. 2461.
110.Almessiere, M.A., et al., *Morphological, structural, and magnetic characterizations of hard-soft ferrite nanocomposites synthesized via pulsed laser ablation in liquid.* Materials Science and Engineering: B, 2021. **273**: p. 115446.

111.Yang, A., et al., *Cation engineering of Cu-ferrite films deposited by alternating target laser ablation deposition.* Journal of Applied Physics, 2008. **103**(7).
112.Sadiq Mohamed, M.J., et al., *Se-Doped Magnetic Co–Ni Spinel Ferrite Nanoparticles as Electrochemical Catalysts for Hydrogen Evolution.* ACS Applied Nano Materials, 2023. **6**(9): p. 7330-7341.
113.Özçelik, S., et al., *Structure, magnetic, photocatalytic and blood compatibility studies of nickel nanoferrites prepared by laser ablation technique in distilled water.* Journal of Alloys and Compounds, 2021. **854**: p. 157279.
114.Yang, A., et al., *Magnetism, Structure, and Cation Distribution in MnFe $ _2 $ O $ _4 $ Films Processed by Conventional and Alternating Target Laser Ablation Deposition.* IEEE transactions on magnetics, 2006. **42**(10): p. 2870-2872.
115.Nakano, M., et al., *Superior magnetic properties of Mn-Zn ferrite thin films prepared by low-temperature process using laser ablation technique.* IEEE transactions on magnetics, 1999. **35**(5): p. 3007-3009.
116.*<Belesso 2000.pdf>.*
117.Reddy, D.H.K. and S.-M. Lee, *Three-dimensional porous spinel ferrite as an adsorbent for Pb (II) removal from aqueous solutions.* Industrial & Engineering Chemistry Research, 2013. **52**(45): p. 15789-15800.
118.Sharma, R. and S. Singhal, *Photodegradation of textile dye using magnetically recyclable heterogeneous spinel ferrites.* Journal of Chemical Technology & Biotechnology, 2015. **90**(5): p. 955-962.
119.Singh, S., et al., *Improved growth of nano tin ferrites with their decoration on carbon foam for wastewater treatment.* Environmental Nanotechnology, Monitoring & Management, 2021. **16**: p. 100546.
120.Mandal, S., et al., *Photocatalytic and antimicrobial activities of zinc ferrite nanoparticles synthesized through soft chemical route: a magnetically recyclable catalyst for water/wastewater treatment.* Journal of environmental chemical engineering, 2016. **4**(3): p. 2706-2712.
121.Zhang, F., et al., *Zinc ferrite catalysts for ozonation of aqueous organic contaminants: phenol and bio-treated coking wastewater.* Separation and Purification Technology, 2015. **156**: p. 625-635.
122.Patil, S., et al., *Sugarcane juice mediated eco-friendly synthesis of visible light active zinc ferrite nanoparticles: application to degradation of mixed dyes and antibacterial activities.* Materials Chemistry and Physics, 2018. **212**: p. 351-362.
123.Jadhav, S.A., et al., *Magnetically retrievable nanoscale nickel ferrites: an active photocatalyst for toxic dye removal applications.* Ceramics International, 2021. **47**(20): p. 28623-28633.
124.Gerbaldo, M.V., et al., *Degradation of anti-inflammatory drug diclofenac using cobalt ferrite as photocatalyst.* Chemical Engineering Research and Design, 2021. **166**: p. 237-247.
125.Udhaya, P.A., et al., *Copper Ferrite nanoparticles synthesised using a novel green synthesis route: Structural development and photocatalytic activity.* Journal of Molecular Structure, 2023. **1277**: p. 134807.
126.Qiu, S., et al., *An efficient and low-cost magnetic heterogenous Fenton-like catalyst for degrading antibiotics in wastewater: Mechanism, pathway and stability.* Journal of Environmental Management, 2022. **302**: p. 114119.
127.Dehghani, F., S. Hashemian, and A. Shibani, *Effect of calcination temperature for capability of MFe2O4 (M= Co, Ni and Zn) ferrite spinel for adsorption of bromophenol red.* Journal of industrial and engineering chemistry, 2017. **48**: p. 36-42.
128.Albalah, M.A., Y.A. Alsabah, and D.E. Mustafa, *Characteristics of co-precipitation synthesized cobalt nanoferrites and their potential in industrial wastewater treatment.* SN Applied Sciences, 2020. **2**: p. 1-9.
129.De la Torre, E., et al., *Activated carbon-spinels composites for Waste Water Treatment.* Metals, 2018. **8**(12): p. 1070.
130.Frolova, L., *Photocatalytic activity of spinel ferrites Co x Fe 3–x O 4 (0.25< x< 1) obtained by treatment contact low-temperature non-equilibrium plasma.* Applied Nanoscience, 2020. **10**: p. 4585-4590.
131.Tatarchuk, T., et al., *Cobalt ferrite as an electromagnetically boosted metal oxide hetero-Fenton catalyst for water treatment.* Chemosphere, 2023. **326**: p. 138364.
132.Wang, G., et al., *Fabrication, characterisation and magneto-responsive performance of manganese ferrite nanospheres for fast separation of oil slicks from water surfaces.* Ceramics International, 2023.
133.Ramu, A., et al., *A facile synthesis of metal ferrites and their catalytic removal of toxic nitro-organic pollutants.* Environmental Pollution, 2021. **270**: p. 116063.
134.Dojcinovic, M.P., et al., *Mixed Mg–Co spinel ferrites: Structure, morphology, magnetic and photocatalytic properties.* Journal of Alloys and Compounds, 2021. **855**: p. 157429.
135.Mondal, N.J., et al., *Nanocrystalline Ni-Zn spinel ferrites: size-dependent physical, photocatalytic and antioxidant properties.* Nanoscale Advances, 2023.
136.Shukrullah, S., et al., *Effective removal of chromium from wastewater with Zn doped Ni ferrite nanoparticles produced using co-precipitation method.* Materials Today: Proceedings, 2021. **47**: p. S9-S12.
137.Jesudoss, S., et al., *Studies on the efficient dual performance of Mn1–xNixFe2O4 spinel nanoparticles in photodegradation and antibacterial activity.* Journal of Photochemistry and Photobiology B: Biology, 2016. **165**: p. 121-132.
138.Chahar, D., et al., *Photocatalytic activity of cobalt substituted zinc ferrite for the degradation of methylene blue dye under visible light irradiation.* Journal of Alloys and Compounds, 2021. **851**: p. 156878.
139.Van Tran, C., et al., *New TiO2-doped Cu–Mg spinel-ferrite-based photocatalyst for degrading highly toxic rhodamine B dye in wastewater.* Journal of hazardous materials, 2021. **420**: p. 126636.
140.Hermosilla, D., et al., *Environmentally friendly synthesized and magnetically recoverable designed ferrite photo-catalysts for wastewater treatment applications.* Journal of hazardous materials, 2020. **381**: p. 121200.
141.Manohar, A., K. Chintagumpala, and K.H. Kim, *Mixed Zn–Ni spinel ferrites: Structure, magnetic hyperthermia and photocatalytic properties.* Ceramics International, 2021. **47**(5): p. 7052-7061.
142.Gul, S., et al., *Al-substituted zinc spinel ferrite nanoparticles: preparation and evaluation of structural, electrical, magnetic and photocatalytic properties.* Ceramics International, 2020. **46**(9): p. 14195-14205.
143.Zhang, B., et al., *Magnetic properties and adsorptive performance of manganese–zinc ferrites/activated carbon nanocomposites.* Journal of Solid State Chemistry, 2015. **221**: p. 302-305.
144.George, M., et al., *Evaluation of Cu–MgFe2O4 spinel nanoparticles for photocatalytic and antimicrobial activates.* Journal of Physics and Chemistry of Solids, 2021. **153**: p. 110010.
145.Singh, S., et al., *Enhanced photocatalytic performance of Ru-doped spinel nanoferrites for treating recalcitrant organic pollutants in wastewater.* Journal of Sol-Gel Science and Technology, 2019. **92**: p. 760-774.
146.Fito, J., O. Ebrahim, and T.T. Nkambule, *The Application Mn-Ni Ferrite Nanocomposite for Adsorption of Chromium from Textile Industrial Wastewater.* Water, Air, & Soil Pollution, 2023. **234**(1): p. 37.
147.An, V.N., et al., *Silver decorated on cobalt ferrite nanoparticles as a reusable multifunctional catalyst for water treatment applications in non-radiation conditions.* RSC advances, 2023. **13**(35): p. 24554-24564.
148.Nandhini, G., et al., *Photocatalytic degradation of methylene blue on strontium-doped cobalt ferrite.* Journal of Materials Science: Materials in Electronics, 2023. **34**(18): p. 1426.

149.Zhang, H., et al., *From waste to waste treatment: Mesoporous magnetic NiFe2O4/ZnCuCr-layered double hydroxide composite for wastewater treatment.* Journal of Alloys and Compounds, 2020. **819**: p. 153053.
150.Ciocarlan, R.-G., et al., *Novel magnetic nanocomposites containing quaternary ferrites systems Co0. 5Zn0. 25M0. 25Fe2O4 (M= Ni, Cu, Mn, Mg) and TiO2-anatase phase as photocatalysts for wastewater remediation under solar light irradiation.* Materials Science and Engineering: B, 2018. **230**: p. 1-7.
151.Ai, J., et al., *Microstructural evolution and catalytic properties of novel high-entropy spinel ferrites MFe2O4 (M= Mg, Co, Ni, Cu, Zn).* Ceramics International, 2023. **49**(14): p. 22941-22951.
152.Jiang, D., et al., *Customized copper/cobalt-rich ferrite spinel-based construction ceramic membrane incorporating gold tailings for enhanced treatment of industrial oily emulsion wastewater.* Separation and Purification Technology, 2023. **320**: p. 124131.
153.Rani, R., et al., *Structural, morphological and temperature dependent electrical traits of Co0. 9Zn0. 1InxFe2-xO4 spinel nano-ferrites.* Ceramics International, 2021. **47**(21): p. 30902-30910.
154.Hu, Z.-T., et al., *Self-cleaning MnZn ferrite/biochar adsorbents for effective removal of tetracycline.* Science of The Total Environment, 2022. **844**: p. 157202.
155.Ahmed, M., et al., *Promising wastewater treatment using rare earth-doped nanoferrites.* Journal of magnetism and magnetic materials, 2014. **350**: p. 73-80.
156.Shakil, M., et al., *Enhanced structural, optical, and photocatalytic activities of Cd–Co doped Zn ferrites for degrading methyl orange dye under irradiation by visible light.* Journal of Physics and Chemistry of Solids, 2022. **161**: p. 110419.
157.Mangood, A.H., et al., *Evaluation of synergistic approach of spinel cadmium–copper nanoferrites as magnetic catalysts for promoting wastewater decontamination: Impact of Ag ions doping.* Environmental Science and Pollution Research, 2023: p. 1-18.
158.Rezlescu, N., et al., *Scandium substituted nickel–cobalt ferrite nanoparticles for catalyst applications.* Applied Catalysis B: Environmental, 2014. **158**: p. 70-75.
159.Dhiman, P., et al., *Co Doped Mg–Zn Spinel Nano-ferrites as a Sustainable Magnetic Nano-photo-catalyst with Reduced Recombination for Photo Degradation of Crystal Violet.* Journal of Inorganic and Organometallic Polymers and Materials, 2023: p. 1-14.
160.Abdo, M. and A. El-Daly, *Sm-substituted copper-cobalt ferrite nanoparticles: Preparation and assessment of structural, magnetic and photocatalytic properties for wastewater treatment applications.* Journal of Alloys and Compounds, 2021. **883**: p. 160796.
161.Singh, S., et al., *Traversing the advantageous role of samarium doped spinel nanoferrites for photocatalytic removal of organic pollutants.* Journal of Rare Earths, 2021. **39**(7): p. 781-789.
162.Abou Hammad, A.B., B.A. Hemdan, and A.M. El Nahrawy, *Facile synthesis and potential application of Ni0. 6Zn0. 4Fe2O4 and Ni0. 6Zn0. 2Ce0. 2Fe2O4 magnetic nanocubes as a new strategy in sewage treatment.* Journal of Environmental Management, 2020. **270**: p. 110816.
163.Basfer, N. and N. Al-Harbi, *Structural, optical and photocatalytic activity of Ce3+ doped Co–Mg nanoparticles for wastewater treatment applications.* Journal of King Saud University-Science, 2023. **35**(1): p. 102436.
164.Irfan, M., et al., *Testing of optical, dielectric and photocatalytic properties of Ce3+ doped cobalt–cadmium nanocomposite for high frequency devices and wastewater treatment.* Ceramics International, 2022. **48**(6): p. 8517-8528.
165.Jasrotia, R., et al., *Photocatalytic degradation of malachite green pollutant using novel dysprosium modified Zn–Mg photocatalysts for wastewater remediation.* Ceramics International, 2022. **48**(19): p. 29111-29120.
166.Keerthana, S., et al., *Pure and Ce-doped spinel CuFe2O4 photocatalysts for efficient rhodamine B degradation.* Environmental Research, 2021. **200**: p. 111528.
167.Sharma, R., et al., *Boosting the catalytic performance of pristine CoFe2O4 with yttrium (Y3+) inclusion in the spinel structure.* Materials Research Bulletin, 2017. **90**: p. 94-103.
168.Keerthana, S., et al., *Rare earth metal (Sm) doped zinc ferrite (ZnFe2O4) for improved photocatalytic elimination of toxic dye from aquatic system.* Environmental Research, 2021. **197**: p. 111047.
169.Abdo, M., R. Al-Wafi, and M. AlHammad, *Highly efficient visible light driven photocatalytic activity of rare earth cerium doped zinc-manganese ferrite: Rhodamine B degradation and stability assessment.* Ceramics International, 2023.
170.Chao, L., et al., *Three-dimensional ordered microporous silica supported p-lanthanum ferrite and n-ceria as heterojunction photocatalyst to activate peroxymonosulfate for bisphenol a degradation.* International Journal of Hydrogen Energy, 2023. **48**(41): p. 15433-15446.
171.Ivanets, A., et al., *Effect of magnesium ferrite doping with lanthanide ions on dark-, visible-and UV-driven methylene blue degradation on heterogeneous Fenton-like catalysts.* Ceramics International, 2021. **47**(21): p. 29786-29794.
172.Meena, S., et al., *Enhanced sunlight driven photocatalytic activity and electrochemical sensing properties of Ce-doped MnFe2O4 nano magnetic ferrites.* Ceramics International, 2021. **47**(10): p. 14760-14774.
173.Kumar, M., H.S. Dosanjh, and H. Singh, *Removal of lead and copper metal ions in single and binary systems using biopolymer modified spinel ferrite.* Journal of environmental chemical engineering, 2018. **6**(5): p. 6194-6206.
174.Sharma, A., et al., *Cobalt ferrite incorporated Ocimum sanctum nanocomposite matrix as an interface for adsorption of organic dyes: A sustainable alternative.* ChemistrySelect, 2023. **8**(5): p. e202203709.
175.Sahare, S.P., et al., *Modified cobalt ferrite entrapped chitosan beads as a magnetic adsorbent for effective removal of malachite green and copper (II) ions from aqueous solutions.* Journal of Inorganic and Organometallic Polymers and Materials, 2023. **33**(1): p. 266-286.
176.Joshi, C.S., R. Srivastava, and A. Joshi, *Polyaniline/Manganese-Cobalt ferrite nanocomposite as an efficient material for crystal violet dye degradation under sunlight irradiation.* Materials Today: Proceedings, 2023.
177.Hosseini, S., et al., *Magnetic cation exchange membrane incorporated with cobalt ferrite nanoparticles for chromium ions removal via electrodialysis.* Journal of Membrane Science, 2019. **583**: p. 292-300.
178.Sadrolhosseini, A.R., M. Naseri, and S.A. Rashid, *Polypyrrole-chitosan/nickel-ferrite nanoparticle composite layer for detecting heavy metal ions using surface plasmon resonance technique.* Optics & Laser Technology, 2017. **93**: p. 216-223.
179.Abou Hammad, A., et al., *A novel electromagnetic biodegradable nanocomposite based on cellulose, polyaniline, and cobalt ferrite nanoparticles.* Carbohydrate polymers, 2019. **216**: p. 54-62.
180.Tatarchuk, T., et al., *Structure, morphology and adsorption properties of titania shell immobilized onto cobalt ferrite nanoparticle core.* Journal of Molecular Liquids, 2020. **297**: p. 111757.
181.Giri, J., et al., *Synthesis and characterizations of water-based ferrofluids of substituted ferrites [Fe1− xBxFe2O4, B= Mn, Co (x= 0–1)] for biomedical applications.* Journal of Magnetism and Magnetic Materials, 2008. **320**(5): p. 724-730.
182.Naushad, M., et al., *Nickel ferrite bearing nitrogen-doped mesoporous carbon as efficient adsorbent for the removal of highly toxic metal ion from aqueous medium.* Chemical Engineering Journal, 2017. **330**: p. 1351-1360.

183.Malana, M.A., R.B. Qureshi, and M.N. Ashiq, *Adsorption studies of arsenic on nano aluminium doped manganese copper ferrite polymer (MA, VA, AA) composite: Kinetics and mechanism.* Chemical Engineering Journal, 2011. **172**(2-3): p. 721-727.
184.Zareei, F. and S.M. Hosseini, *A new type of polyethersulfone based composite nanofiltration membrane decorated by cobalt ferrite-copper oxide nanoparticles with enhanced performance and antifouling property.* Separation and Purification Technology, 2019. **226**: p. 48-58.
185.Jayalakshmi, R. and J. Jeyanthi, *Dynamic modelling of Alginate-Cobalt ferrite nanocomposite for removal of binary dyes from textile effluent.* Journal of Environmental Chemical Engineering, 2021. **9**(1): p. 104924.
186.Katowah, D.F., et al., *Ternary nanocomposite based poly (pyrrole-co-O-toluidine), cobalt ferrite and decorated chitosan as a selective Co2+ cationic sensor.* Composites Part B: Engineering, 2019. **175**: p. 107175.
187.Mahmoodi, N.M., *Magnetic ferrite nanoparticle–alginate composite: Synthesis, characterization and binary system dye removal.* Journal of the Taiwan Institute of Chemical Engineers, 2013. **44**(2): p. 322-330.
188.Cui, H.-J., et al., *Synthesis of porous magnetic ferrite nanowires containing Mn and their application in water treatment.* Journal of Materials Chemistry A, 2013. **1**(19): p. 5902-5907.
189.Martins, P., et al., *Tailored magnetic and magnetoelectric responses of polymer-based composites.* ACS applied materials & interfaces, 2015. **7**(27): p. 15017-15022.
190.Jayalakshmi, R. and J. Jeyanthi, *Synthesis and structural characterization of polymer-based cobalt ferrite nanocomposite with core–shell structure.* Journal of Inorganic and Organometallic Polymers and Materials, 2018. **28**: p. 1286-1293.
191.Lakroun, S.E., et al., *Enhanced fermentative biohydrogen production from milk processing wastewater by magnetic spinel ferrites nanoparticles.* Energy Sources, Part A: Recovery, Utilization, and Environmental Effects, 2023. **45**(1): p. 3138-3153.
192.Moradi, M., et al., *Intensification of persulfate-mediated elimination of bisphenol A by a spinel cobalt ferrite-anchored g-C3N4 S-scheme photocatalyst: catalytic synergies and mechanistic interpretation.* Separation and Purification Technology, 2022. **285**: p. 120313.
193.Wu, D., et al., *Effective degradation of diatrizoate by electro-peroxone process using ferrite/carbon nanotubes based gas diffusion cathode.* Electrochimica Acta, 2017. **236**: p. 297-306.
194.Yao, J., et al., *Role of magnetic substances in adsorption removal of ciprofloxacin by gamma ferric oxide and ferrites co-modified carbon nanotubes.* Journal of Colloid and Interface Science, 2023. **638**: p. 872-881.
195.Nadeem, N., et al., *Coal fly ash-based copper ferrite nanocomposites as potential heterogeneous photocatalysts for wastewater remediation.* Applied Surface Science, 2021. **565**: p. 150542.
196.Jelokhani, F., S. Sheibani, and A. Ataie, *Adsorption and photocatalytic characteristics of cobalt ferrite-reduced graphene oxide and cobalt ferrite-carbon nanotube nanocomposites.* Journal of Photochemistry and Photobiology A: Chemistry, 2020. **403**: p. 112867.
197.Ansari, F., F. Soofivand, and M. Salavati-Niasari, *Eco-friendly synthesis of cobalt hexaferrite and improvement of photocatalytic activity by preparation of carbonic-based nanocomposites for waste-water treatment.* Composites Part B: Engineering, 2019. **165**: p. 500-509.
198.Wang, J., et al., *One-pot synthesis of multifunctional magnetic ferrite–MoS 2–carbon dot nanohybrid adsorbent for efficient Pb (ii) removal.* Journal of Materials Chemistry A, 2016. **4**(10): p. 3893-3900.
199.Ahangari, A., S. Raygan, and A. Ataie, *Capabilities of nickel zinc ferrite and its nanocomposite with CNT for adsorption of arsenic (V) ions from wastewater.* Journal of Environmental Chemical Engineering, 2019. **7**(6): p. 103493.
200.Verma, B. and C. Balomajumder, *Magnetic magnesium ferrite–doped multi-walled carbon nanotubes: an advanced treatment of chromium-containing wastewater.* Environmental Science and Pollution Research, 2020. **27**(12): p. 13844-13854.
201.Wu, D., et al., *Adsorptive removal of aqueous bezafibrate by magnetic ferrite modified carbon nanotubes.* RSC advances, 2017. **7**(63): p. 39594-39603.
202.Luan, H., et al., *Adsorptive filtration of As (III) from drinking water by CuFe2O4 particles embedded in carbon nanotube membranes.* Journal of Chemical Technology & Biotechnology, 2019. **94**(9): p. 2816-2825.
203.Ramaraj, S., et al., *Synthesis and application of bismuth ferrite nanosheets supported functionalized carbon nanofiber for enhanced electrochemical detection of toxic organic compound in water samples.* Journal of colloid and interface science, 2018. **514**: p. 59-69.
204.Guo, Z., et al., *Synthesis of amino-functionalized biochar/spinel ferrite magnetic composites for low-cost and efficient elimination of Ni (II) from wastewater.* Science of the Total Environment, 2020. **722**: p. 137822.
205.Lv, S., et al., *Rice hull/MnFe2O4 composite: preparation, characterization and its rapid microwave-assisted COD removal for organic wastewater.* Journal of Hazardous Materials, 2009. **171**(1-3): p. 634-639.
206.Suba, V., et al., *Enhanced adsorption and antimicrobial activity of fabricated apocynaceae leaf waste activated carbon by cobalt ferrite nanoparticles for textile effluent treatment.* Journal of Inorganic and Organometallic Polymers and Materials, 2019. **29**: p. 550-563.
207.Saleh, T.S., et al., *Design and development of novel composites containing nickel ferrites supported on activated carbon derived from agricultural wastes and its application in water remediation.* Materials, 2023. **16**(6): p. 2170.
208.Bai, M., et al., *Enhancing cadmium removal efficiency through spinel ferrites modified biochar derived from agricultural waste straw.* Journal of Environmental Chemical Engineering, 2023. **11**(1): p. 109027.
209.Grewal, J.K., et al., *Carbon quantum dot-titanium doped strontium ferrite nanocomposite: Visible light active photocatalyst to degrade nitroaromatics.* Catalysts, 2022. **12**(10): p. 1126.
210.Perveen, S., et al., *Biochar-mediated zirconium ferrite nanocomposites for tartrazine dye removal from textile wastewater.* Nanomaterials, 2022. **12**(16): p. 2828.
211.Algethami, J.S., et al., *Manganese Ferrite–Hydroxyapatite Nanocomposite Synthesis: Biogenic Waste Remodeling for Water Decontamination.* Nanomaterials, 2022. **12**(10): p. 1631.
212.Shabelskaya, N., et al., *Formation of biochar nanocomposite materials based on CoFe2O4 for purification of aqueous solutions from chromium compounds (VI).* Water, 2022. **15**(1): p. 93.
213.Maksoud, M.A., et al., *Novel adsorbent based on carbon-modified zirconia/spinel ferrite nanostructures: evaluation for the removal of cobalt and europium radionuclides from aqueous solutions.* Journal of Colloid and Interface Science, 2022. **607**: p. 111-124.
214.Alizadeh, M., et al., *Surface magnetization of hydrolyzed Luffa Cylindrica biowaste with cobalt ferrite nanoparticles for facile Ni2+ removal from wastewater.* Environmental Research, 2022. **212**: p. 113242.
215.Zinatloo-Ajabshir, S. and M. Salavati-Niasari, *Preparation of magnetically retrievable CoFe2O4@ SiO2@ Dy2Ce2O7 nanocomposites as novel photocatalyst for highly efficient degradation of organic contaminants.* Composites Part B: Engineering, 2019. **174**: p. 106930.
216.Hassaneen, F.Y., et al., *Innovative nanocomposite formulations for enhancing biogas and biofertilizers production from anaerobic digestion of organic waste.* Bioresource technology, 2020. **309**: p. 123350.
217.Chang, S., et al., *High-efficiency and selective adsorption of organic pollutants by magnetic CoFe2O4/graphene oxide adsorbents: Experimental and molecular dynamics simulation*

study. Separation and Purification Technology, 2020. **238**: p. 116400.
218.Dhiman, P., et al., *Magnetic Ni–Zn ferrite anchored on g-C3N4 as nano-photocatalyst for efficient photo-degradation of doxycycline from water.* Environmental Research, 2023. **216**: p. 114665.
219.Wabaidur, S.M., et al., *Oxygenated functionalities enriched MWCNTs decorated with silica coated spinel ferrite–A nanocomposite for potentially rapid and efficient de-colorization of aquatic environment.* Journal of Molecular Liquids, 2020. **317**: p. 113916.
220.Arsalani, N., Y. Panahian, and R. Nasiri, *Fabrication of novel magnetic F-TiO2 (B)/carbon nanostructures nanocomposites as photocatalysts for malachite green degradation under visible light.* Materials Science and Engineering: B, 2019. **251**: p. 114448.
221.Ghosh, B.K., et al., *Preparation of TiO2/cobalt ferrite/reduced graphene oxide nanocomposite based magnetically separable catalyst with improved photocatalytic activity.* Journal of Nanoscience and Nanotechnology, 2017. **17**(7): p. 4694-4703.
222.Kodasma, R., et al., *Photocatalytic activity of copper ferrite graphene oxide particles for an efficient catalytic degradation of Reactive Black 5 in water.* Ceramics International, 2020. **46**(5): p. 6284-6292.
223.Liu, S.-Q., et al., *Smart photocatalytic removal of ammonia through molecular recognition of zinc ferrite/reduced graphene oxide hybrid catalyst under visible-light irradiation.* Catalysis Science & Technology, 2017. **7**(15): p. 3210-3219.
224.Saputra, E., et al., *Fabrication of hybrid covalent triazine framework-zinc ferrite spinel to uplift visible light–driven photocatalytic organic pollutant degradation.* Environmental Science and Pollution Research, 2023. **30**(14): p. 39961-39977.
225.Shu, R., et al., *Facile synthesis of cobalt-zinc ferrite microspheres decorated nitrogen-doped multi-walled carbon nanotubes hybrid composites with excellent microwave absorption in the X-band.* Composites Science and Technology, 2019. **184**: p. 107839.
226.Yamaguchi, N.U., R. Bergamasco, and S. Hamoudi, *Magnetic MnFe2O4–graphene hybrid composite for efficient removal of glyphosate from water.* Chemical Engineering Journal, 2016. **295**: p. 391-402.
227.Tran, N.B.T., N.B. Duong, and N.L. Le, *Synthesis and characterization of magnetic Fe3O4/zeolite NaA nanocomposite for the adsorption removal of methylene blue potential in wastewater treatment.* Journal of Chemistry, 2021. **2021**: p. 1-14.
228.Raghavendra, N., et al., *Electrochemical sensor studies and optical analysis of developed clay based CoFe2O4 ferrite NPs.* Sensors International, 2021. **2**: p. 100083.
229.Sun, F., et al., *Magnetic MFe2O4-Ag2O (M= Zn, Co, & Ni) composite photocatalysts and their application for dye wastewater treatment.* Journal of Environmental Chemical Engineering, 2019. **7**(2): p. 103011.
230.Li, Z., et al., *Spinel ferrite-enhanced Cr (VI) removal performance of micro-scale zero-valent aluminum: synergistic effects of oxide film destruction and lattice spacing expansion.* Separation and Purification Technology, 2022. **294**: p. 121110.
231.Fayyaz, A., et al., *Catalytic oxidation of naproxen in cobalt spinel ferrite decorated Ti3C2Tx MXene activated persulfate system: Mechanisms and pathways.* Chemical Engineering Journal, 2021. **407**: p. 127842.
232.Balakrishnan, R.M., et al., *Cobalt ferrite nanoparticles and peroxymonosulfate system for the removal of ampicillin from aqueous solution.* Journal of Water Process Engineering, 2021. **40**: p. 101823.
233.Qu, J., et al., *A novel magnetic silica supported spinel ferrites NiFe2O4 catalyst for heterogeneous Fenton-like oxidation of rhodamine B.* Chinese Chemical Letters, 2019. **30**(6): p. 1198-1203.
234.Latif, S., et al., *Development of zinc ferrite nanoparticles with enhanced photocatalytic performance for remediation of environmentally toxic pharmaceutical waste diclofenac sodium from wastewater.* Environmental Research, 2023. **216**: p. 114500.
235.Appiah-Ntiamoah, R., et al., *In-situ prepared ZnO-ZnFe2O4 with 1-D nanofiber network structure: An effective adsorbent for toxic dye effluent treatment.* Journal of hazardous materials, 2019. **373**: p. 459-467.
236.Al-Najar, B., et al., *Thermally induced oxygen related defects in eco-friendly ZnFe2O4 nanoparticles for enhanced wastewater treatment efficiencies.* Chemosphere, 2022. **288**: p. 132525.
237.Shah, P., et al., *Photocatalytic dye degradation using nickel ferrite spinel and its nanocomposite.* Environmental Science and Pollution Research, 2022. **29**(52): p. 78255-78264.
238.Adel, M., M.A. Ahmed, and A.A. Mohamed, *A facile and rapid removal of cationic dyes using hierarchically porous reduced graphene oxide decorated with manganese ferrite.* FlatChem, 2021. **26**: p. 100233.
239.Ivanets, A., et al., *Methylene blue adsorption on magnesium ferrite: Optimization study, kinetics and reusability.* Materials Today Communications, 2022. **31**: p. 103594.
240.Wang, L., et al., *Adsorption capability for Congo red on nanocrystalline MFe2O4 (M= Mn, Fe, Co, Ni) spinel ferrites.* Chemical Engineering Journal, 2012. **181**: p. 72-79.
241.Jadhav, S.A., et al., *Magneto-structural and photocatalytic behavior of mixed Ni–Zn nano-spinel ferrites: visible light-enabled active photodegradation of rhodamine B.* Journal of Materials Science: Materials in Electronics, 2020. **31**: p. 11352-11365.
242.Hasan, I., et al., *Sonophotocatalytic degradation of malachite green by nanocrystalline chitosan-ascorbic Acid@ NiFe2O4 spinel ferrite.* Coatings, 2020. **10**(12): p. 1200.
243.Rashid, M., et al., *Solar-light-driven and magnetically recoverable doped nano-ferrite: an ideal photocatalyst for water purification applications.* Optical Materials, 2023. **135**: p. 113192.
244.Musajan, Z. and P. Xiao, *Facile fabrication of mesoporous carbon-anchored cobalt ferrite nanoparticles as a heterogeneous activator of peroxymonosulfate for efficient degradation of Congo red.* Environmental Science and Pollution Research, 2023. **30**(16): p. 48088-48106.
245.Debnath, S. and R. Das, *Strong adsorption of CV dye by Ni ferrite nanoparticles for waste water purification: Fits well the pseudo second order kinetic and Freundlich isotherm model.* Ceramics International, 2023. **49**(10): p. 16199-16215.
246.Ramadevi, P., et al., *Photocatalytic dye degradation efficiency and reusability of aluminium substituted nickel ferrite nanostructures for wastewater remediation.* Inorganic Chemistry Communications, 2023. **150**: p. 110532.
247.Naik, M.M., et al., *A facile green synthesis of nickel ferrite nanoparticles using Tamarindus Indica seeds for magnetic and photocatalytic studies.* Nanotechnology for Environmental Engineering, 2023. **8**(1): p. 143-151.
248.Sukumar, M., et al., *Synthesize and characterization of copper doped nickel ferrite nanoparticles effect on magnetic properties and visible light catalysis for rhodamine dye degradation mechanism.* Journal of Alloys and Compounds, 2023. **953**: p. 169902.
249.Mishra, S., P. Kumar, and S.K. Samanta, *Microwave catalytic degradation of antibiotic molecules by 2D sheets of spinel nickel ferrite.* Industrial & Engineering Chemistry Research, 2020. **59**(36): p. 15839-15847.
250.Sayğılı, G.A. and H. Sayğılı, *Pharmaceutical analysis by a novel spinel ferrite nanocomposite derived from a biomaterial-based activated carbon.* Journal of pharmaceutical and biomedical analysis, 2020. **179**: p. 112957.
251.Mushtaq, S., et al., *Biocompatibility and cytotoxicity in vitro of surface-functionalized drug-loaded spinel ferrite nanoparticles.* Beilstein Journal of Nanotechnology, 2021. **12**(1): p. 1339-1364.

252.Jasrotia, R., et al., *Nickel ions modified CoMg nanophotocatalysts for solar light-driven degradation of antimicrobial pharmaceutical effluents.* Journal of Water Process Engineering, 2022. **47**: p. 102785.
253.Xiao, S., A. Fakhri, and B.J. Janani, *Synthesis of spinel Tin ferrite decorated on Bismuth ferrite nanostructures for synergetic photocatalytic, superior drug delivery, and antibacterial efficiencies.* Surfaces and Interfaces, 2021. **27**: p. 101490.
254.Adewuyi, A., O.A. Ogunkunle, and R.A. Oderinde, *Zirconium ferrite incorporated zeolitic imidazolate framework-8: a suitable photocatalyst for degradation of dopamine and sulfamethoxazole in aqueous solution.* RSC advances, 2023. **13**(14): p. 9563-9575.
255.Al-Hetlani, E., et al., *An effective magnetic nanoadsorbent based on a carbonaceous/spinel ferrite nanocomposite for the removal of pharmaceutical pollutants from wastewater.* Environmental Science: Water Research & Technology, 2022. **8**(5): p. 998-1010.
256.Jadhav, S.A., et al., *Visible light photocatalytic activity of magnetically diluted Ni–Zn spinel ferrite for active degradation of rhodamine B.* Ceramics International, 2021. **47**(10): p. 13980-13993.
257.Behura, R., R. Sakthivel, and N. Das, *Synthesis of cobalt ferrite nanoparticles from waste iron ore tailings and spent lithium ion batteries for photo/sono-catalytic degradation of Congo red.* Powder technology, 2021. **386**: p. 519-527.
258.Kaur, P., et al., *Synergizing hexagonal ferrite with transition metals in core-shell-shell nanostructures (SrFe@ Dop@ M) as dualistic probe for detoxification and electrochemical detection of pharmaceutical drugs.* Ceramics International, 2023. **49**(4): p. 6199-6212.
259.Dhiman, P., et al., *Solar active nano-Zn1− xMgxFe2O4 as a magnetically separable sustainable photocatalyst for degradation of sulfadiazine antibiotic.* Journal of Molecular Liquids, 2019. **294**: p. 111574.
260.Makofane, A., D.E. Motaung, and N.C. Hintsho-Mbita, *Photocatalytic degradation of methylene blue and sulfisoxazole from water using biosynthesized zinc ferrite nanoparticles.* Ceramics International, 2021. **47**(16): p. 22615-22626.
261.Daf, S.R., et al., *Effect of hydrothermal processing duration on physical and antimicrobial properties of Mg0. 2Zn0. 5Mn0. 3 Fe2O4 ferrite nanoparticles.* Materials Science and Engineering: B, 2023. **298**: p. 116879.
262.Kumari, S., et al., *Nano Ca–Mg–Zn ferrites as tuneable photocatalyst for UV light-induced degradation of rhodamine B dye and antimicrobial behavior for water purification.* Ceramics International, 2023. **49**(8): p. 12469-12480.
263.El-Bassuony, A.A., W. Gamal, and H. Abdelsalam, *Impact of different magnetic materials added to silver–magnetite nanoparticles on the structural, magnetic and antimicrobial properties.* The European Physical Journal Special Topics, 2023: p. 1-13.
264.Bessy, T., et al., *Photocatalytic Degradation of Toxic Dyes and Antimicrobial Activities by Cadmium Doped Magnesium Ferrites Synthesized by Combustion Method.* Journal of Inorganic and Organometallic Polymers and Materials, 2023: p. 1-18.
265.Mordekar, R.K., et al., *Silver substituted cobalt zinc ferrites as magnetic antimicrobials.* Ceramics International, 2023.
266.Dhanda, N., et al., *Green-synthesis of Ni-Co nano ferrites using Aloe Vera extract: structural, optical, magnetic, and antimicrobial studies.* Applied Organometallic Chemistry, 2023: p. e7110.
267.Nigam, A., et al., *Physio-chemical characterization, in-vitro biocompatibility, and antimicrobial activity of magnetite nanoparticles synthesized via sol-gel route.* Inorganic and Nano-Metal Chemistry, 2023: p. 1-11.
268.El-Khawaga, A.M., et al., *Promising photocatalytic and antimicrobial activity of novel capsaicin coated cobalt ferrite nanocatalyst.* Scientific Reports, 2023. **13**(1): p. 5353.
269.Wendari, T.P., et al., *CuFe2O4/hydroxyapatite magnetic nanocomposite synthesized using pensi clam shells as a source of calcium for degradation of dye and anti-bacterial applications.* Case Studies in Chemical and Environmental Engineering, 2023: p. 100482.
270.Babukutty, B., et al., *Structural influence of chromium substituted magnetite ferrofluids on the optical and antibacterial characteristics.* Materials Today Communications, 2023. **34**: p. 105439.
271.Hatami Kahkesh, K., et al., *Synthesis, Characterization, Antioxidant and Antibacterial Activities of Zinc Ferrite and Copper Ferrite Nanoparticles.* Materials Chemistry Horizons, 2023. **2**(1): p. 49-56.
272.Goud, G.S., et al., *Synthesis, Characterization, Morphological, Antimicrobial, Electrical and Magnetic Properties of Cd Substituted Mg Nano Ferrites.* Available at SSRN 4379587.
273.Shokri, S., et al., *Synthesis and characterization of a novel magnetic chitosan–nickel ferrite nanocomposite for antibacterial and antioxidant properties.* Scientific Reports, 2023. **13**(1): p. 15777.
274.Reddy, R.A., et al., *Structural, magnetic and antibacterial studies of gadolinium doped cobalt ferrite nanoparticles synthesized at low temperature.* Advances in Natural Sciences: Nanoscience and Nanotechnology, 2023. **14**(1): p. 015005.
275.Ravichandran, D., et al., *Ulva lactuca L. extract bio-templated fabrication of CuO/ZnFe2O4 nanocomposites for photodegradation organic dye pollutants and in vitro biological activities.* Colloids and Surfaces A: Physicochemical and Engineering Aspects, 2024. **689**: p. 133701.
276.Kousar, T., et al., *Facile synthesis of graphene anchored rare earth doped mixed metal ferrite nanorods: a potential candidate for azo dye mineralization.* Journal of Rare Earths, 2024. **42**(5): p. 907-916.
277.Punyasamudram, S., et al., *Multifunctional characteristics of biosynthesized CoFe2O4@ Ag nanocomposite by photocatalytic, antibacterial and cytotoxic applications.* Chemosphere, 2024. **349**: p. 140892.
278.Razavi, F.S., D. Ghanbari, and M. Salavati-Niasari, *Green synthesis of SrFe12O19@ Ag and SrFe12O19@ Au as magnetic plasmonic nanocomposites with high photocatalytic performance for degradation of organic pollutants.* Chemosphere, 2022. **291**: p. 132741.
279.Abou Taleb, M.F., et al., *Binary metal doped spinel ferrite nanoparticles and their Nano hybrid with MXene matrix to enhance catalytic properties.* Optical Materials, 2023. **145**: p. 114485.
280.Phor, L., et al., *Magnetically separable NiZn-ferrite/CeO2 nanorods/CNT ternary composites for photocatalytic removal of organic pollutants.* Journal of Molecular Liquids, 2023. **390**: p. 123064.
281.Razavi, F.S., D. Ghanbari, and M. Salavati-Niasari, *Comparative study on the role of noble metal nanoparticles (Pt and Pd) on the photocatalytic performance of the BaFe12O19/TiO2 magnetic nanocomposite: Green synthesis, characterization, and removal of organic dyes under visible light.* Industrial & Engineering Chemistry Research, 2022. **61**(36): p. 13314-13327.
282.Abdel Aziz, Y.S., et al., *In-situ construction of Zr-based metal-organic framework core-shell heterostructure for photocatalytic degradation of organic pollutants.* Frontiers in Chemistry, 2023. **10**: p. 1102920.
283.Asadi, R., et al., *Effective removal of Zn (II) ions from aqueous solution by the magnetic MnFe2O4 and CoFe2O4 spinel ferrite nanoparticles with focuses on synthesis, characterization, adsorption, and desorption.* Advanced Powder Technology, 2020. **31**(4): p. 1480-1489.
284.Lingamdinne, L.P., et al., *Studies on removal of Pb (II) and Cr (III) using graphene oxide based inverse spinel nickel ferrite nano-composite as sorbent.* Hydrometallurgy, 2016. **165**: p. 64-72.
285.Jung, K.-W., S.Y. Lee, and Y.J. Lee, *Facile one-pot hydrothermal synthesis of cubic spinel-type manganese ferrite/biochar composites for environmental remediation of*

heavy metals from aqueous solutions. Bioresource technology, 2018. **261**: p. 1-9.
286.Sezgin, N., et al., *Synthesis, characterization and, the heavy metal removal efficiency of MFe2O4 (M= Ni, Cu) nanoparticles.* Ekoloji, 2013. **22**(89): p. 89-96.
287.Khoso, W.A., et al., *Synthesis, characterization and heavy metal removal efficiency of nickel ferrite nanoparticles (NFN's).* Scientific Reports, 2021. **11**(1): p. 3790.
288.Ramadan, R. and M.M. El-Masry, *Effect of (Co and Zn) doping on structural, characterization and the heavy metal removal efficiency of CuFe2O4 nanoparticles.* Journal of the Australian Ceramic Society, 2024. **60**(2): p. 509-524.
289.Camacho-González, M.A., et al., *Synthesis and characterization of magnetic zinc-copper ferrites: Antibacterial activity, photodegradation study and heavy metals removal evaluation.* Materials Chemistry and Physics, 2019. **236**: p. 121808.
290.Lingamdinne, L.P., et al., *Biogenic reductive preparation of magnetic inverse spinel iron oxide nanoparticles for the adsorption removal of heavy metals.* Chemical Engineering Journal, 2017. **307**: p. 74-84.
291.Al Yaqoob, K., et al., *Selectivity and efficient Pb and Cd ions removal by magnetic MFe2O4 (M= Co, Ni, Cu and Zn) nanoparticles.* Materials Chemistry and Physics, 2019. **232**: p. 254-264.
292.Narayana, P., et al., *Predictive capability evaluation and optimization of Pb (II) removal by reduced graphene oxide-based inverse spinel nickel ferrite nanocomposite.* Environmental Research, 2022. **204**: p. 112029.
293.Tatarchuk, T., et al., *Magnesium-zinc ferrites as magnetic adsorbents for Cr (VI) and Ni (II) ions removal: Cation distribution and antistructure modeling.* Chemosphere, 2021. **270**: p. 129414.
294.Tran, C.V., et al., *Effective removal of Pb (II) from aqueous media by a new design of Cu–Mg binary ferrite.* Acs Omega, 2020. **5**(13): p. 7298-7306.
295.Tavares, D.S., et al., *Spinel-type ferrite nanoparticles for removal of arsenic (V) from water.* Environmental Science and Pollution Research, 2020. **27**: p. 22523-22534.
296.Iqbal, Z., M.S. Tanweer, and M. Alam, *Reduced graphene oxide-modified spinel cobalt ferrite nanocomposite: synthesis, characterization, and its superior adsorption performance for dyes and heavy metals.* ACS omega, 2023. **8**(7): p. 6376-6390.
297.Kumari, S., et al., *Alkaline earth metal doped nickel ferrites as a potential material for heavy metal removal from waste water.* Materials Chemistry and Physics, 2023. **301**: p. 127582.
298.Bafana, A., S.S. Devi, and T. Chakrabarti, *Azo dyes: past, present and the future.* Environmental Reviews, 2011. **19**(NA): p. 350-371.
299.Burkinshaw, S., *Application of dyes*, in *The chemistry and application of dyes*. 1990, Springer. p. 237-379.